MODELING DRIVER BEHAVIOR DURING AUTOMATED VEHICLE TAKEOVERS

A Dissertation

by

HANANEH ALAMBEIGI

Submitted to the Office of Graduate and Professional Studies of
Texas A&M University
in partial fulfillment of the requirements for the degree of

DOCTOR OF PHILOSOPHY

Chair of Committee,	Anthony D. McDonald
Committee Members,	Maryam Zahabi
	Thomas Ferris
	Reza Langari
Head of Department,	Lewis Ntaimo

May 2022

Major Subject: Industrial Engineering

ABSTRACT

Driving crashes are a leading cause of death and injuries worldwide. Automated vehicles are expected to reduce these crashes and provide safety benefits. However, the safety of partially automated vehicles is limited by the driver ability to takeover when automation fails. Understanding factors that influence takeover performance is a critical first step in designing safer systems. Additional steps are required to integrate these factors into a design process. One method of integration is through simulation frameworks that join technology with driver models and produce safety-related predictions. Despite the considerable amount of modeling work during manual emergencies, models of automated vehicle takeover behavior are rare. This research addresses this gap by investigating the influential factors and their impacts on takeover performance, identifying promising driver models that accurately capture the impact of influential factors, and developing a comprehensive modeling framework that provides accurate predictions of driver behavior.

This work collected data from a driving simulator experiment to investigate the impact of automation design issues (e.g., silent failure) on driver performance across various transitions of control. Drivers' takeover time and quality are explored using Bayesian regression models and a significant impact of silent failures on takeover safety, especially in critical events, is found. To capture the effects of each factor, the drivers' reaction and control maneuver are modeled using visual looming-based models. An evidence accumulation and a piecewise linear model are proposed to predict the drivers' braking behavior. The steering avoidance is modeled by a looming-based open-loop

Gaussian model followed by a closed-loop two-point visual control model for stabilization steering. The developed braking and steering models are leveraged and a holistic algorithm is proposed that ties two parallel evidence accumulators to the developed models to account for the onset of each decision alternative as well as the drivers' response behavior.

The development of a comprehensive and realistic model that closely matches real-life driver behaviors is vital to assess the safety-related effectiveness of automated systems following a takeover. These evaluations can guide the design of automated technologies and reduce the consequences of failures.

DEDICATION

To my husband, Ali, for showing me what the true Love is.

ACKNOWLEDGEMENTS

This dissertation would not have been possible without incredible individuals, who were directly or indirectly involved, during my PhD journey. I would like to take this opportunity to thank all of them for their contribution, support, and encouragement.

First and foremost, I would like to express my deepest gratitude to my advisor, Dr. Anthony (Tony) McDonald, whom I had the privilege to be his first PhD student. Tony is a wonderful mentor and a brilliant researcher. His unwavering support and sincere caring always inspires me in my academic and real life. Tony, thank you for all your dedication, patience, insightful advice, and for allowing our work relationship to grow into one of mutual trust and appreciation. I consider myself very fortunate indeed to have had the opportunity to work with you every day throughout this journey.

I would also like to extend my appreciation to my remarkable committee members, Dr. Maryam Zahabi, Dr. Thomas Ferris, and Dr. Reza Langari for providing insight, valuable feedback, and support throughout this journey. It was an honor to have you on my committee.

I am very grateful for the funding support received throughout my PhD from the U.S. Department of Transportation University Transportation Center.

My sincere thanks to all my friends in the Human Factors & Machine Learning (HFML) lab for all the constructive feedback, helpful suggestions, and unforgettable memories. I look forward to our continued friendships and future collaborations.

Very special thanks to the fantastic and supporting faculty, staff, and students of the Industrial and Systems Engineering department at the Texas A&M University for making my graduate school experience enjoyable.

I would also like to thank my friends and family, my amazing parents, for always believing in me and providing me with the opportunities to follow my dreams, my brother, Mohsen, for his unwavering support, my sister in-law, Yasaman, for being the wonderful sister that I could have ever wished for, and my nephews, Parsa and Kasra, for making my life more beautiful and cheerful. Thank you for your endless love, support, and inspiration with my academic pursuit and my life in general.

Last but definitely not the least, to my lovely husband, Ali, who has always been a constant source of love, joy, and support in my life. Ali, you are my best friend and companion, my soulmate, and the closest person to my heart. Thank you for your unconditional love, understanding, sacrifice, and for always encouraging me to pursue my dreams. Without your tremendous love and support, this journey would not have been possible. This degree is yours as much as it is mine.

CONTRIBUTORS AND FUNDING SOURCES

Contributors

This work was supervised by a dissertation committee consisting of committee chair, Dr. Anthony McDonald, and committee members, Dr. Maryam Zahabi and Dr. Thomas Ferris of the Wm Michael Barnes '64 Department of Industrial and Systems Engineering, and Dr. Reza Langari of the Department of Engineering Technology and Industrial Distribution (ETID).

All work conducted for the dissertation was completed independently by the student under the advisement of Dr. Anthony McDonald of the Wm Michael Barnes '64 Department of Industrial and Systems Engineering.

Funding Sources

Graduate study was supported by a research assistantship from Texas A&M University.

This work was also made possible in part by a grant from the U.S. Department of Transportation, University Transportation Centers Program to the Safety through Disruption (SAFE-D) University Transportation Center under grant number 451453-19C36. Any opinions, findings, conclusions, or recommendations expressed in this material are solely the responsibility of the author and do not necessarily reflect the official views of the funding organizations.

TABLE OF CONTENTS

Page

LIST OF FIGURES

Page

LIST OF TABLES

Page

1. INTRODUCTION

Driving crashes have a significant impact on the world economy (Blincoe et al., 2015) and are a leading cause of death and injuries worldwide (World Health Organization, 2015) causing over 1.2 million deaths and 50 million injuries each year (Road safety facts, 2019). One promising method of reducing these costs is the introduction of advanced automated vehicle technologies such as forward collision warning and automated emergency braking (Fildes et al., 2015). Forward collision warning and automated emergency braking have been associated with a reduction in read-end crashes of 27% (Cicchino, 2017a) and between 38% and 43% (Fildes et al., 2015), respectively. Additionally, advanced automated technologies such as automated vehicles are expected to provide even greater safety benefits (Blanco et al., 2016; Eriksson et al., 2017). Moreover, the advent of these vehicles promised a number of socio-economic advantages including an increase in shared mobility, a reduction in fuel consumption, and an improvement in traffic flow (Casner et al., 2016; Fagnant & Kockelman, 2015).

But despite impressive demonstrations and technical advances of automated vehicles, many obstacles remain on the road to achieve the expected safety outcomes. Depending on the scheme of function allocation between the driver and the automation, automated vehicle can encompass several varieties. Forming an incorrect mental model of the function allocation can lead to various human factors-related issues (Casner et al., 2016; Inagaki & Sheridan, 2018). Understanding the responsibilities of the automation and human driver across the new automation technologies can facilitate these issues. To

classify these technologies, the Society of Automotive Engineers (SAE) has introduced a levels of vehicle automation framework (SAE International, 2021). The levels of this framework define the responsibilities for controlling the vehicle (i.e., steering, acceleration, and braking), monitoring the driving environment, and serving as a fallback when the automation hits operational domain limits. Table 1.1 shows the narrative descriptions of different levels of automation as defined by SAE International (2021).

Table 1.1 SAE Levels of Automation and Their Definition

SAE Level of Automation	SAE Name	Description
0	No Automation	The driver performs all aspects of the driving task
1	Driver Assistance	Automated vehicle performs either steering or acceleration/braking, while the driver monitors the driving environment
2	Partial Automation	Automated vehicle performs both steering and acceleration/braking, while the driver monitors the driving environment
3	Conditional Automation	Automated vehicle performs both steering and acceleration/braking as well as monitoring the driving environment in some circumstances, while expecting the driver to takeover the vehicle control and respond appropriately to automation failures
4	High Automation	Automated vehicle performs both steering and acceleration/braking as well as monitoring the driving environment in some circumstances and does not require the driver to takeover the vehicle control
5	Full Automation	Automated vehicle performs all aspects of the driving task

Note. The grey highlighted rows indicate the area of focus for this dissertation.

Although automated vehicles promise to offer several benefits, some safety issues remain in the interaction between human drivers and automation, in particular, with the transition from driver assistance systems (SAE Level 1) to partially automated vehicles

(SAE Level 2) or higher levels of automation. Previous research on human-automation interaction shows that a high level of automation takes the operator out of the control loop, leads to mental underload (as a result of reduced workload from driving task) and overload issues (as a result of automation failure), and causes loss of situation awareness, skill degradation, and under and over trust and reliance on the automation (Bainbridge, 1983; Endsley & Kiris, 1995; Hancock et al., 2013; Kaber & Endsley, 2004; J. Lee & See, 2004; Parasuraman & Riley, 1997; Sarter & Woods, 2000). Similar challenges have been found in automated vehicle driving (Banks et al., 2017, 2018; de Winter et al., 2014; B. Seppelt & Victor, 2016; Young & Stanton, 2002).

Driving technologies at higher levels of automation shift monitoring and the execution of steering and braking to the automation. This shift has been shown to increase the drivers' inclination to perform non-driving-related tasks (Carsten et al., 2012; de Winter et al., 2014; Jamson et al., 2013), which could impede their ability to avoid a crash when an intervention is required (Louw & Merat, 2017). Thus, the safety of automated vehicles is limited by the ability of the automation and human driver to perform their responsibilities, their ability to transfer control to and from one another, and their ability to conduct appropriate interactions with the transportation network (Banks & Stanton, 2015; Brown, 2017; J. D. Lee, 2018; Lu & de Winter, 2015). As a result, the transition of control from automation to driver is perhaps the most critical aspect of the safety limits in design considerations of automated driving systems.

An automated vehicle takeover is a process in which an automated vehicle fails in its control responsibility or faces an operational limit, and the driver has to resume control

from the automation. A takeover can be initiated by the driver or the automation (Lu et al., 2016) and is usually prompted by a precipitating event such as a cut-in maneuver from a passing vehicle or an object in the road (e.g., Gold, Körber, Lechner, & Bengler, 2016; Li, Blythe, Guo, & Namdeo, 2018). Takeovers consist of completing visual, cognitive, and physical readiness processes (SAE International, 2016; Wintersberger et al., 2017; Zeeb et al., 2015) along with performing a mitigating action to avoid crashes. The safety of a takeover is limited by the time taken for the drivers to complete the takeover process and the effectiveness of the executed action. This is equivalent to the notion of speed-accuracy tradeoff, in which decisions can be made faster, sacrificing accuracy, or more accurate, sacrificing speed (Ratcliff et al., 2016). Therefore, the negative impacts of the visual, cognitive, and physical readiness processes on takeover time (i.e., the time between the precipitating event and the first demonstration of an evasive maneuver from the driver), even if not tremendous, can be carried over to the quality of the mitigating action resulting in a more aggressive behavior (Alambeigi & McDonald, 2021b; Zeeb et al., 2016). This emphasizes that the takeover time alone does not guarantee a safe evasive maneuver and the post-takeover control aspect should also be taken into account. If drivers perform all components of a takeover within the time budget (i.e., time to collide at the precipitating event onset), and execute an avoidance maneuver, the takeover is deemed safe and a crash is avoided. Understanding factors that influence takeover time and action quality is a critical first step in designing safer systems; however, additional steps are required to integrate the effects of these factors into the design process.

One method of integration is through simulation frameworks. Simulation frameworks capture bounds on human physical and cognitive performance and provide realistic predictions of human behavior. Within these frameworks, driver models, pre-crash kinematic driving data (from driving simulation or naturalistic studies), and automated vehicle algorithms are integrated to produce safety-related predictions. The driver model is a significant component of this process, as poor model selection may undermine the accuracy of the safety-related predictions (Bärgman et al., 2017; Roesener et al., 2017). Over the past decade, there has been a considerable amount of work in the modeling of driver behavior during manual driving (Markkula et al., 2012; Saifuzzaman & Zheng, 2014); however, studies are rare in the automated vehicle takeover context. In particular, there is no holistic model of driver behavior following an automated vehicle takeover, that can capture all components of a takeover process (e.g., action selection or action execution) and perform under various traffic or environmental conditions. Different components of a takeover process can be translated into models of driver behavior (e.g., decision-making, steering and/or braking) to assess the effectiveness of a takeover performance within the limits of driver-related factors, vehicle kinematics, and traffic or environmental context.

1.1. Research Objectives

Developing effective driver takeover models that capture the underlying influential factors is contingent on investigating how humans behave under various traffic and environmental conditions and how the effects of those conditions can be integrated

into the models. Such knowledge can then be used to develop models of takeover behavior and assess the degree to which the models can replicate observed driver behavior. Thus, the objectives of my dissertation are to answer the following questions:

1. To what degree does the system design influence the takeover time and post-takeover performance during automated vehicle driving?

   One of the most prevalent issues with the automated vehicles' design is a silent failure, where the automation fails or encounters an operational limit without a preceding takeover request (e.g., due to sensor limitations). In this situation, the system implicitly relies on the driver to perceive the failure and resume the control from the automation. Although it is expected that it elongates the takeover time, the exact impact on takeover performance is not known. Another issue is the takeover time budget related to the time that the system disengages when a failure happens. Time budget refers to the time to collision (TTC) or time to lane crossing (TLC) at the time of the takeover request or the event onset in case of a silent failure. Investigating and quantifying the impacts of these factors and their interaction across different environmental and traffic situations (e.g., an unexpected braking lead vehicle) is important to design a safer system.

2. To what degree do contemporary models of manual driving capture the drivers' braking and steering behavior after automated transitions of control?

   Prior work on models of drivers' braking and steering behavior in manual emergencies showed that TTC plays an important role in determining drivers' decision to initiate

the brake (Kiefer et al., 2006; D. Lee, 1976). Drivers have direct access to a visual estimate of inverse TTC (i.e., visual looming) and react to this stimulus only when the accumulated evidence exceeds a threshold. This is aligned with the finding in automated vehicle driving, which showed TTC at the time of the failure is one of the principal determinants of a takeover performance (McDonald et al., 2019), suggesting that existing models of manual driving can be extended to automated vehicle takeovers; however, there is a need for more detailed driver braking reaction and control models, and for formal model validation processes that assess the degree to which driver models replicate observed driver behavior. Effective models of post-takeover control steering must include both the initial avoidance maneuver and the subsequent stabilization steering given that it may take drivers up to 40 s following a takeover to fully return to normal steering behavior (Merat et al., 2014)., these models have not been validated against drivers' post-takeover steering avoidance and stabilization behavior.

3. Does integrating individual decision-making, braking, and steering models capture drivers' comprehensive takeover behavior?

   Several independent models have been developed that predict driver behavior in different phases of a takeover process. However, there has not been a holistic modeling framework of drivers' perceptual decision-making and control response after a takeover process. In particular, models of the takeover have been focused on an avoidance strategy by either braking or steering alone, while in real life, drivers perform steering and braking with close temporal proximity, if not at the same time.

The concept of parallel information processing follows the leaky competing accumulator models, in which the human brain can accumulate two sets of evidence in parallel, rather than having a single accumulator with different thresholds, allowing them to have different choice alternatives (Usher & McClelland, 2001). Developing and validating such a comprehensive model can be used as a guideline to improve the design of advanced automated vehicle-related technologies.

1.2. Dissertation Overview

This dissertation has seven chapters including this chapter. Figure 1.1 maps these chapters onto a takeover event. Chapter 2 provides background information on current automated vehicle technologies, elaborates on findings from a comprehensive literature review about automated vehicle takeovers, as well as models of driver behavior, and identifies several research gaps in the current literature. Chapter 3 through 6 address the research questions discussed in section 1.1. All four chapters use the data from the driving simulator experiment collected in response to the first research question.

Chapter 3 addresses the first question of the dissertation regarding the impacts of system design issues (silent failures and time budgets) on takeover performance. To answer this question, a driving simulator experiment with two takeover scenarios was conducted. Simulator experiment was selected as it provides a controllable, cost-effective, and safe environment to investigate the driving performance (Eriksson et al., 2017; Risto & Martens, 2014) and driver behavior models have been successfully developed from the data collected in simulator studies (Piccinini et al., 2019; Xue et al., 2018). To quantify

the impacts, Bayesian multilevel regression models were used comparing silent and alerted failures across different time budgets. The Bayesian approach provides the distribution of takeover performance variables for a given parameter, which is more informative for safety. The driving performance data set from the experiment is published on the Virginia Tech Transportation Institute data repository (Alambeigi & McDonald, 2021a).

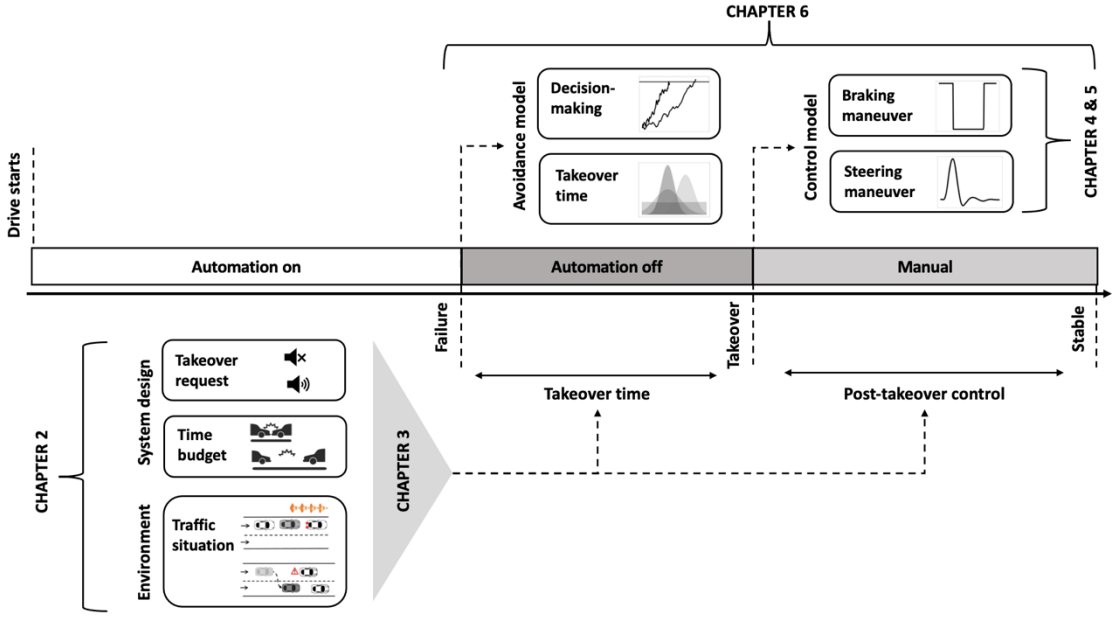

Figure 1.1 An illustration of this dissertation chapters mapped on a takeover process

Chapter 4 answers the second research question regarding the models of post-takeover braking behavior. To address this question, a baseline comparison model was developed and the fit results were compared with a promising model identified in the literature review (i.e., the visual looming-based models, in particular, evidence

accumulation). The driver braking reaction was modeled by an evidence accumulation. In this model, drivers receive various pieces of evidence such as the changes in the visual looming of the lead vehicle (i.e., the ratio of the angular size of the forward vehicle and its rate of change; D. N. Lee, 1976) and respond with braking when the mismatch between their expected looming and actual looming exceeds a threshold. To evaluate the performance of this model in capturing the effects of the presence of an alert and time budget, it was compared with a simple reaction time distribution. The simulated brake reaction times were fed to a piecewise linear function to model the driver's braking control behavior.

Chapter 5 provides answers to the question regarding the models of post-takeover steering behavior. The steering maneuvers were modeled using a two-part visual-based avoidance and stabilization model. The two-part model contained an open-loop avoidance and a closed-loop stabilization component. The open-loop avoidance component followed a visual looming-based Gaussian function and the stabilization steering modeled based on a visual-based optimal control process to minimize the angles between the vehicle's heading and near and far anchor points. The open- and closed-loop models were then compared with a baseline closed-loop model fitted to the entire post-takeover control.

Chapter 6 addresses the last question regarding the holistic model of a takeover process using two evidence accumulation models that work in parallel to simulate the drivers' decision-making, braking, and steering behavior across the investigated system design and environmental factors. The basic accumulator model was modified to better account for the drivers' perceptual decision-making and response time process (e.g.,

memory decay or multiple responses at a single time). The basic piecewise linear and open-loop avoidance models were extended to capture the urgency of the events. An Approximate Bayesian Computation (ABC) approach was used to fit the entire model to the collected data. This approach was employed as it explores the parameter space and replaces the likelihood ratio computation with simulations of the model (Turner & Van Zandt, 2012). The output of this model is summary statistics of the parameters that can be used to simulate the drivers' decision-making, takeover time, and braking and steering control maneuvers.

Chapter 7 presents the conclusion of this dissertation. It summarizes the key findings, practical implications and theoretical contributions to the body of literature, limitations, and future work.

2. LITERATURE REVIEW*

The prior chapter established that investigating factors that influence takeover performance and identifying models of driver behavior during takeovers are critical elements of automated vehicles' safety. This chapter briefly introduces the current state of the art in automated vehicles and then reviews the literature on automated vehicle takeovers and models of driver behavior.

2.1. Current Automated Vehicle Technologies

Advanced safety technologies such as forward collision warnings, blind spot monitoring, and automated emergency braking have reduced crashes and crash severity (Cicchino, 2017a, 2017b; Fildes et al., 2015; Isaksson-Hellman & Lindman, 2016). Automated vehicle technologies—such as the "Tesla Autopilot" (Tesla Motors, 2018), "IntelliSafe Autopilot" (Volvo Cars, 2018), "GM Cruise" (General Motors, 2018), and Waymo's self-driving car (Waymo, 2018) may continue this trend and provide even greater comfort and safety benefits (Blanco et al., 2016; Eriksson et al., 2017). The safety impact (i.e., the reduction in crashes resulting in injuries or deaths) of these automated vehicle technologies will be limited by the ability of the automation and human to perform their responsibilities, their ability to transfer control to and from one another, their ability

* Parts of this chapter are reprinted with permission from "McDonald, A. D., Alambeigi, H., Engström, J., Markkula, G., Vogelpohl, T., Dunne, J., & Yuma, N. (2019). Toward Computational Simulations of Behavior During Automated Driving Takeovers: A Review of the Empirical and Modeling Literatures. Human Factors, 61(4), 642–688."

to conduct appropriate interactions with the transportation network, and appropriate levels of trust and reliance of the human driver on the automation (Banks & Stanton, 2015; Brown, 2017; J. D. Lee, 2018; J. Lee & Kolodge, 2018; Lu & de Winter, 2015; McDonald et al., 2019; B. Seppelt & Victor, 2016).

The human factors and driving safety research communities have primarily focused on transitions of control (Lu et al., 2016; McDonald et al., 2019) although some efforts have been made to analyze interactions between vehicles in automated mode and the transportation network (Brown, 2017; Brown & Laurier, 2017). In parallel with these efforts, companies have continued to pursue the development and testing of automated vehicle technologies on public roadways. In the state of California, USA, these tests must be documented in two reports documenting automation disengagements and crashes (State of California Department of Motor Vehicles, 2014). The disengagement reports document the number and nature of transitions of control for each company and the crash reports contain a set of required fields along with an unstructured narrative report. The databases containing these reports offer a unique opportunity to augment the findings from controlled laboratory and on road studies.

Prior research has used these databases to compare automated and manual vehicle safety (Blanco et al., 2016; Schoettle & Sivak, 2015; Teoh & Kidd, 2017), analyze transitions of control (Dixit et al., 2016; Favarò et al., 2017, 2019), and identify trends in collision types and crash dynamics (Favarò et al., 2017). These studies have found that automated vehicles tend to be safer than manually driven vehicles, although there are open issues regarding the impact of transitions of control on safety (Teoh & Kidd, 2017).

Analyses of the crash database have found that the majority of crashes occur when the vehicle in automated mode is stopped, that approximately 20% of the crashes occur following a manual transition, and that no crashes have been reported during an automated initiated transition of control to the driver (Favarò et al., 2017, 2019). The findings have been derived primarily from frequency analyses of the fields in the crash database and manual reviews of crash narratives. These findings are aligned with those of Alambeigi et al. (2019) that showed in addition to rear-end collisions at intersections, crashes associated with manual transitions, and crashes involving a side-swipe during overtake are prominent themes in the automated vehicle crash database. This illustrates the need for investigations of silent automation failures in which the automation fails to detect an imminent crash and requires driver input in different situations (e.g., an overtake or a rear-end situation).

2.2. Automated Vehicle Takeovers

Given the importance of transitions of control in current automated vehicle technology safety, a substantial amount of recent research has focused on identifying and quantifying characteristics of the driver, environment, and transition mechanism that correlate with safe transfers of control (Eriksson & Stanton, 2017b; Lu et al., 2016; McDonald et al., 2019; Zhang et al., 2019). Automated vehicle takeovers are either driver-initiated or automation-initiated. In case of the automation-initiated, humans are expected to assume control of the vehicle with or without a preceding alert. If the precipitating event is recognized by the automation, an alert will be provided to the driver; otherwise, in cases where the automation fails to detect the precipitating event or unexpectedly disengages,

the driver will not receive a takeover request (i.e., silent failures). Takeovers consist of visual, cognitive, and physical components. The visual component comprises redirecting eyes from non-driving related tasks to the driving scene and scanning the roadway to assess action alternatives. The cognitive component involves situation perception, action selection, and evaluation of the action. The physical component consists of motor readiness and steering or braking action execution. Drivers establish motor readiness by repositioning their hands to the steering wheel and their feet to the pedals. The cognitive perception and physical readiness components might be executed parallel to each other (Zeeb et al., 2015). At the end of a takeover, drivers perform their selected action, evaluate it, and they modify and update their action if it is necessary. Figure 2.1 shows a conceptual model of the physical, visual, and cognitive components of the takeover process. In this figure, the durations of motor, gaze, and cognitive readiness, and action selection represent one possible scenario; in practice, any readiness component could have maximum latency (McDonald et al., 2019). For instance, if the driver is engaged with a handheld secondary task (e.g., holding a cell phone or a tablet in hands), in an emergency situation, he/she might need to select an action before initiating the hand movements to place the device in a safe position and take the steering wheel. In this case, motor readiness takes longer times than cognitive readiness. To ensure safe takeovers, it is important to examine the factors and environments that impact these components and undermine takeover performance.

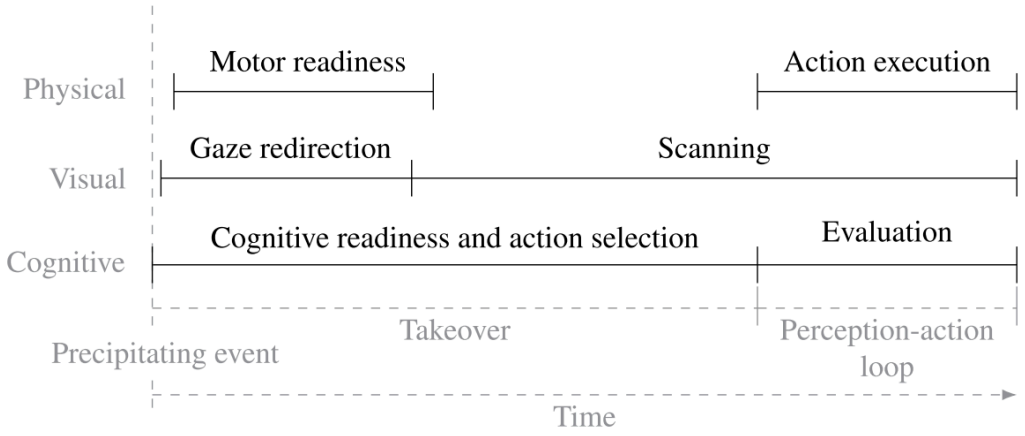

Figure 2.1 A conceptual model of the physical, visual, and cognitive components of the takeover process. Reprinted with permission from McDonald et al. (2019).

2.2.1. Takeover Performance Metrics

From the safety perspective, the time taken for the drivers to complete all components of a takeover process and the quality of the executed action are both important. Thus, the remainder of this section covers the metrics used in the literature for both time and quality of a takeover process.

2.2.1.1. Takeover Time

While a variety of temporal measures have been used to assess takeover performance, the takeover time is most often measured as the time between the takeover request, or event presentation for silent failures, and the first evidence of demonstrable braking or steering input. Demonstrable input is typically defined by the first exceedance of control input thresholds. The most common thresholds are 2 degrees for steering and a threshold of 10 % actuation from braking (Gold et al., 2017; Louw, Markkula, et al., 2017;

Zeeb et al., 2015). Other temporal measures of takeover performance include the time between the warning (or failure) and the redirection of the driver's gaze (Eriksson et al., 2019), repositioning of the hands or feet to the controls (Petermeijer, Bazilinskyy, et al., 2017; Petermeijer, Cieler, et al., 2017; Petermeijer, Doubek, et al., 2017), automation deactivation (Dogan et al., 2017; Vogelpohl, Kühn, Hummel, Gehlert, et al., 2018), or the initiation of the last evasive action (Louw, Markkula, et al., 2017). Table 2.1 summarizes these measures and their link to driver behaviors.

Table 2.1 Temporal Measures of Takeovers and Related Driver Actions Following a Precipitating Event. Reprinted With Permission From McDonald et al. (2019).

Takeover Temporal Measure	Driver Action	Example Reference
Gaze reaction time	Driver redirects gaze to the forward roadway	(Eriksson et al., 2019)
Feet-on reaction time	Driver repositions feet to the pedals	(Petermeijer, Bazilinskyy, et al., 2017)
Hands-on reaction time	Driver repositions hands to the steering wheel	(Petermeijer, Bazilinskyy, et al., 2017)
Side mirror gaze time	Driver redirects gaze to the side mirror	(Vogelpohl, Kühn, Hummel, Gehlert, et al., 2018)
Speedometer gaze time	Driver redirects gaze to the instrument panel	(Vogelpohl, Kühn, Hummel, Gehlert, et al., 2018)
Indicator time	Driver activates turn signal (or indicator light)	(S. Li et al., 2018)
Automation deactivation time	Driver deactivates the automation by braking/steering action or pressing a button	(Dogan et al., 2017)
Takeover time	Driver depresses brake pedal more than 10% or turns the steering wheel more than 2 degrees	(Gold et al., 2017)
Action time	Driver initiates the final evasive action	(Louw, Markkula, et al., 2017)

Many of these measures are situation dependent—for example, drivers may already have their hands on the steering wheel at the time of a takeover request and thus would not have a measurable "hands-on reaction time." From a modeling perspective, these measures present opportunities for model validation. For example, if a model's structure includes an eye glance component, one can partially validate the model based on the predicted time to return a driver's glance to the forward roadway.

2.2.1.2. Takeover Quality

Takeover quality, or post-takeover control, comprises a broad range of metrics intended to measure the takeover performance. Metrics explored in the literature include lateral and longitudinal acceleration (or their combined magnitude), time to collision statistics (TTC), inverse TTC, time to lane crossing (TLC), time headway to the lead vehicle, distance headway to the lead vehicle, lane position statistics, frequency of collision occurrence, time to complete an evasive maneuver, steering wheel angle based metrics, maximum derivative of the control input that drivers used to avoid the collision, speed statistics, and lane change error rates (Eriksson & Stanton, 2017b; Feldhütter et al., 2017; Körber et al., 2016; Merat et al., 2014; Naujoks et al., 2017; Schmidt et al., 2017; Wandtner et al., 2018a; Zeeb et al., 2016, 2017). The complete set of metrics used to measure takeover quality in the reviewed studies is shown in Table 2.2. The diverse definitions of takeover quality make summative analysis difficult and thus there is a significant need for a convergence of measures in future studies. From a modeling perspective, these metrics provide a similar opportunity for validation, but also provide

insight into the impact of various factors on lateral (i.e., steering) and longitudinal control. Such impacts can be used to guide model selection for braking (longitudinal) and steering (lateral) control models. In the following sections, we separate the impacts of each factor on lateral and longitudinal control in order to align with this model selection process.

Table 2.2 Summary of Takeover Quality Metrics Used in the Reviewed Studies. Reprinted With Permission From McDonald et al. (2019).

Takeover Quality Metric	Unit	Example Studies Employing the Metric
Max, min, mean lateral acceleration	[m/s^2]	(Gold et al., 2016; Gonçalves et al., 2016; Kreuzmair & Meyer, 2017; Lorenz et al., 2014)
Max, min, mean longitudinal acceleration	[m/s^2]	(Feldhütter et al., 2017; Gold et al., 2015; Gold, Damböck, Bengler, et al., 2013)
Max resultant acceleration	[m/s^2]	(Gold, Damböck, Bengler, et al., 2013; Hergeth et al., 2017; Kerschbaum et al., 2015; S. Li et al., 2018)
Brake input rate	Count	(Eriksson et al., 2019)
Min, mean, inverse time to collision	[s]	(Gold et al., 2015; Hergeth et al., 2017; Körber et al., 2018)
Min time to lane crossing	[s]	(Zeeb et al., 2017)
Min time headway	[s]	(Schmidt et al., 2017; Strand et al., 2014; Zeeb et al., 2017)
Min distance headway	[m]	(Louw, Kountouriotis, et al., 2015; Schmidt et al., 2017)
Max, mean, standard deviation of lane position	[m] or [ft]	(Vogelpohl, Kühn, Hummel, Gehlert, et al., 2018; Wiedemann et al., 2018)
Crash rate	Count	(Körber et al., 2016; Radlmayr et al., 2014)
Time to complete a lane change	[s]	(Bueno et al., 2016; Louw, Merat, et al., 2015)
Lane change error rate	Count	(Mok, Sirkin, et al., 2015; Wandtner et al., 2018a)
Max, standard deviation of steering wheel angle	[rad] or [deg]	(Bueno et al., 2016; Clark & Feng, 2017; Eriksson & Stanton, 2017a; Shen & Neyens, 2014)
Max steering wheel velocity	[rad/s]	(Wiedemann et al., 2018)
High frequency steering control input	Count	(Merat et al., 2014)
Min, max, mean, standard deviation of velocity	[m/s] or [km/h]	(Brandenburg & Skottke, 2014; Clark & Feng, 2017; Merat et al., 2014; Naujoks et al., 2017)
Max derivative of the control input	[deg] or [rad/s]	(Louw, Markkula, et al., 2017)

2.2.2. Influential Factors on Takeover Performance

The topic of transfers of control between humans and automation has been extensively explored by human factors researchers (Bainbridge, 1983; Dekker & Woods, 2002; Endsley & Kaber, 1999; Endsley & Kiris, 1995; Hancock, 2007; Kaber & Endsley, 2004; Sarter & Woods, 2000). However, transitions of automated vehicle control present several new and complex challenges (B. Seppelt & Victor, 2016). A significant amount of research has been dedicated to exploring these nuances and identifying factors that influence takeover performance. These factors, their definitions, and example studies are summarized in Table 2.3.

Table 2.3 Factors and Definitions for Key Terms Associated with Automated Vehicle Takeovers. Reprinted With Permission From McDonald et al. (2019).

Measure	Definition	Example Reference
Time budget	The time-to-collision (or time to line crossing) at first presentation of a precipitating event	(Gold, Damböck, Lorenz, et al., 2013)
Secondary task	A non-driving task performed by the driver at the time of the precipitating event (e.g., interacting with in-vehicle technology)	(Radlmayr et al., 2014; Zeeb et al., 2016)
Takeover request modality	The modality (e.g., auditory, visual, vibrotactile) of the takeover request	(Naujoks et al., 2014)
Driving environment	The weather conditions and road type during a takeover, traffic density in vehicles per kilometer, or the available escape paths	(Gold et al., 2016; Radlmayr et al., 2014)
Presence of takeover request	Whether the takeover was preceded by a request	(Strand et al., 2014)
Level of automation	SAE automation level 0 to level 4	(Madigan et al., 2018; Radlmayr et al., 2018)
Driver factors	Driver specific factors such as fatigue or alcohol impairment	(Vogelpohl, Kühn, Hummel, & Vollrath, 2018; Wiedemann et al., 2018)

As this table shows the factors that have been found to influence takeover performance include time budget, secondary task engagement, the presence and modality of a takeover request, the external driving environment, level of automation, and driver factors (e.g., age or trust). This section reviews these factors, and provides a summary of their impacts, and consolidates the findings into requirements for driver models.

2.2.2.1. Time Budget

Time budget refers to the TTC or TLC at the time of the takeover request or onset of the precipitating event for silent failures. A broad range of takeover time budgets have been explored in the literature, where the most common time is 7 s (Eriksson et al., 2017; Eriksson & Stanton, 2017b). While nearly all the reviewed studies included a time budget for control transitions, several specifically evaluated the effects of varying time budgets on take-over time and post-take-over control. Time budget has been shown to significantly increase the takeover time with an approximately 0.3 s increase per a 1 s increase in time budget (Gold et al., 2017; McDonald et al., 2019). In addition, time budget significantly impacts lateral and longitudinal aspects of the post-takeover control by decreasing the minimum TTC and increasing the maximum lateral and longitudinal accelerations. Choice of maneuver is also affected by this factor, where lower time budgets lead to more braking responses. Collectively these results align with findings from analyses of manual driving (Markkula et al., 2016), which suggests that models used for manual driving may be translated to automated vehicle takeovers.

2.2.2.2. Secondary Task

Secondary tasks refer to any non-driving related activity that drivers perform during automated driving. Studies have explored visual, cognitive, and motoric task modalities (McDonald et al., 2019). A wide range of secondary tasks have been explored in the literature including both artificial, defined as highly controlled and validated interactions, and naturalistic tasks, defined as any real-life activity or interaction with in-vehicle technology even if it is not partially controlled. Table 2.4 shows a comprehensive summary of the secondary tasks explored in the takeover literature. The impact of secondary tasks on takeover time is strongly related to the manual load of the task. These tasks can be performed on a handheld or a mounted device where handheld secondary tasks in particular, significantly increase takeover time (Zhang et al., 2019). This additional time is composed of increases in both visual and physical readiness time (Dogan In addition, secondary tasks significantly impact post-takeover control and the choice of maneuver. Drivers are more likely to brake if engaged in a secondary task (Louw, Merat, et al., 2015; Naujoks et al., 2017). However, there is a confound between the increases in takeover time and the resulting post-takeover control, wherein the source of post-takeover control decrements is unclear. This confound may be resolved through driver modeling analyses.

Table 2.4 Summary of Secondary Tasks Used in the Reviewed Studies. Reprinted With Permission From McDonald et al. (2019).

Type of task	Modality	Secondary task	Description		Example References
Artificial	Visual Motoric	Surrogate reference task (SuRT)	Presentation of targets that have to be identified by their columns		(Feldhütter et al., 2017; Gold, Damböck, Lorenz, et al., 2013)
	Visual	Rapid serial visual presentation (RSVP)	Serial presentation of targets and distractors, targets have to be reacted to by pressing a button		(Wiedemann et al., 2018)
	Cognitive	Twenty-question task	20 yes/no verbal questions		(Merat et al., 2012)
	Cognitive	n-back	Serial presentation of targets and distractors, target n steps before current stimulus has to be recalled		(Gold et al., 2015; Louw, Markkula, et al., 2017; Radlmayr et al., 2014)
	Cognitive Motoric	Manual shape identification	Fitting different shapes through the holes in a bag		(Gold et al., 2015)
	Cognitive Motoric	Oddball task	Presentation of a series of auditory stimuli and distractors, target stimuli have to be reacted to by pressing a button		(Körber et al., 2015)
	Visual Cognitive	Heads-up display interaction	Projection of a series of IQ test questions on a heads-up display requiring verbal answers		(Louw, Madigan, et al., 2017; Louw, Markkula, et al., 2017)
	Visual Cognitive Motoric	Visual adaptation of the Remote Association Test	Finding the target word that links three presented images among the mixed letters		(Bueno et al., 2016)
Naturalistic	Visual Cognitive Motoric	Composing text	Writing an email, completing a missing word or transcribing a given sentence	Handheld device	(Wandtner et al., 2018a, 2018b)
	Visual Cognitive Motoric			Mounted device	(Zeeb et al., 2015, 2016)

Table 2.5 Continued Summary of Secondary Tasks Used in the Reviewed Studies. Reprinted With Permission From McDonald et al. (2019).

Type of task	Modality	Secondary task	Description		Example References
	Visual Cognitive Motoric	Reading text	Reading a magazine, newspaper, article, book or a given sentence	Handheld device	(Eriksson & Stanton, 2017b; Wan & Wu, 2018; Wandtner et al., 2018a; Zeeb et al., 2017)
	Visual Cognitive			Mounted device	(Louw, Merat, et al., 2015; Zeeb et al., 2016)
	Visual Cognitive Motoric	Proofreading text	Reading the mistakes of a given sentence aloud	Handheld device	(Zeeb et al., 2017)
	Visual Cognitive			Mounted device	(Zeeb et al., 2017)
	Visual Cognitive Motoric	Watching a video	Watching video stream w/wo instruction to answer questions	Handheld device	(Miller et al., 2015; Mok, Johns, et al., 2015; Wan & Wu, 2018)
	Visual Cognitive			Mounted device	(Petermeijer, Doubek, et al., 2017; Walch et al., 2015)
	Visual Cognitive Motoric	Playing a game	Playing a game (e.g., quiz game or Tetris)	Handheld device	(Melcher et al., 2015)
	Visual Cognitive Motoric			Mounted device	(Eriksson et al., 2019; van den Beukel & van der Voort, 2013)
	Visual Cognitive Motoric	Device interaction	Internet search or retrieving information from an application	Handheld device	(Dogan et al., 2017; Zhang et al., 2017)
	Visual Cognitive Motoric			Mounted device	(Naujoks et al., 2017; Zeeb et al., 2015)
	Cognitive	Hearing text and repeating	Hearing a sentence and repeating		(Wandtner et al., 2018a)
	Visual Cognitive	Sleeping	Taking a nap		(Wan & Wu, 2018)
	Visual Cognitive Motoric	Free choice of tasks	Free choice by participant (e.g., listening to music)		(Clark & Feng, 2017; Jamson et al., 2013)

2.2.2.3. Takeover Request Modality

Takeover request modality is the modality of alert that is used to warn the driver about a takeover request. The takeover request could be a generic alert involving auditory feedback, visual feedback, vibrotactile feedback, or a combination. Ecological alerts, which provide a description or an instruction to the driver, have also been explored. Studies have found that multimodal alerts lead to shorter takeover times compared to unimodal alerts (Petermeijer, Bazilinskyy, et al., 2017). The impact of ecological alerts on takeover time is strongly dependent on conciseness of the alert design (Forster et al., 2017; Lorenz et al., 2014). Further research is needed to clarify the impact of ecological alerts and multimodal takeover requests on post-takeover control. Although preliminary findings suggest that multimodal alerts may be a promising future design direction for automated vehicle manufacturers.

2.2.2.4. Driving Environment

Traffic situations, road elements, and weather conditions surrounding the takeover are considered as driving environments. Among these environmental factors, traffic density, available escape paths, weather conditions, and road types (e.g., city roads, highways, curved roads, marked and unmarked lanes) have significantly impact takeover time and post-takeover performance. Traffic density is defined as the average number of vehicles occupying a distance of the roadway (e.g., per kilometer, per mile), whereas escape paths refer to paths of travel that the driver can take without being involved in a crash. Traffic density has been explored through several studies as increases or decreases

in the number of vehicles per mile (Dogan et al., 2017; Gold et al., 2016, 2017). The range of traffic densities explored in the literature includes 0-30 vehicles per mile. High traffic density (representing the level of service D in traffic flow categories; Margiotta & Washburn, 2017), fewer escape paths, driving in highway environments, and adverse weather conditions delay the takeover time and deteriorate post-takeover control (Gold et al., 2016; Körber et al., 2016; S. Li et al., 2018). However, further work is needed to clarify the findings of the studies here, particularly those on weather conditions and road type. In general, driver models must be robust to the various driving environments where takeovers occur.

2.2.2.5. Presence of a Takeover Request

Presence of a takeover request refers to presence or absence of a warning, notifying the driver about the need to resume control where the automation fails or encounters an operational limit. The absence of an alert is typically referred to as a silent failure. In such conditions, the system implicitly relies on the driver to perceive the failure and resume control. Few current studies have addressed the impacts of silent failures directly, especially compared to manual driving (Blommer et al., 2017; Piccinini et al., 2019). These studies showed that silent failure increased the brake reaction time and the takeover time compared to manual driving and resulted in higher standard deviation of lane position and more high-frequency steering corrections; however, no significant differences were found between silent and alerted failure. The conflicting findings across these studies and

the limited analyses of the impact of silent failures on post-transition control highlight the need for additional studies.

2.2.2.6. Level of Automation

Most studies have explored level of automation (see Table 1.1) effects through a comparison between automated driving and a manual emergency baseline. In these cases, automation has been shown to significantly increase takeover time (Gold, Damböck, Lorenz, et al., 2013; Happee et al., 2017) and decrease post-takeover performance (Dogan et al., 2017; Madigan et al., 2018) relative to the manual baseline. Few studies were identified that directly compared levels of automation. These studies have shown conflicting findings between the higher levels of automation. Some studies have shown that an increase in the level of automation has been associated with increase in takeover time (Neubauer et al., 2014) and decrease in min TTC (Strand et al., 2014) while Madigan et al. (2018) found a decrease in reaction time and increase in time headway with higher levels of automation during non-critical transitions of control. Further research is needed to clarify the specific impact of higher levels of automation (level 1 to level 4) on takeover performance.

2.2.2.7. Driver Factors

In addition to the primary factors mentioned above, prior work has explored the effects of various driver factors on takeover performance. Driver factors found in the literature include repeated exposure to takeovers, training, prior real-world automation

experience, trust in automation, age, fatigue, and alcohol consumption. Of these factors repeated exposure has the strongest impact on takeover time and post-takeover control, where it decreases the takeover time, maximum accelerations, and crash rate and increases the minimum TTC (Gold et al., 2017; Payre et al., 2016). Task-related fatigue and drowsiness (Feldhütter et al., 2017; Vogelpohl, Kühn, Hummel, & Vollrath, 2018), and alcohol (Wiedemann et al., 2018) may influence takeover time and performance, however, significant future work is needed to confirm the findings of preliminary studies. The findings on age (Clark & Feng, 2017; Gold et al., 2017) and trust (Körber et al., 2018; Payre et al., 2016) are inconclusive. Consistency in measurement techniques and statistical analyses may clarify these findings.

Table 2.6 presents the specific impacts of factors on takeover time and post-takeover lateral and longitudinal control that have been found in the literature. The grey areas show the factors with limited number of studies as well as inconclusive findings. The findings suggest that time budget, handheld secondary task, presence and modality of takeover request, driving environment, levels of automation, and driver factors including repeated exposure to takeovers, alcohol consumption, and trust in automation influence the takeover time. With respect to the post-takeover control, the results show that with longer time budget, engagement in a handheld secondary task, increase in traffic density, decrease in escape paths, adverse weather conditions, alcohol consumption, and less exposure to takeover, the increase in takeover time led to the deterioration of post-takeover performance as measured by TTC or lateral and longitudinal accelerations.

Table 2.6 The Impacts of Factors on Takeover Performance. Reprinted With Permission From McDonald et al. (2019).

Factor	Levels or direction of change	Impact on takeover time	Impact on lateral control	Impact on longitudinal control
Time budget	Increasing	Increasing	Decrease in max lateral acceleration	Decrease in max longitudinal acceleration
			Decrease in SD of lane position	Decrease in collision rates
			Decrease in SD of SWA	Increase in min TTC
Secondary task	Handheld	Increasing	Increase in SD of lane position	Decrease in Min TTC
			Decrease in min TLC	Decrease in time headway
	Non-handheld	No to minor increase	Increase in max/mean lateral acceleration	Decrease in min TTC
			Increase in SD of lane position	Increase in collision rates
			Increase in max SWA	
			Increase in TLC	
			Increase in lane change error rates	
Presence of a takeover request	Absent (silent failure)	Increasing compared to manual, Insufficient evidence compared to presence of a request	Increase in high-freq. steering corrections	Insufficient evidence
			Increase in SD of lane position	
Levels of automation	Increasing	Insufficient evidence	Insufficient evidence	Insufficient evidence

Table 2.7 Continued The Impacts of Factors on Takeover Performance. Reprinted With Permission From McDonald et al. (2019).

Factor		Levels or direction of change	Impact on takeover time	Impact on lateral control	Impact on longitudinal control
Takeover request modality		Multimodal	Decreasing	Decrease in SD of lane position	Insufficient evidence
				Decrease in max lateral acceleration	
Driving environment		Traffic density	Increasing	Increase in max lateral acceleration	Increase in mean/max longitudinal acceleration
				Increase in SD of SWA	Increase in brake application frequency
		Escape path	Decreasing		Increase in collision rates
					Decrease in min/mean TTC
		Weather condition	Adverse		Decrease in min distance headway
Driver factors	Repeated exposure to takeovers	Increasing	Decreasing	Decrease in max lateral acceleration	Increase in min TTC
					Decrease in Collision rates
	Alcohol consumption	Increasing	Increasing	Increase in SD of lane position	Increase in longitudinal acceleration
	Trust in automation	Increasing	Increasing	Insufficient evidence	Insufficient evidence
	Age	Increasing	Insufficient evidence	Insufficient evidence	Insufficient evidence
	Fatigue	Increasing	Insufficient evidence	Increase in max lateral acceleration	Insufficient evidence

Note. TTC: time to collision; TLC: time to lane crossing; SD: standard deviation; SWA: steering wheel angle; Max: maximum; Min: minimum. The grey highlighted rows indicate the factors with insufficient evidence of impact on takeover time or post-takeover control.

In addition to identifying these factors, few empirical studies have investigated the interaction effects between the factors presented in Table 2.6. Table 2.8 summarizes these findings. Few prior studies have explored the interaction effects between the factors identified in this review. Significant interaction effects on takeover time have been observed for age and time budget (Clark & Feng, 2017), age and weather condition (S. Li et al., 2018), and repeated exposure and takeover request modality (Forster et al., 2017). The findings suggest that older drivers had lower takeover times with longer time budgets than younger drivers. Also, adverse weather condition (e.g., snow or fog) delayed the younger drivers' reaction time. The drivers who received a multimodal takeover request had a lower takeover time in the first exposure to takeover compared to the drivers who received a unimodal takeover request. Regarding the post-takeover control, significant interactions have been found for time budget and secondary task (Wan & Wu, 2018) and traffic density and age (Körber et al., 2016). The findings of Wan and Wu (2018) showed that lower time budgets led to lower minimum TTC when drivers were engaged in tasks that disengaged them from the driving environment (e.g., sleeping, watching a movie, or typing) as compared to tasks such as monitoring the roadway or reading. Körber et al. (2016) observed that younger drivers braked less than older drivers at low traffic densities. Beyond this finding, further work is needed to understand the interaction between specific factors.

Table 2.8 Summary of the Findings in Interaction Effects for Takeover Time and Post-takeover Control. Reprinted With Permission From McDonald et al. (2019).

Factor		Interactive Factor	Findings
Time budget		Secondary task (handheld and non-handheld)	Minimum TTC was higher for lower time budgets and tasks where drivers were disengaged from the forward roadway
		Age	Older drivers had lower hands-on and feet-on reaction times with longer time budgets
Secondary task	Non-handheld	Request modality	No significant findings
	Non-handheld	Driving environment (Traffic density)	No significant findings
		Age	No significant findings
	Non-handheld	Task-related fatigue	No significant findings
	Non-handheld	Level of automation (L0 vs. L3)	No significant findings
Driving environment	Traffic density	Repeated exposure	No significant findings
		Age	Younger drivers brake less than older drivers at low traffic densities (0 and 10 vehicles/km)
	Weather condition	Age	Younger drivers' reaction time increased in poor weather conditions (rain, snow, fog)
		Level of automation (L0 vs. L2)	Difference in maximum longitudinal acceleration between manual and automated vehicle was greater in light fog condition compared to heavy fog
Repeated exposure		Age	No significant findings
		Request modality	Drivers who received multimodal alert had a lower automation deactivation time and hands-on time in the first exposure to takeover compared to the drivers who received a unimodal takeover request
		Level of automation (L0 vs. L2)	Maximum lateral acceleration has been reduced with repeated exposure to takeovers for drivers in L2 of automation
Fatigue		Level of automation (L0 vs. L3)	No significant findings

Note. TTC = Time to collision; L = Level of automation

2.2.3. Automated Vehicle Takeover Insights

The findings of automated vehicle takeover literature highlight the need to investigate the impact of factors that are not well studied and their interaction with other driver- or environmental-related factors. Specifically, more evidence is needed for a rigorous conclusion on the impacts of absence of a takeover request (i.e., silent failure), modality of a takeover request, age, trust, fatigue, and levels of automation on takeover performance. In addition, the findings suggest that process models of human takeover behavior should capture the negative impacts of low time budget, handheld secondary tasks, uncertainty in the driving environment, and driver factors (e.g., alcohol) on takeover time and post-takeover control. The takeover empirical literature provides a clear guidance on the link between these factors and post-takeover driving behavior, e.g., models of a takeover process should predict higher deceleration (i.e., more intense braking) with lower time budgets. In addition, considering the increase in takeover time, models should predict a delay between manual and automated driving, although the decision-making component in models of automated vehicle takeovers should be similar to those in manual driving emergencies (Lu et al., 2016). The exact mechanisms by which models capture the influence of these factors remains unclear.

2.3. Models of Driver Behavior

One approach to assess the safety-related effectiveness of automated systems is to use simulation frameworks which join predicted human behavior with technology (Bärgman et al., 2017; Roesener et al., 2017). Designing simulation frameworks requires

a combination of three different components including a driving environment data, an automated vehicle algorithm, and a model of driver behavior (Anund et al., 2013; Bärgman et al., 2017). The driving environment data describes pre-crash kinematic driving data such as speed or acceleration, and is necessary to describe the driving scenario. In addition, the algorithm behind automated vehicle technologies such as autonomous emergency braking should be entered as an input to the simulation framework. Driver model, which is the third component in the simulation framework, can be used to guide the design process and calibrate design parameters. Markkula (2013) classified the driver models into three types: conceptual, statistical, and process models. Conceptual models provide a description of driver behavior without quantifying the specific factors (e.g., Banks & Stanton, 2019). In contrast, statistical models give a quantitative description such as probability distribution of driver behavior (e.g., Gold, Happee, & Bengler, 2017). Among the three types, process models are able to mathematically describe and predict driver behavior based on theories of driver control and can be applied to a simulation framework (Bärgman et al., 2017).

One potential outcome of this framework is the assessment of crash risk (e.g., crash percentage variations) resulted from the combination of inputs. To improve the design of automated technologies different driver models will be entered into the framework and their impacts on crash risk will be compared. Figure 2.2 presents the integration of the essential components in a simulation framework. It has been shown that the validity of a simulation framework is reasonably dependent on the model's accuracy (Markkula et al.,

2012). Thus, it is vital to design accurate and realistic models that closely match with real-life human driver behaviors.

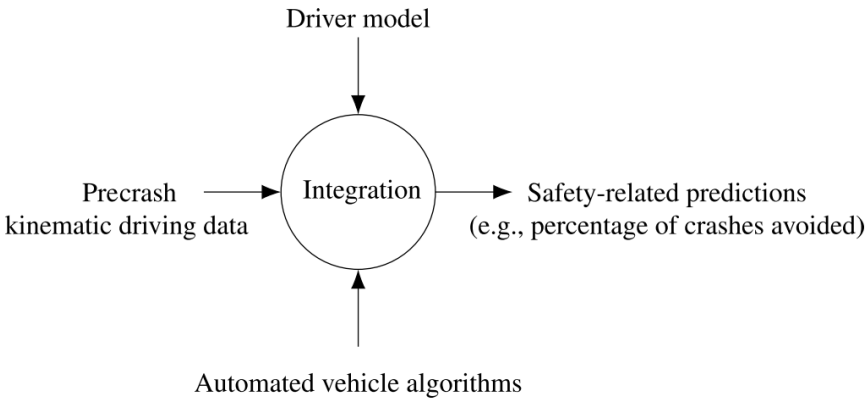

Figure 2.2 An example of a simulation framework for using driver behavior models to improve safety. Reprinted with permission from McDonald et al. (2019).

Models of driving behavior have a rich history in the human factors and vehicle dynamics literatures (Markkula et al., 2012; Michon, 1985; Plöchl & Edelmann, 2007; Saifuzzaman & Zheng, 2014). The models developed in the literature seek to describe driver acceleration, braking, or decision-making. Often models focus on acceleration/braking or steering in a specific context, for example, car-following situations (Markkula et al., 2012; Saifuzzaman & Zheng, 2014). While most of these models are designed to depict manual driving behavior, the prior section suggests that there is significant overlap between manual emergency avoidance behavior and automated vehicle takeover behavior. By extension, models of manual driving behavior may be useful for modeling automated vehicle takeovers. As illustrated in Figure 2.1, a takeover process consists of a readiness and decision-making process and executing an action. The

actions available to drivers include braking, steering, or a combination of braking and steering. A complete model of a takeover would therefore, include components to predict drivers' recognition of the need to takeover, decision-making, and braking and steering behavior. Studies that model all of these behaviors are rare, therefore the remainder of this chapter reviews the driver behavior models that fall into these categories, individually.

2.3.1. Recognizing the Need to Takeover

Prior studies suggest that the timing and the quality of driver reactions in unexpected emergency situations (e.g., rear-end) is to a large extent determined by situation kinematics (Kiefer et al., 2006; D. Lee, 1976; B. D. Seppelt, 2009). This statement is aligned with the literature on automated vehicle takeovers that revealed that the driver's reaction time to an emergency situation is highly dependent to the parameters such as TTC (Gold et al., 2017; McDonald et al., 2019; Zhang et al., 2019). Kiefer et al. suggested that driver's ability to perceive the lead vehicle's relative motion is based on an inverse TTC threshold that decreases linearly with driver speed. In this study the inverse TTC was calculated as the difference in speed between the lead and following vehicles divided by the distance between the two vehicles (Kiefer et al., 2005).

Studies in manual and automated driving introduced the concept of response threshold models and showed that rather than relative distance and speed, drivers have access to a visual estimate of TTC and their reactions to a precipitating event are significantly driven by perceptual cues (Engström, 2010; Engström et al., 2018; Markkula et al., 2016; Pekkanen et al., 2018; B. Seppelt & Lee, 2015; Xue et al., 2018). One

representation of these perceptual cues is visual looming, which is the perceived optical expansion of the closing object on driver's retina and can be described by inverse tau (Engström, 2010). Inverse tau is a visual-based estimate of inverse TTC (D. Lee, 1976) and is calculated as follows:

$$\boldsymbol{\tau^{-1} = \dot{\theta}/\theta} \qquad \textbf{Equation 2.1}$$

In this equation, θ is visual angle and is defined as the projected angle of the visual object (e.g., lead vehicle) on driver's retina, and $\dot{\theta}$ is defined as the visual angle expansion rate. Visual angle and expansion rate can be calculated as the following formulas (D. Lee, 1976).

$$\boldsymbol{\theta = 2arctan\left(\frac{w}{2D}\right)} \qquad \textbf{Equation 2.2}$$

$$\boldsymbol{\dot{\theta} = \frac{W|v_f - v_l|}{D^2 + 4w^2}} \qquad \textbf{Equation 2.3}$$

In these equations, W is the width of the object, D is the distance from the driver's eyes to the object, and $|v_f - v_l|$ is the relative speed of the driver's vehicle to the object. Figure 2.3 visualizes the visual angle of a lead vehicle at the following vehicle driver's eyes in which θ, W, and D indicate the driver's visual angle of the lead vehicle, width of the lead vehicle, and distance to the lead vehicle, respectively. As the driver gets closer to the potential collision, inverse tau increases.

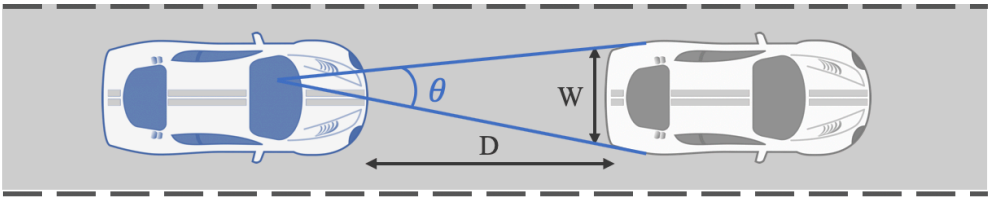

Figure 2.3 Visual angle of a lead vehicle at the following vehicle driver's eyes

In a lead vehicle braking scenario, Xue et al. showed that the visual looming threshold model always captured the brake reaction times better that expansion rate as measured by AIC values. However, they showed that the threshold models of visual looming could not capture the variability of observed brake response timing (Xue et al., 2018). This implies that the perception behind drivers' brake onset is more likely based on evidence accumulation than a particular threshold (Jin et al., 2011; Y. Li et al., 2016; Markkula et al., 2016; Svärd et al., 2017; Xue et al., 2018).

Visual evidence accumulation models work based off of the perceived looming rather than looming per se. In these models, drivers receive various pieces of evidence such as the red brake light of the leading vehicle or changes in the visual looming of the lead vehicle. This evidence encourages or discourages the driver to perform a control action, where the action is taken if sufficient evidence is accumulated (Markkula, Boer, et al., 2018). The evidence accumulation models in emergency situations are strongly correlated with the process of situation awareness recovery (Goncalves et al., 2019) and were introduced by a dynamic and interactive notion of predictive processing (Engström et al., 2018). Predictive processing model suggests that the driver's recognition of the need to initiate a response is likely driven by the difference between actual and expected

looming (Engström et al., 2018; Xue et al., 2018); For instance, in a situation where the driver is following a lead vehicle, if there is a fixed gap between the two vehicles then the driver predicts that there should be no visual expansion of the lead vehicle. The issue arises when the lead vehicle starts slowing down and makes a mismatch between driver's predicted and actual looming (Victor et al., 2018). The looming prediction error, which drives initiation of avoidance actions (Engström et al., 2018), is defined as:

$$\boldsymbol{\varepsilon(t) = \tau_{actual}^{-1} - \tau_{predicted}^{-1}} \qquad \textbf{Equation 2.4}$$

In equation 4, τ_{actual}^{-1} is the actual and $\tau_{predicted}^{-1}$ is the predicted looming. The following equation shows the accumulative part of a basic evidence accumulation model:

$$\boldsymbol{\frac{dA}{dt} = k\varepsilon(t) - M + v(t)} \qquad \textbf{Equation 2.5}$$

In which, $\varepsilon(t)$ is the looming prediction error, $v(t)$ is a zero-mean Gaussian white noise with standard deviation of sigma (σ). σ, k, and M are free model parameters. Brake adjustment will be executed if A exceeds a threshold. Studies have estimated the reaction times—particularly the brake reaction times—by fitting the model to a set of data and optimizing the free parameters (Piccinini et al., 2019; Svärd et al., 2020). Piccinini et al. (2019) applied this model to a lead vehicle braking scenario and captured the effect of fatigue, that arises due to using the automation, on driver's braking time. Markkula et al. (2016) proposed that drivers' braking initiation are based on the accumulation of various stimuli such as visual looming, brake lights, or warnings. They showed that evidence

accumulation models can perfectly explain the variability of brake timing. Engström et al. (2017) extended this model by including a cognitive distraction on drivers' reactions to a braking lead vehicle situation. In this study they compared the accumulation models of cognitively-distracted drivers with non-distracted drivers. The results showed that the non-distracted braking responses reached the response threshold earlier than cognitively-distracted responses. They showed that the response of cognitively-distracted drivers were driven by looming, while, the other group's responses were additionally driven by brake light. Xue et al. (2018) compared a looming-only accumulator model with a looming accumulator that includes the brake light and included that the latter model was fit best on a simulator-based braking lead vehicle data. Collectively, these results show that the evidence accumulation models can effectively capture the reaction time.

2.3.2. Decision-making Models

Drivers' avoidance strategies could be categorized into four different responses including braking, steering, *both* braking and steering, and no action. Prior research has shown that few models have been developed to predict drivers' avoidance maneuver selection. Gold et al. (2017) modeled the brake application by using a logistic regression model. They found time budget, traffic density, age, and repeated exposure to takeovers as significant predictors of braking. Kaplan and Prato (2012) used a mixed logit model to show that road and vehicle characteristics, driver attributes (e.g., fatigue or alcohol consumption), type of precipitating event, and environmental conditions affect the selection of avoidance maneuver. For example, they showed that drivers are more inclined

to brake when entering an intersection and steer when encountering an object or an animal in the road. Another study by Hu et al. (2017) predicts braking or steering maneuvers using a decision-tree model in cut-in scenarios. They showed that driving kinematics such as TTC and distance to the cut-in vehicle as well as driver attributes such as neuroticism and extraversion affect the drivers' avoidance strategies. The choice of steering maneuver was adopted by a minority of the drivers that were in low-risk driving conditions, male, and young.

In addition to these studies, a few studies have used the perceptual cues to model the driver's decision-making behavior. A study by Venkatraman et al. (2016) used logistic regression models to predict drivers' braking or steering maneuver in response to a lead vehicle braking scenario. They analyzed different perceptual variables including visual angle of the lead vehicle, expansion rate, and visual looming as well as timing and modality of the warning that the driver received. They showed that only a combination of visual angle and visual looming is the best predictor of choice of response as compared to the other predictors and their combinations. For example, with a unit increase in visual angle or tau, drivers are more likely to brake rather than steer into the adjacent lane. In another study by Markkula et al., they developed a simulation-ready model in which a driver makes an action decision based on a couple of perceptual decisions. These perceptual decisions are evidence accumulators that could be activated by sensory inputs (e.g., visual looming). In this model, the driver responds to the visual looming cues that build up in the evolving event. Driver's gaze determines what sensory inputs should be fed into the model. For example, if the driver's gaze is on the road, the visual looming of

the lead vehicle will be compared to a threshold and could lead to an avoidance maneuver. The decision to brake functions when the increase in brake pedal position of the lead vehicle makes a discrepancy between the actual and predicted looming and that accumulates to a threshold. The decision to steer arises when the driver is catching up to the lead vehicle (integration of looming over time is more than a threshold) or when the driver's braking does not solve the conflict (Markkula, Romano, et al., 2018).

2.3.3. Braking Models

Models of braking behavior were by far the most extensively explored area in the literature. These models were originally known with the concept of car-following in which the driver's braking behavior was modeled in reaction to a lead vehicle (Brackstone & McDonald, 1999; Gazis et al., 1961; Gipps, 1981; Pipes, 1953). These models were mostly based off of the distance headway and relative velocity to the lead vehicle. One of the leading studies in this regard is a model in Gazis, Herman, and Rothey (GHR; 1961) in which the driver's braking depended on the relative velocity to the lead vehicle along with a time lag. Several researchers tried to modify the GHR model by adding various parameters to the model. Sultan, Brackstone, and McDonald (2004) added an acceleration term to GHR to make a more realistic model that can perceive the lead vehicle's deceleration/acceleration. Yang and Peng (2010) extended the GHR model by taking into account error-inducing behaviors, as well as unpredictability of driver behavior but they still used the distance and velocity to the lead vehicle as the main elements of their model. In a model developed by Gipps, the maximum braking depends on the speed and headway

distance, in a way that the speed should not pass the driver's desired threshold (Gipps, 1981). The distribution of desired velocity, the reaction time of the driver, the ratio of mean braking rate to driver's estimates of the mean braking rate, distributions of acceleration and braking, and length of the vehicle are the parameters that are included in this model. van Winsum argued that in a car-following situation the distance that the driver attempts to maintain from the lead vehicle is based on a time headway that is constant in given similar circumstances, thus, the difference between the actual and such a desired time headway is the key element in the model (van Winsum, 1999). Based on this model, if distance to the lead vehicle is larger than a threshold, there is no safety-related reason for the driver to brake. However, if distance to the lead vehicle is smaller than this threshold, the driver initiates the deceleration which is a function of TTC. A model by Hamdar et al. (2008) took into account the stochastic character of the cognitive processes used by the drivers in a car-following model. They proposed a model that reflects the psychological and cognitive aspects of driving and captures risk-taking behavior under uncertainty. Based on their model, the driver first estimates the probability of a rear-end collision. Afterwards, the driver enters the evaluation process where a prospect theory is adapted for modeling this process. With the understanding that human drivers are limited in perception of absolute kinematics of other vehicles (Boer, 1999) as opposed to estimating the visual cues (Gray & Regan, 1998), we can argue that these models cannot effectively capture the drivers' braking responses.

Using evidence accumulation models, Svärd et al. showed that the brake is applied by the driver to minimize accumulated looming prediction error in a braking lead vehicle

situation. This model then separated the braking response into two categories of brake onset and brake control. In this model the driver receives evidence for the brake onset by accumulating looming. The braking action is taken when the accumulated evidence exceeds a certain threshold. When taking the braking action, the driver estimates how the looming will gradually decay as a result of the braking. This estimation is then compared to the actual looming and this process is continued until either the situation is resolved, maximum braking is achieved, or a collision occurs (Svärd et al., 2020). Prior studies fed the brake reaction time—estimated from the evidence accumulation model—to a piecewise linear model and showed that this model can be successfully fit to a braking control maneuver in rear-end emergencies (Markkula et al., 2016; Svärd et al., 2020). These studies showed that the rate at which drivers increased their deceleration was highly dependent on urgency of the situation.

2.3.4. Steering Models

Steering or lane changing behavior has not been studied as much as the braking models, however, these models have a long history in human behavior and traffic safety domains (Michon, 1985). The steering models are typically based on a control theory description of path-following tasks and needs a predefined desired path containing lateral road position as an input to the model (Jurgensohn, 2007; Markkula et al., 2012). Steering models can be divided into two major categories of closed-loop and open-loop. In a closed-loop model, the driver is considered as an active controller that minimizes the error between the desired and predicted values of certain parameters such as position and

velocity. In contrast, in an open-loop model, the driver reacts based on a set of pre-learned control inputs without receiving any feedback.

A closed-loop model by McAdam (2003) gets the steering wheel angle as an input to minimize the predicted lateral deviation from a desired path by minimizing the expected value of the total mean square error. Similar to McAdam's model, Sharp et al. (2000) uses the steering wheel angle as a control input; however, they proposed the idea of multi point preview for steering modeling. The driver experiences deviations between a set of points on an optical lever and corresponding points on the desired path. Steering wheel angle is then calculated as the weighted sum of all the previewed path deviations, in which the weights are free parameters. Salvucci and Gray (2004) proposed a similar model by leveraging only two points. The distinction is using the rate of change in the steering wheel angle as a control input instead of using the steering wheel angle itself. All these models try to minimize the deviation from a desired path; thus, they could be considered as an optimization effort. This model has been validated in a study by Markkula et al. that showed the effectiveness of a closed-loop two-point model in capturing the post-event stabilization steering (Markkula et al., 2014). Breuer (1998) proposed an open-loop model that applied steering wheel angle as an input during a limited time interval until reaching a certain steering wheel angle. Markkula et al. (2012) tested five variations of this model. In these variations, the amplitude of the steering wheel angle was determined based on different factors such as looming.

The automated vehicle takeover literature suggests that a steering maneuver can include a crash avoidance maneuver and a subsequent stabilization maneuver (Eriksson

& Stanton, 2017a; Merat et al., 2014; Russell et al., 2016). As defined in Markkula et al. (2014), an avoidance maneuver begins when the lead vehicle starts decelerating and ends when the driver rotates the steering wheel more than a threshold and the stabilization maneuver begins with the steering wheel rotation and ends either 250 m after passing the lead vehicle, or when the driver's vehicle falls below 10 km/h, whichever happens first. Markkula et al. (2014) compared different aforementioned closed-loop and open-loop steering models in predicting the avoidance and stabilization steering. Based on the results of this comparison, the open-loop models provided the best fit for the avoidance maneuver, while, the closed-loop models better explained the stabilization maneuver.

Prior research has found few studies that have investigated steering models in an evidence accumulation context (Markkula, Boer, et al., 2018). This study developed a steering model that integrates evidence accumulator, kinematic motor primitives, and prediction of motor actions. This framework works based on the assumption that a calculated estimate of currently needed control adjustment is compared to a prediction of the consequences of actions. This comparison yields a prediction error that will be entered into an evidence accumulation model (with a gain) where it is integrated over time to a threshold of ± 1 to execute the patterns of behavior based on the input.

2.3.5. Models of Driver Behavior Insights

The evidence from the empirical review of automated takeovers suggests that there is a strong link between TTC and driver responses. Extrapolating similar results from manual driving suggests that drivers may make decisions based on visual quantities such

as visual looming, which by extension suggests that models based on such visual quantities may be preferred to relative velocity- and distance-based models. Furthermore, the finding that visual quantities cannot explain the variability in the reaction time suggests that evidence accumulation models should be preferred to simpler stimulus-response visual angle models. These models were also successful in capturing the drivers' braking control maneuver when combined with a piecewise linear model. Evidence accumulation models can also, in theory, capture the difference between silent and alerted failures, by integrating warning as a source of evidence for the need of an action.

The literature on automated vehicle takeovers suggests that drivers tend to use steering in response to emergency takeovers with long time budgets (Gold et al., 2017). The pattern of steering avoidance follows an anticipatory and compensatory process where drivers provide a large initial steering input followed by a series of smaller corrective inputs. The anticipatory and compensatory process can be captured in the open-loop and closed-loop models.

The literature on models of driver decision-making is notably lighter than that of the steering and braking models. A notable trait of the models reviewed here is the link between visual parameters and driver decision-making (Venkatraman et al., 2016). This link facilitates a connection between models of decision-making, steering, and braking reviewed earlier that are also driven by looming (e.g., Markkula, 2014; Markkula, Boer, et al., 2018).

2.4. Gap Analysis

The prior sections illustrate the need to investigate the impact of factors that are not well studied (e.g., silent failure) and their interaction with other driver-related or environmental factors on takeover performance. In addition, the findings showed that commonalities exist across models that may explain driver behaviors across various aspects of takeovers; however, there has not been an extensively validated modeling framework in this context. As illustrated in Figure 2.1, such a model would have to capture the driver's perception of the need for a takeover, the loop of decisions to steer or brake, and braking and/or steering action execution under various factors. The lack of a thorough understanding of the effect size of driver, system, and environmental factors on takeover performance and models of driver behavior that can capture these impacts, prompt the following research questions:

1. To what degree system's design (silent failure and time budget) influence the takeover time and post-takeover performance during automated vehicle driving?
2. To what degree do contemporary models of manual driving capture the drivers' braking and steering behavior after automated transitions of control?
3. Does integrating individual decision-making, braking, and steering models capture drivers' comprehensive takeover behavior?

The goal of this dissertation is to address these questions over one empirical and three modeling studies. The questions generate four corresponding chapters of my

research including a driving simulation study of automated vehicle takeover behavior, modeling the driver's braking behavior, modeling the driver's steering behavior, and a holistic model of driver takeover behavior. The remainder of this dissertation will discuss the data collection process, provide methodologies, results, and discussions for all studies, and conclude with theoretical and practical implications of these results for transportation safety research and the field of Human Factors.

3. SIMULATOR STUDY OF TAKEOVER BEHAVIOR*

The findings of previous chapter highlight that developing models of takeover requires an investigation of the impacts of various factors (e.g., silent failure) on takeover behavior. The goal of the current chapter is to investigate the degree to which silent failure and time budget influence the takeover time and post-takeover performance during automated vehicle driving. To accomplish this goal, a driving simulator experiment is conducted. Simulator experiment has been selected, as driver behavior models have been successfully developed from the data collected in driving simulation studies (Piccinini et al., 2019; Xue et al., 2018). The driving simulators provide a high level of relative validity and a controllable, cost-effective, and safe environment to investigate the driving performance (Eriksson et al., 2017; Risto & Martens, 2014), while, given the safety-critical nature of automated vehicle takeovers, a naturalist setting may expose the drivers to greater risks.

3.1. Methods

The driving simulator experiment used a 2×2×2 factorial design including a between-subjects factor of takeover request presence (silent vs. alerted) and within-subjects factors of scenario criticality (critical vs. non-critical) and takeover scenario

* Reprinted with permission from "Alambeigi, H., & McDonald, A. D. (2021). A Bayesian Regression Analysis of the Effects of Alert Presence and Scenario Criticality on Automated Vehicle Takeover Performance. Human Factors."

(obstacle reveal and unexpected braking). The takeover scenarios were chosen based on the findings of an automated vehicle crash database analysis that sideswipe crashes during left-side overtakes and rear-end collisions were among the most common automated vehicle crashes (Alambeigi et al., 2019). In both scenarios, participants drove the middle vehicle of a three-vehicle platoon. This setup created the possibility of a collision with the rear of the participant's vehicle, which is the most commonly observed automated vehicle collision type (Biever et al., 2020; Favarò et al., 2017). This study complied with the American Psychological Association Code of Ethics and was approved by the Texas A&M University Institutional Review Board (IRB2018-1362D). Informed consent was obtained from each participant.

3.1.1. Participants

Sixty-four participants (32 male, 32 female) between 19 and 65 years old with the mean age of 41.44 (SD = 15.14) years were recruited to participate in this study. Recruitment was conducted over email from participants who had previously participated in a research study with the Texas A&M Transportation Institute (TTI), as well as students and employees of Texas A&M University. All participants were English-speakers, reported normal or corrected-to-normal visual acuity and normal color vision, held a valid driver's license, reported driving experience of at least 1.5 years (M = 25.36, SD=16.26), were not taking any medications that may have affected the operation of a moving vehicle, had not previously participated in an experiment involving automated vehicles, and had

no prior experience driving automation-enabled vehicles (e.g., Tesla autopilot). Participants were compensated $50 for their participation.

3.1.2. Apparatus

The study was conducted in the TTI driving simulation lab. The lab consists of a Realtime Technologies Inc. (RTI) quarter-cab driving simulator with three screens that provide 165° horizontal and 35° vertical fields of view, a speaker system to provide ambient roadway noise, and a physiological and eye-tracking data collection suite. The simulator collects continuous steering wheel position, accelerator and brake pedal positions, velocity, time to lane crossing, time headway to an upstream object, and lane position at a 60 Hz sampling rate. The glance behavior and physiological data collection suite consisted of a dashboard-mounted FOVIO eye-tracking system (Seeing Machines, Canberra, Australia), a Zephyr BioHarness 3.0 (Zephyr Technology, Annapolis, MD, USA), and a Shimmer3 wireless Galvanic Skin Response (GSR) sensor (Shimmer, Dublin, Ireland). The glance behavior and physiological data have been analyzed in a different study to predict the driver error following the failures using machine learning algorithms (Alambeigi, McDonald, Manser, et al., 2022; Alambeigi, McDonald, Shipp, et al., 2022). The complete lab setup including the driver seat and the three forward view screens is illustrated in Figure 3.1. The eye-tracking system is positioned on top of the dashboard.

Figure 3.1 The driving simulation lab setup. Reprinted with permission from Alambeigi & McDonald (2021b).

3.1.3. Automation

The simulator's automated driving system provided lateral and longitudinal control on highway roads and could be activated with a button on a touch screen display located to the right of the steering wheel. Figure 3.2 shows the center console with the automation touch screen including an activation/deactivation button. When the system encountered a failure or an operational limit, the vehicle's lateral and longitudinal control was disabled. The driver could manually deactivate the automation either by braking or pressing the activation button on the touch screen display. The status of the automation, if engaged, was indicated by two green icons (iconic lane markings and steering wheel) in the instrument cluster. Figure 3.3 illustrates the instrument cluster with a graphical representation of the system state. The left and right figures show the cluster when the automation is off and on, respectively.

Figure 3.2 The center console with the automation activation/deactivation screen. Reprinted with permission from Alambeigi & McDonald (2021b).

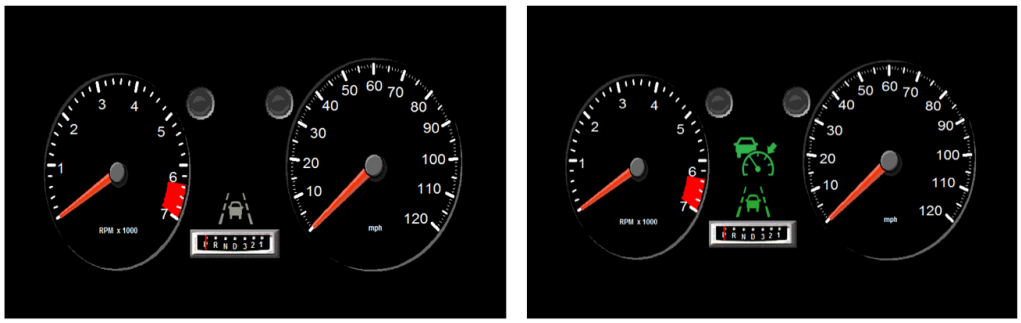

Figure 3.3 Instrument cluster when the automation is off (left) and is on (right). Reprinted with permission from Alambeigi & McDonald (2021b).

3.1.4. Study Process

Participants were consented and then completed a pre-experiment questionnaire. This questionnaire consisted of demographic and technology acceptance (Ghazizadeh et al., 2012) questions. Participants then received information (through a document) about the simulator and the automated system's capabilities and limitations. The information

indicated that the automation was not capable of driving on all types of roadways, that there were some driving situations where the automation reached an operational limit, and that the automation would transition control back to the driver when it hit an operational limit. In addition, participants were instructed to keep at least one hand on the steering wheel while the automation was enabled. After receiving training on the automation, the participants toured the simulator. The tour consisted of a demonstration of the automation controls by the experimenter while the participant sat in the driver's seat of the simulator. When the participant indicated they were comfortable with the controls, they completed two practice drives and four experimental drives. Finally, the participant was asked to complete a post-experiment questionnaire including simulator realism and technology acceptance questions.

3.1.5. Simulator Scenario

The simulator scenario consisted of two practice (manual and automated) and four experimental drives separated by two-minute breaks. Each drive took place on a four-lane straight highway with two lanes in each direction and a posted speed limit of 65 mph (104.6 kph). The drives had natural surroundings (woods, farms, buildings) and ambient traffic of approximately 10 cars per mile (approximately 6 cars per km) on the oncoming traffic lanes (representing the level of service A in traffic flow categories; Margiotta & Washburn, 2017). During all six drives, the participants drove in a three-vehicle platoon with a 1 s time headway in which the speed of all vehicles where kept constant at 65 mph. In the manual practice drive, the participants were instructed to maintain the 1 s time

headway and the 65-mph constant speed, while in the automated drives, the system was capable of maintaining the time headway and the constant speed.

The manual and automated practice drives were approximately 5 minutes long. The goals of these drives were to screen for simulator sickness and allow participants to familiarize themselves with the simulator controls. In the drives, participants practiced controlling the simulator, driving in the platoon, and engaging and disengaging the automation. In the automated practice drive, the lead vehicle in the platoon exited the highway approximately 5 miles into the drive and a visual and auditory takeover request was issued to the driver. Participants were permitted to repeat either of the practice drives until they felt comfortable driving and operating the automation (3 participants requested to repeat the drives, post hoc analyses suggested that there were no substantial differences between the performance of these participants and the others).

The four experimental drives were conducted on a 10 mi (16 km) section of the highway. After approximately 7 miles of driving, an event that required a takeover happened. The event differed by the takeover scenario (see Figure 3.4). In both scenarios, the distance headway to the lead vehicle at the event onset was approximately 29 m which corresponded to the 1 s time headway with 65 mph. In the obstacle reveal scenario, the lead vehicle suddenly changed lanes to avoid an obstacle in the participant's lane. The obstacle was a stationary vehicle with brake lights and the participant had 5 or 10 s to respond at the time of the failure depending on the scenario criticality. In the braking scenario, the lead vehicle suddenly braked due to approaching a construction zone on the road shoulder while the participant's vehicle maintained speed. In this event, the criticality

of the scenario was manipulated using the deceleration rates of the lead vehicle where the constant deceleration rate of 2 m/s2 represented the non-critical and 5 m/s2 represented the critical scenario. Figure 3.4 shows both takeover scenarios from the driver's view. The left figure represents the unexpected braking scenario with the construction zone on the road shoulder and the right figure shows the obstacle reveal scenario after the lead vehicle changed lanes, exposing the stalled vehicle in the driver's lane.

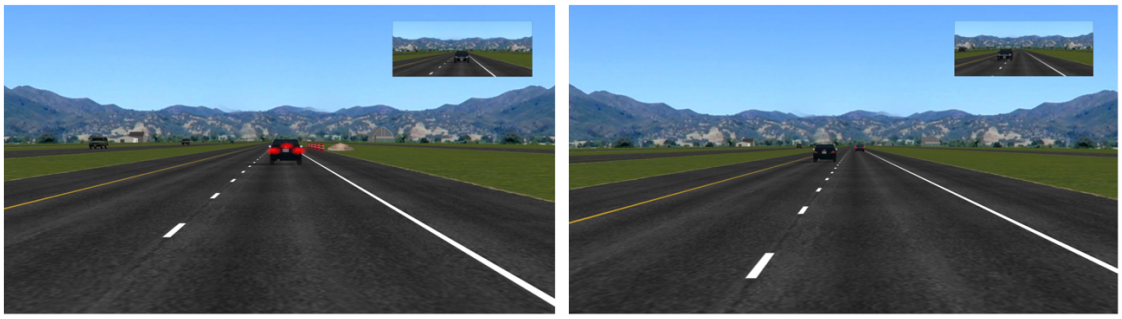

Figure 3.4 Takeover scenarios from the driver's view with left and right figures representing the unexpected braking and obstacle reveal scenarios, respectively. Reprinted with permission from Alambeigi & McDonald (2021b).

3.1.6. Dependent Variables

Regardless of the scenario and criticality, the participants in the silent failure group did not receive any indication of the automation failure. The participants in the alerted group received an auditory and visual alert. The auditory alert consisted of a loud beep, and the visual alert consisted of a change of color on the instrument cluster and an automation activation screen (as shown in Figure 3.3). All participants in both groups drove all four combinations of scenario criticality and scenario type. The order of these drives was counterbalanced across participants using a Latin square technique (Allen,

2018). All 64 drivers completed the four experimental drives producing 256 completed driving datasets.

The takeover performance was assessed with takeover time, crash frequency, minimum TTC, and maximum longitudinal and lateral accelerations. These metrics were selected because they were direct or indirect indicators of safety (Driver Metrics Performance Behaviors and States Committee, 2015). In particular, minimum TTC is an established surrogate safety metric for longitudinal vehicle control that has been used in several prior studies to evaluate the effects of the criticality of the scenario and other factors on post-takeover control (McDonald et al., 2019). Table 3.1 provides a list of the dependent variables used to analyze the takeover performance in the study along with a description of their calculation.

Table 3.1 Overview of the Dependent Measures Used to Analyze the Takeover Performance. Reprinted With Permission From Alambeigi & McDonald (2021b).

Dependent Variable	Unit	Description
Takeover time	[s]	Time elapsed between the event onset and start of maneuver greater than a threshold (2° steering wheel angle and 10% brake pedal actuation)
Minimum time to collision	[s]	Minimum time to collision to the lead vehicle/obstacle between the takeover time and 35 s after the event onset
Maximum longitudinal accelerations	[m/s²]	Maximum longitudinal acceleration between the takeover time and 35 s after the braking event onset
Maximum lateral accelerations	[m/s²]	Maximum lateral acceleration between the takeover time and 35 s after the obstacle-reveal event onset
Crash frequency	[n]	Frequency of crashes

The minimum TTC and maximum accelerations were calculated between the event onset and 35 s after the event or when the participant's vehicle exited the initial lane. The threshold of 35 s was chosen based on findings in the literature that drivers need as much as 35-40 s to stabilize the control of the vehicle after a transition (Merat et al., 2014). The takeover time was defined as the time between the event onset and the start of the maneuver. The thresholds for the start of the maneuver were 2 degrees for steering wheel angle rotation and 10% for brake pedal position and were selected based on a review of the literature (McDonald et al., 2019).

3.1.7. Data Analysis

Separate statistical analyses were conducted for the takeover scenarios (obstacle reveal and unexpected braking) as initial observations suggested that the scenarios produced qualitatively different responses. The count data from crashes were analyzed with a two-sided Fisher's exact test. Fisher's exact test was used as it can deal with small sample sizes (Bower, 2003). The continuous dependent measures were analyzed with separate Bayesian multilevel regression models fitted using the "brms" package in R 4.0.0 (Bürkner, 2018). In contrast to the frequentist null-hypothesis testing approach which relies on the mean or median values for model fitting, the Bayesian approach focuses on the distribution of response variables for a given parameter, which may be more informative for safety (Eriksson & Stanton, 2017b). The Bayesian multilevel (i.e., mixed-effects) model applied in this study incorporated both population-level and group-level effects (also referred to as fixed and random effects in frequentist vocabulary; Bürkner,

2018; Nalborczyk, Batailler, Lœvenbruck, Vilain, & Bürkner, 2019). The population-level effects were assumed to be constant across observations and in this study included the scenario criticality, alert type, and their interaction. The group-level effects accounted for the variability of the individual-specific estimates that were associated with the repeated measures from the same participant. The order of the scenario was not included in the analysis as it was accounted for with the counterbalanced design and post hoc graphical analysis suggested that there were no substantial differences in dependent measures associated with the order. The models for maximum accelerations were fit in one direction for each scenario type—longitudinal for the braking scenario and lateral for the obstacle reveal scenario—because most driver responses included only one evasive maneuver (i.e., steering or braking).

The models were estimated using the Markov chain Monte Carlo (MCMC) algorithm in the brms package (Bürkner, 2017). Posterior distributions were estimated using 4 MCMC chains and 2,000 samples per chain. The first 1,000 samples were used to tune the parameters of the sampling algorithm and were not included in the analysis. For each model, the mean, standard deviation, lower and upper bounds of 95% credible interval of the posterior distribution were estimated from the remaining 4,000 samples (1,000 per chain). The credible interval can be understood as the region where there is a 95% probability that the true mean falls within the lower and upper bounds (Kruschke & Liddell, 2018). All models were fit with uninformative priors. The selection of uninformative priors was guided by prior analyses of automated vehicle studies (DinparastDjadid et al., 2019; Pipkorn et al., 2021). In addition, this decision allowed for

more direct comparisons with the prior Ordinary Least Squares linear regression analyses (Elster & Wübbeler, 2015) of silent failures and is consistent with the conflicting findings observed across previous studies.

3.2. Results

3.2.1. Takeover Time

Figure 3.5 shows the takeover time data and boxplots for the obstacle reveal and unexpected braking events, critical and non-critical scenarios, and alerted and silent failures. The results of the Bayesian regressions are summarized in Table 3.2 including the mean (estimate), standard deviation (estimated error), and the two-sided 95% credible interval for the fitted posterior distribution. Each row of the table illustrates the estimated change in takeover time attributable to the level of a factor compared to its alternative, e.g., the scenario criticality coefficient (β_C) indicates the estimated change in takeover time attributable to non-critical scenarios compared to critical scenarios. The interaction term (β_{CA}) indicates the estimated change in takeover time when the scenario is non-critical given the alert type.

In the unexpected braking scenario, the estimate of the scenario criticality predicts a mean increase of 0.76 s for the non-critical scenario, and the credible interval shows a 95% probability that the non-critical scenario increases the takeover time between 0.40 and 1.12 s. The alert type regression coefficient estimates a mean takeover time increase of 0.16 s with a credible interval from -0.17 to 0.50 s for silent failures.

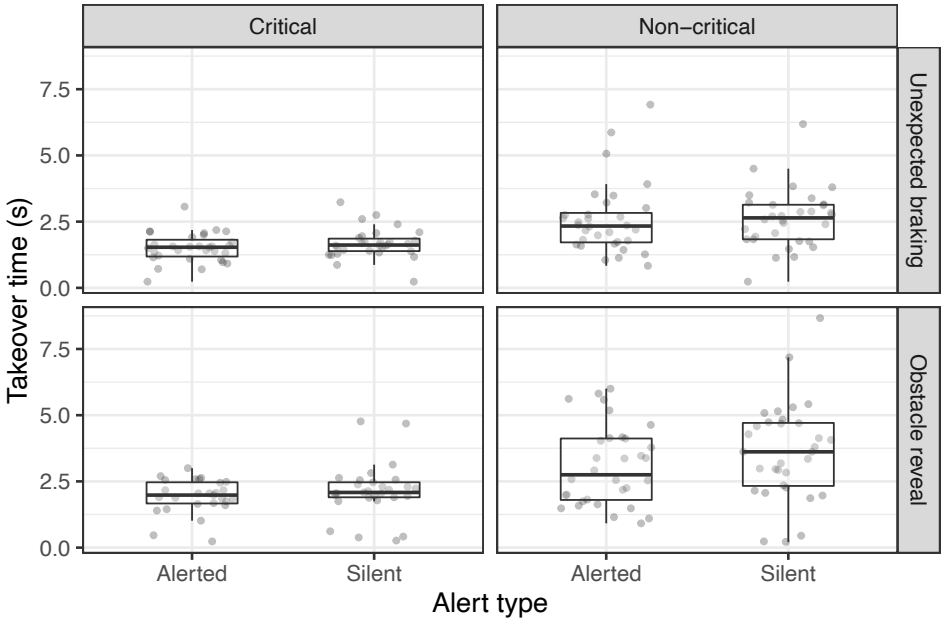

Figure 3.5 Boxplot of takeover time under criticality of the event and alert type for the unexpected braking (top) and obstacle reveal (bottom) events. Reprinted with permission from Alambeigi & McDonald (2021b).

Figure 3.6 shows the posterior density of regression coefficient of silent failure and the interaction between non-critical event and silent failure on takeover time across the two events. The circle represents the estimated mean takeover time and the dark and light shaded areas indicate the estimated takeover times greater than and lower than zero, respectively. The posterior density of the alert type shows silent failures increase the takeover time for 84% of participants (see Figure 3.6 top left plot). Similarly, the estimated posterior distribution of the interaction between alert type and scenario criticality has a mean of 0.19 s and a credible interval from -0.37 to 0.63. Figure 3.6 (the top right plot) shows that there is a 70% probability that the takeover time increases between critical and non-critical events for silent failures.

In the obstacle reveal scenario, the scenario criticality regression coefficient predicts a mean increase of 1.05 s for the non-critical scenario. The credible interval shows a 95% probability that this mean value lies within the 0.40 to 1.72 s interval. The estimate of the alert type shows a mean of 0.19 s increase in takeover time with the range from -0.45 to 0.84 s credible interval as a result of the silent failure. Figure 3.6 shows a 72% probability of an increase in takeover time with silent failure. Similarly, the interaction between alert type and scenario criticality 0.41 s increases the mean takeover time with a credible interval that ranges from -0.53 to 1.33. Figure 3.6 (the bottom right plot) shows that there is an 82% probability that the takeover time increases when the scenario criticality changes from critical to non-critical and when the alert is not present.

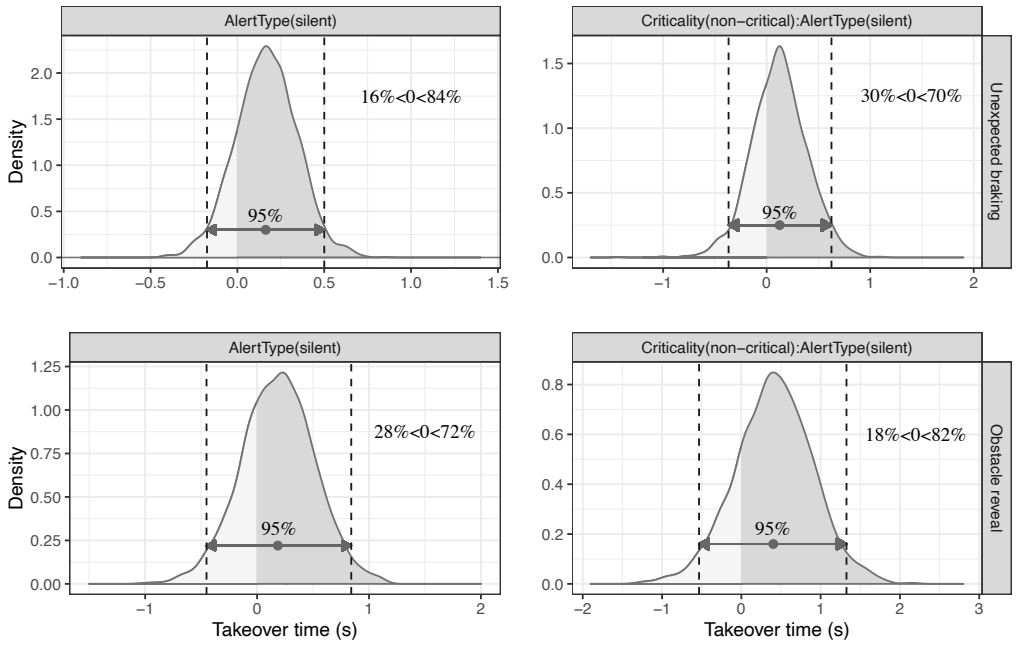

Figure 3.6 Posterior density of regression coefficient of silent failure and the interaction effects on takeover time across the unexpected braking (top) and obstacle reveal (bottom) events. Reprinted with permission from Alambeigi & McDonald (2021b).

Table 3.2 Summary of the Posterior Coefficients for the Takeover Time Across the Obstacle Reveal and Unexpected Braking Events. Reprinted With Permission From Alambeigi & McDonald (2021b).

Scenario	Model	Parameter	Independent measure (effect)	Estimate (s)	Est. Error	Lower 95%-CI	Upper 95%-CI
Unexpected braking	Population-level	$\boldsymbol{\beta_0}$	**Intercept**	**1.50**	**0.12**	**1.26**	**1.74**
		$\boldsymbol{\beta_C}$	**Scenario criticality (non-critical)**	**0.76**	**0.18**	**0.40**	**1.12**
		β_A	Alert type (silent)	0.16	0.17	-0.17	0.50
		β_{CA}	Scenario criticality (non-critical) x alert type (silent)	0.19	0.25	-0.37	0.63
	Group-level	σ_s	sd (Intercept)	0.25	0.12	0.02	0.48
	Family-specific	σ_e	error	0.53	0.09	0.37	0.71
Obstacle reveal	Population-level	$\boldsymbol{\beta_0}$	**Intercept**	**1.95**	**0.23**	**1.48**	**2.39**
		$\boldsymbol{\beta_C}$	**Scenario criticality (non-critical)**	**1.05**	**0.33**	**0.40**	**1.72**
		β_A	Alert type (silent)	0.19	0.32	-0.45	0.84
		β_{CA}	Scenario criticality (non-critical) x alert type (silent)	0.41	0.47	-0.53	1.33
	Group-level	σ_s	sd (Intercept)	0.23	0.16	0.01	0.60
	Family-specific	σ_e	error	1.15	0.13	0.87	1.40

Note. Text in bold refers to the estimated credible intervals at population-level that do not include 0. σ_s at the group-level effect denotes the standard deviation of the individuals varying intercept and σ_e at the family-specific effect indicates the standard deviation of the residuals.

3.2.2. Post-takeover Control

3.2.2.1. Crash Frequency

From the 256 drives, 11 drives resulted in crashes (Table 3.3). The majority of crashes (8/11) occurred in the obstacle reveal scenario. The crashes included rear-end collisions (2), a side-swipe with the trailing vehicle while executing a lane change (1), a rear-end collision with the following vehicle after the execution of lane change (6), and single-car run off-road incidents to the right and left (2). No crashes occurred in the non-critical scenarios. Fisher's exact test showed a significant difference between the critical and non-critical scenarios in the obstacle reveal event (p<0.001). The effect of the alert type was not significant.

Table 3.3 Number of Crashes Occurred During the Experiment by Condition. Reprinted With Permission From Alambeigi & McDonald (2021b).

Takeover request type	Unexpected braking		Obstacle avoidance	
	Critical	Non-critical	Critical	Non-critical
Silent	2	0	3	0
Alerted	1	0	5	0

3.2.2.2. Time to Collision

Figure 3.7 shows the minimum TTC following the obstacle reveal and unexpected braking events for critical and non-critical scenarios and under alerted and silent failures overlaid on a boxplot. Table 3.4 contains the posterior summaries of coefficients including the mean, standard deviation, and the two-sided 95% credible interval for minimum TTC. In the unexpected braking scenario, the scenario criticality coefficient indicates a mean difference of 1.49 s with 95% most credible values between 0.89 and 2.11 s in minimum

TTC associated with non-critical scenario compared to critical. The results show a decrease of 0.45 s TTC for silent failures with a 95% credible interval of -1.11 – 0.18 s. Figure 3.8 shows the posterior density of regression coefficient of silent failure and the interaction between non-critical event and silent failure on minimum TTC in the unexpected braking (top) and the obstacle reveal (bottom) scenarios. The circle represents the estimated mean of minimum TTC and the dark and light shaded areas indicate the estimated minimum TTC greater than and lower than zero, respectively. This figure shows that 92% of drivers would be expected to have a lower minimum post-takeover TTC in the silent failure case. The interaction between silent failure and non-critical scenario indicates the estimated mean of 0.56 s with a 95% credible interval of -0.15 and 1.29 s.

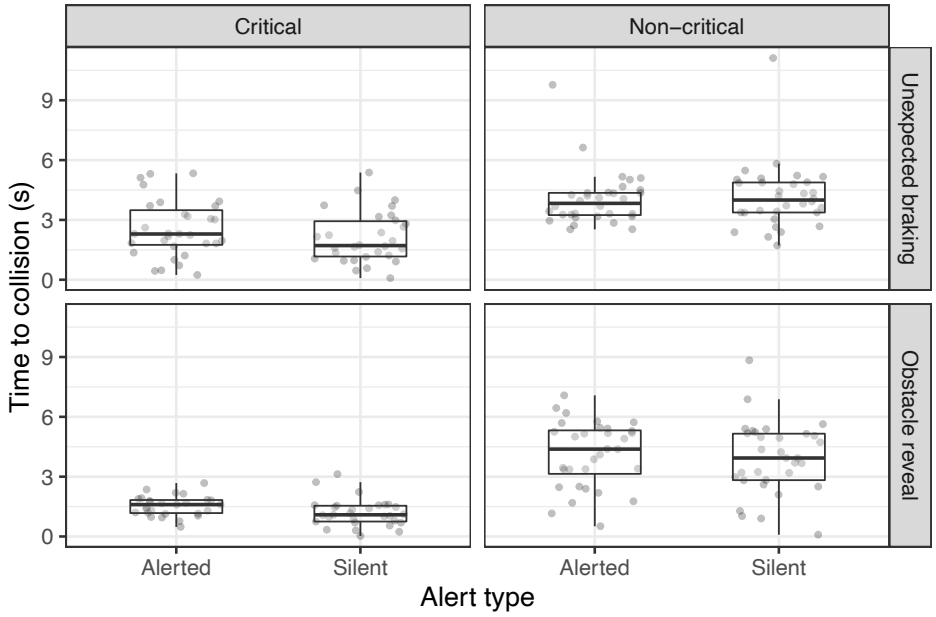

Figure 3.7 Boxplot of minimum TTC under criticality of the event and alert type for obstacle reveal and unexpected braking events. Reprinted with permission from Alambeigi & McDonald (2021b).

Table 3.4 Summary of the Posterior Coefficients for the Minimum TTC Across the Obstacle Reveal and Unexpected Braking Events. Reprinted With Permission From Alambeigi & McDonald (2021b).

Scenario	Model	Parameter	Independent measure (effect)	Estimate	Est. Error	Lower 95%-CI	Upper 95%-CI
Unexpected braking	Population-level	$\boldsymbol{\beta_0}$	**Intercept**	**2.49**	**0.24**	**2.02**	**2.96**
		$\boldsymbol{\beta_C}$	**Scenario criticality (non-critical)**	**1.49**	**0.31**	**0.89**	**2.11**
		β_A	Alert type (silent)	-0.45	0.33	-1.11	0.18
		β_{CA}	Scenario criticality (non-critical) x alert type (silent)	0.56	0.36	-0.15	1.29
	Group-level	σ_s	sd (Intercept)	0.72	0.17	0.37	1.03
	Family-specific	σ_e	error	0.80	0.12	0.55	1.10
Obstacle reveal	Population-level	$\boldsymbol{\beta_0}$	**Intercept**	**1.51**	**0.23**	**1.05**	**1.95**
		$\boldsymbol{\beta_C}$	**Scenario criticality (non-critical)**	**2.73**	**0.33**	**2.10**	**3.35**
		β_A	Alert type (silent)	-0.35	0.31	-0.95	0.26
		β_{CA}	Scenario criticality (non-critical) x alert type (silent)	0.05	0.45	-0.82	0.92
	Group-level	σ_s	sd (Intercept)	0.33	0.20	0.02	0.75
	Family-specific	σ_e	error	1.08	0.14	0.80	1.34

Note. Text in bold refers to the estimated credible intervals at population-level that do not include 0. σ_s at the group-level effect denotes the standard deviation of the individuals varying intercept and σ_e at the family-specific effect indicates the standard deviation of the residuals.

In the obstacle reveal scenario, the estimate of the scenario criticality predicts a mean increase of 2.73 s for the non-critical event with a 95% probability that the mean of

minimum TTC falls between 2.10 to 3.35 s. The alert type regression coefficient shows a mean decrease of 0.35 s in minimum TTC as a result of the silent failure with a 95% credible interval of -0.95 to 0.26 s. Similar to the unexpected braking event, analysis of the posterior density on the alert type shows that with 88% probability the silent failure decreases the minimum TTC (see Figure 3.8). Similarly, the interaction between alert type and scenario criticality reveals a 0.05 s increase in the mean takeover time with a credible interval that ranges from -0.82 to 0.92. Posterior distribution of this parameter (see the bottom right plot in Figure 3.8) shows that there is a 55% probability that the minimum TTC increases when the scenario criticality changes from critical to non-critical and alert is not present.

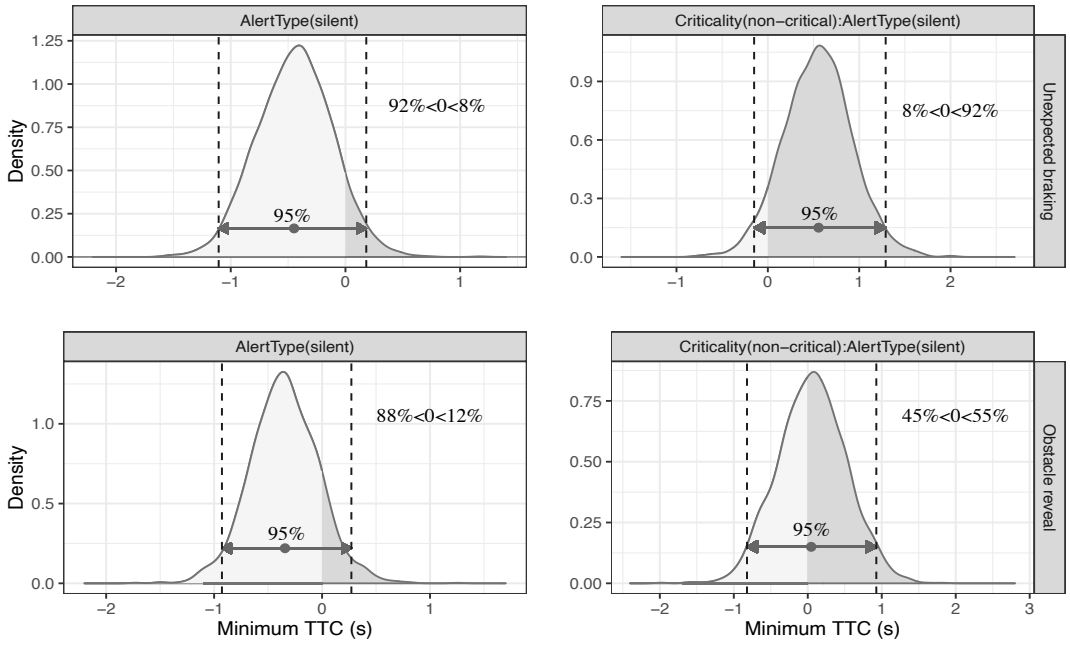

Figure 3.8 Posterior density of regression coefficient of silent failure and the interaction effects on minimum TTC in the unexpected braking (top) and obstacle reveal (bottom) events. Reprinted with permission from Alambeigi & McDonald (2021b).

3.2.2.3. Longitudinal and Lateral Acceleration

Figure 3.9 shows the boxplot of maximum longitudinal acceleration following the unexpected braking event for critical and non-critical scenarios and under alerted and silent failures. The posterior summaries of coefficients including the mean, standard deviation, and the two-sided 95% credible interval for maximum longitudinal acceleration corresponding to the unexpected braking scenario is presented in Table 3.5. Note that lower (i.e., more negative) values of acceleration imply more aggressive braking maneuver while higher (i.e., more positive) values suggest more gradual braking. At the population level, the parameter coefficient of scenario criticality indicates a mean change in maximum longitudinal acceleration of 2.7 m/s^2 (95% credible interval 1.92-3.48 m/s^2) for the non-critical compared to the critical event. The alert type coefficient predicts 0.70 m/s^2 higher longitudinal acceleration intensity for silent failure.

Although the 95% credible interval includes zero, Figure 3.10 shows the posterior density of regression coefficient of silent failure and the interaction between non-critical event and silent failure on maximum longitudinal acceleration in the unexpected braking scenario. The circle represents the estimated mean of maximum longitudinal acceleration and the dark and light shaded areas indicate the estimated maximum longitudinal accelerations greater than and lower than zero, respectively. This figure shows that 91% of the posterior distribution for this parameter is below zero meaning an increase in braking. The β_{CA} indicates the estimated mean of 0.59 m/s^2 for the interaction between silent failure and non-critical scenario with a 95% credible interval of -0.52 and 1.68 s.

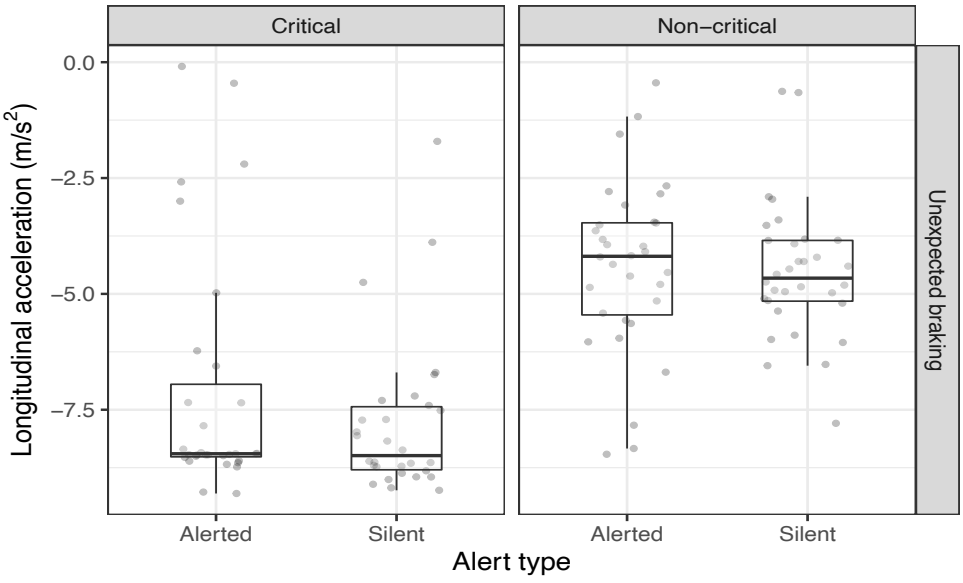

Figure 3.9 Boxplot of maximum longitudinal acceleration under criticality of the event and alert type for unexpected braking event. Reprinted with permission from Alambeigi & McDonald (2021b).

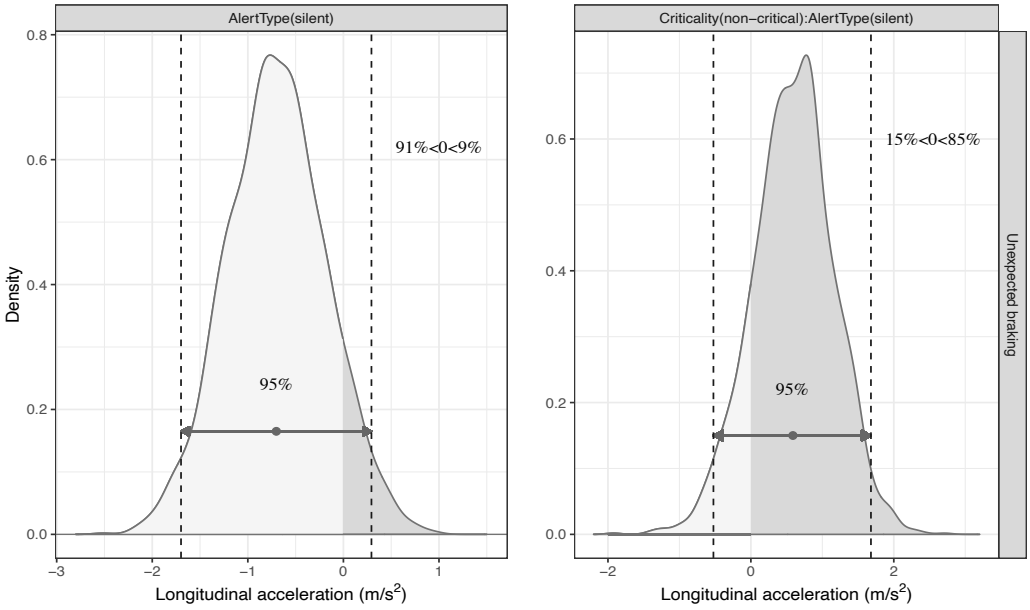

Figure 3.10 Posterior density of regression coefficient of silent failure and the interaction effects on maximum longitudinal acceleration in the unexpected braking event. Reprinted with permission from Alambeigi & McDonald (2021b).

Table 3.5 Summary of the Posterior Coefficients for the Maximum Longitudinal Acceleration in Unexpected Braking Event. Reprinted With Permission From Alambeigi & McDonald (2021b).

Scenario	Model	Parameter	Independent measure (effect)	Estimate	Est. Error	Lower 95%-CI	Upper 95%-CI
Unexpected braking	Population-level	$\boldsymbol{\beta_0}$	**Intercept**	**-7.11**	**0.35**	**-7.79**	**-6.43**
		$\boldsymbol{\beta_C}$	**Scenario criticality (non-critical)**	**2.70**	**0.40**	**1.92**	**3.48**
		β_A	Alert type (silent)	-0.70	0.51	-1.70	0.29
		β_{CA}	Scenario criticality (non-critical) x alert type (silent)	0.59	0.56	-0.52	1.68
	Group-level	σ_s	sd (Intercept)	1.16	0.25	0.61	1.63
	Family-specific	σ_e	error	1.59	0.16	1.32	1.95

Note. Text in bold refers to the estimated credible intervals at population-level that do not include 0. σ_s at the group-level effect denotes the standard deviation of the individuals varying intercept and σ_e at the family-specific effect indicates the standard deviation of the residuals.

Figure 3.11 shows the boxplot of maximum lateral acceleration following the obstacle reveal event across scenario criticality and alert type. The posterior summary of coefficients for this independent measure is shown in Table 3.6. The estimate of the scenario criticality predicts a mean change of 0.89 m/s^2 with the 95% credible interval of 0.50 to 1.28 m/s^2 for the non-critical compared to critical event. The alert type regression coefficient shows 0.11 m/s^2 more severe maximum lateral acceleration as a result of the silent failure. The credible interval includes a range from -0.53 to 0.34 m/s^2. Similar to the unexpected braking event, analysis of the posterior density on the alert type shows that with a 70% probability the silent failure increases the severity of the lateral acceleration

(see Figure 3.12). Similarly, the interaction between alert type and scenario criticality shows a 0.08 m/s^2 increase in the mean lateral acceleration with a credible interval that ranges from -0.67 to 0.46. Figure 3.12 (right plot) shows that there is 85% probability that the maximum lateral acceleration decreases with a non-critical silent failure.

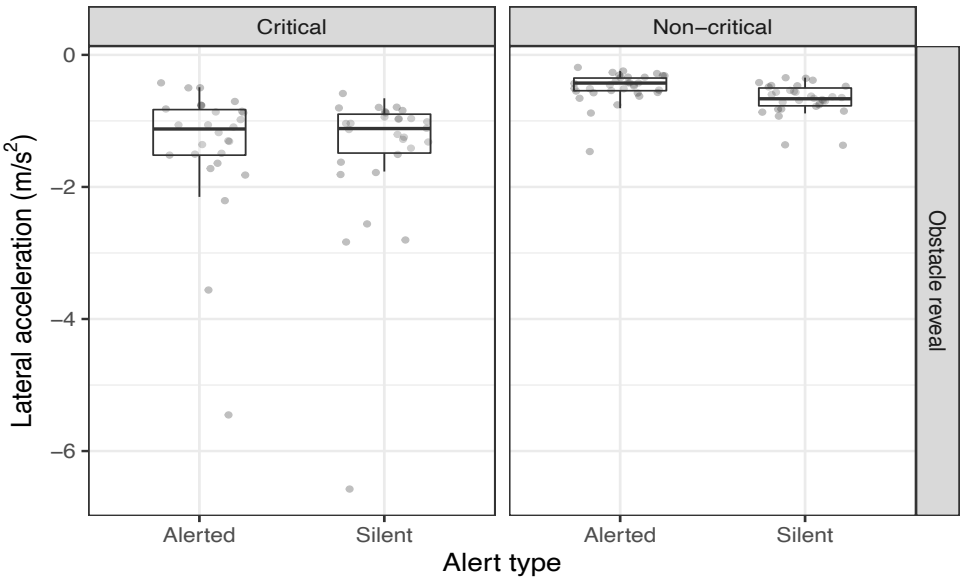

Figure 3.11 Boxplot of maximum lateral acceleration under criticality of the event and alert type for obstacle reveal event. Reprinted with permission from Alambeigi & McDonald (2021b).

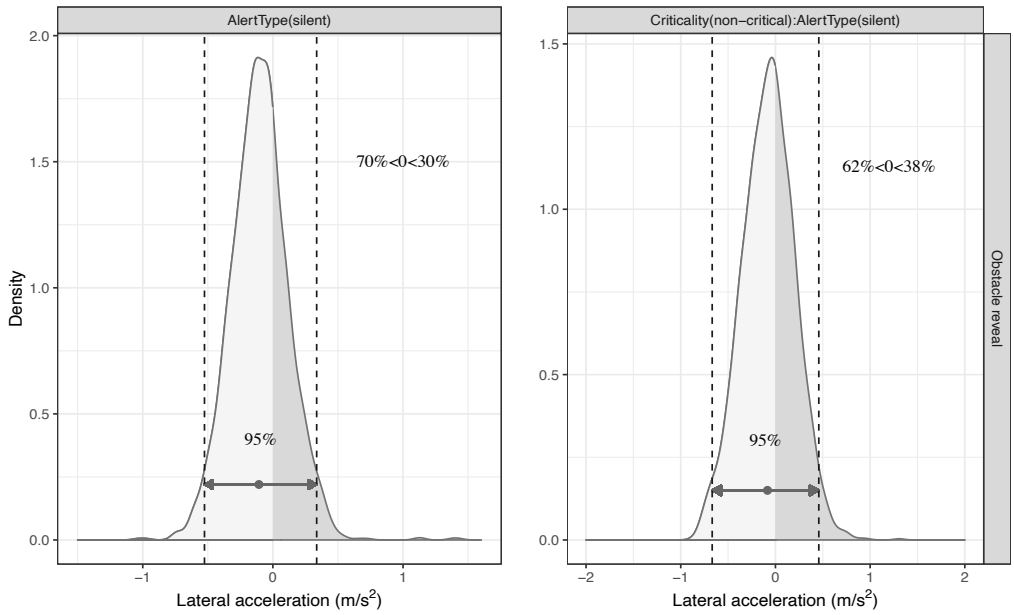

Figure 3.12 Posterior density of regression coefficient of silent failure and the interaction effects on maximum lateral acceleration in the obstacle reveal event. Reprinted with permission from Alambeigi & McDonald (2021b).

Table 3.6 Summary of the Posterior Coefficients for the Maximum Lateral Acceleration in the Obstacle Reveal Event. Reprinted With Permission From Alambeigi & McDonald (2021b).

Scenario	Model	Parameter	Independent measure (effect)	Estimate	Est. Error	Lower 95%-CI	Upper 95%-CI
Obstacle reveal	Population-level	$\boldsymbol{\beta_0}$	**Intercept**	**-1.37**	**0.15**	**-1.67**	**-1.07**
		$\boldsymbol{\beta_C}$	**Scenario criticality (non-critical)**	**0.89**	**0.20**	**0.50**	**1.28**
		β_A	Alert type (silent)	-0.11	0.22	-0.53	0.34
		β_{CA}	Scenario criticality (non-critical) x alert type (silent)	-0.08	0.28	-0.67	0.46
	Group-level	σ_s	sd (Intercept)	0.22	0.13	0.01	0.46
	Family-specific	σ_e	error	0.74	0.06	0.63	0.86

Note. Text in bold refers to the estimated credible intervals at population-level that do not include 0. σ_s at the group-level effect denotes the standard deviation of the individuals varying intercept and σ_e at the family-specific effect indicates the standard deviation of the residuals.

3.3. Discussion

The Bayesian regression modeling analyses show a consistent and substantial effect of scenario criticality on takeover time, crashes, and post-takeover control metrics. The effect of silent failures was comparably less across all measures, although the regressions predicted that most drivers would have increased takeover times (84% for unexpected braking and 72% for obstacle reveal), lower post-takeover TTC (92% and 88%), and higher post-takeover maximum acceleration (91% and 70%). While the predicted average impact of silent failures on takeover time (0.16 s for unexpected braking and 0.19 s for obstacle reveal) may have a minimal practical impact, the effects on minimum TTC (-0.45 s and -0.35 s) and maximum acceleration (-0.7 m/s^2 and -0.1 m/s^2) could be a safety concern. Although it is challenging to ground the magnitude of this change in actual avoided crashes, recent counterfactual analyses have shown that even a 0.5 m/s^2 change in maximum acceleration could increase crash likelihood (Bärgman et al., 2017). Collectively, these results partially confirm our first hypothesis and suggest that silent failures could result in more aggressive post-takeover maneuvers ultimately greater risk of crashes and near-crashes. The effect of the scenario criticality and alert type interaction on takeover time was smaller than that of silent failure in the unexpected braking scenario; however, this interaction effect was larger than the effect of silent failures in the obstacle reveal scenario. The estimated mean takeover time shows that the impact of alert depends on scenario criticality, specifically in a non-critical silent failure, drivers use up to 0.6 s additional time to take over compared to the drivers in non-critical alerted failures. However, the difference in mean response times for drivers in critical

silent and alerted failures was less—drivers required approximately 0.2 s additional time to takeover in critical silent condition compared to the alerted. The effect of silent failures on post-takeover control was higher for critical scenarios compared to non-critical. Overall, these results also partially confirm our second hypothesis and suggest that longer time budgets may alleviate the impact of silent failure on takeover performance.

The findings on scenario criticality are aligned with those of prior studies investigating the impact of deceleration rates and time budget on takeover performance (Bianchi Piccinini et al., 2020; Gold et al., 2017; Mole et al., 2020; Zhang et al., 2019). The predicted increase in takeover time (0.76 s) for the unexpected braking scenario (5 m/s^2 vs. 2 m/s^2) matches the findings of Bianchi Piccinini et al. (Bianchi Piccinini et al., 2020) who observed 0.80 s increase in braking reaction time for lower (2.5 m/s^2) compared to higher (4.5 m/s^2) deceleration rates. The takeover time increase for the obstacle reveal scenario is similar to the 1.35 s calculated in the meta-analysis in Zhang et al. (2019) for larger time budgets (>15 s) compared to smaller time budgets (<8 s). In addition, the 1.05 s increase in takeover time for the non-critical obstacle reveal scenario compared to the critical approximately aligns with the results of the meta-analyses in Gold et al. (2017) and McDonald et al. (2019) who found a 1.65 s and 1.35 s increase in takeover time for 5 s increase in time budget, respectively. The predicted increase in TTC (0.55 s) for the obstacle reveal scenario also follows the findings of the meta-analysis by Gold et al. (2017) who attributed an impact of 0.50 s increase in TTC for each second increase in takeover time budget. Contrary to the findings in Gold et. al (2017), the time budget in this study showed a significant impact on crash risk. The predicted impact of time budget

on longitudinal acceleration in the unexpected braking (2.7 m/s^2 less intense acceleration in non-critical) and lateral acceleration in the obstacle reveal scenario (0.9 m/s^2 less intense acceleration in non-critical) are novel findings of this study.

The predicted 0.16 s and 0.19 s increase in takeover time associated with silent failures is consistent with the results of Blommer et al. (Blommer et al., 2017) who observed a 0.10 s increase in mean takeover time attributable to silent failures. This predicted increase is notably less than the meta-analysis in Zhang et al. (2019) which attributed an average increase of 0.58 s to silent failures. This difference is likely associated with the fact that the meta-analytic model averaged over multiple other factors known to influence takeover time including the alert modality, surrounding environment, and driver impairment (McDonald et al., 2019). The findings on post-takeover control are novel and show that silent failures are associated with more extreme post-takeover maneuvers. The regression models suggest that on average a 0.5 s reduction (and up to a 2.5 s reduction) in minimum TTC is associated with silent failures. Moreover, silent failure resulted in higher post-takeover longitudinal and lateral accelerations. The more intense maximum accelerations after silent failures represent an abrupt and aggressive braking or lane change maneuver. The interaction effects in the fitted models suggest that during non-critical silent failures it takes longer for drivers to accumulate sufficient visual looming evidence of the need to initiate an avoidance maneuver which makes their responses different from drivers that receive an alert. The effect of the interaction was less prominent for the unexpected braking compared to the obstacle reveal scenario. One possible reason might be that the unexpected appearance of the lead vehicle's brake light

(after a prolonged period of non-braking) may have accelerated the accumulation of non-looming evidence and led to the initiation of braking.

Although the findings are consistent with those of prior work, the findings showed a less-than-expected decremental effect of silent failures on takeover performance. There might be several possible explanations associated with that. First, the experiment represented a "best-case scenario", in which, the drivers' cognitive state (e.g., drowsiness, emotion, distraction) was not taken into account. For example, the drivers did not perform any non-driving tasks (e.g., text reading) while driving, which could have softened the negative impacts associated with them. In line with multiple resource theory, it should be noted that such conditions might have a selective impact on a single component of a takeover process rather than all, depending on the required processing resources (Wickens, 1984; Zeeb et al., 2016). In addition, drivers were, specifically, instructed to keep their hands on the steering wheel and informed that it was their responsibility to monitor the automation and the driving environment. While there is some evidence that hands-on-wheel requirements alone do not substantially affect takeover performance (Pipkorn et al., 2021; Victor et al., 2018), our instructions may have led the drivers to be more engaged than might otherwise be expected, especially for longer drives (Merat et al., 2014). Second, the takeover event in this study occurred after approximately 6 minutes of automated driving, which may have been insufficient to induce significant vigilance decrements. For example, Feldhütter, Gold, Schneider, and Bengler (2017) observed takeover performance decrements after 20 minutes but not after 5 minutes, and in a comparison of 10-minute increments from 10 to 40 minutes, Greenlee, DeLucia, and

Newton (2018) observed the largest performance decrement between 10 and 20 minutes. A third explanation is that the drivers under—or appropriately—trusted the automation. If drivers calibrated their trust to an expectation that the automation would fail, they may have been motivated to stay engaged and quicker to respond. This explanation is supported by comments from several participants during the study indicating that they did not trust automated vehicles as well as analyzing the technology acceptance questionnaires.

Future work should investigate these findings with specific protocols to address the driver's cognitive state, such as distraction by having the driver to engage in a non-driving-related task, vigilance by investigating a longer drive, and trust by providing information to the driver. Transparent information on automated vehicle capabilities and limitations can alleviate the negative sentiment towards these technologies and impact their future acceptance and adoption (Alambeigi et al., 2021; J. Lee & Kolodge, 2018).

3.3.1. Requirements on Models of Driver Behavior

The findings suggest that the takeover time budget—or TTC at the time of the failure—is one of the principal determinants of the takeover performance. As the findings of chapter 2 on driver behavior modeling literature showed, this finding is aligned with prior work on models of driver braking behavior in manual emergencies (Markkula et al., 2016). These models showed that TTC plays an important role in determining drivers' decision to initiate an action in response to a threat (Kiefer et al., 2006; D. Lee, 1976). Studies have shown that drivers have direct access to a visual estimate of inverse TTC (i.e., visual looming), where as a potential collision gets closer, the visual looming gets

higher (Markkula et al., 2016). To capture the impact of time budget, the process models of automated vehicle takeovers that take into account the scenario kinematics and urgency (using a visual looming-based term) should be preferred. In addition to the impacts of time budgets, the models should be designed to capture the impacts of silent failures. Receiving a takeover request increases the urgency of the scenario for the driver and might impact the driver's decision-making process. Thus, the received alert can be considered as an environmental cue for the need to initiate an action. By virtue of having the non-looming evidence term in the looming-based evidence accumulation models, the impact of presence/absence of an alert can be explained by this model.

Collectively, the visual looming-based models, in particular evidence accumulation models, seem to be a promising direction for capturing the impacts of presence of an alert and time budget on takeover performance. The next chapters use this model to estimate the drivers' post-takeover behavior.

4. MODELS OF POST-TAKEOVER BRAKING BEHAVIOR

The findings of chapter 2 show that the process models of manual driving can be extended to automated vehicle transitions of control with similar efficacy. In addition, a considerable amount of work was found in the modeling of driver braking behavior (Markkula et al., 2012; McDonald et al., 2019). Aligned with the findings of chapter 3, these studies have highlighted the visual looming-based models and the evidence accumulation framework as a promising direction for driver behavior modeling (McDonald et al., 2019). Despite the wealth of research on evidence accumulation models in manual driving rear-end emergencies, the models on post-takeover performance are rare. Thus, the goal of the current chapter is to develop and analyze a visual looming-based evidence accumulation model that accounts for the driver's braking reaction time as well as a piecewise linear model that predicts the driver's post-takeover braking control. To accomplish this goal, we have used the collected data from the unexpected braking event explained in chapter 3.

4.1. Methods

From the total number of 128 unexpected braking drives, 3 drives resulted in crashes and 19 drives did not include braking. The data from these drives were excluded from the analysis resulting in a total of 106 complete drives. The critical events including the event onset to the time that the driver stopped braking were extracted from the data

for further analysis. An example of the brake pedal position across the two scenario criticalities is shown in Figure 4.1.

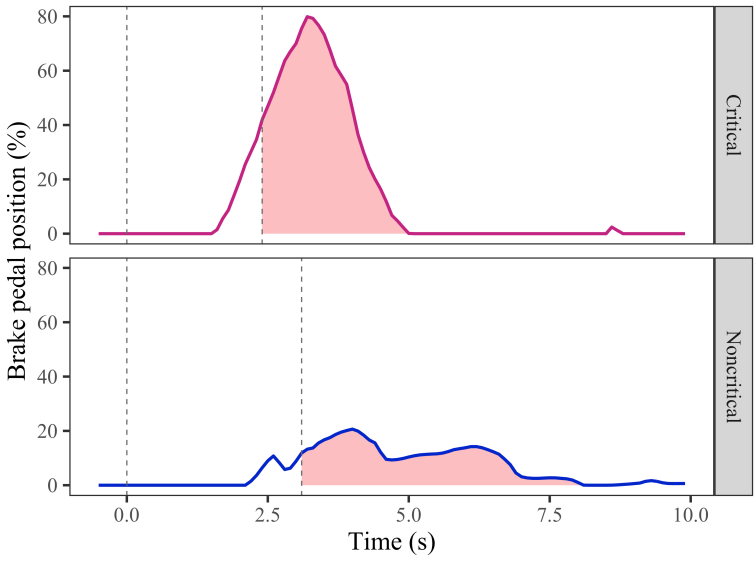

Figure 4.1 An example of brake pedal position for the critical and non-critical unexpected braking events

To increase the generalizability of the models, the drivers' original kinematics have been substituted by counterfactual kinematics. To this end, it is assumed that the drivers did not decelerate and continued with the same speed as the time of the event until they crash. Figure 4.2 represents an example of the original and counterfactual speed following the event onset. In this figure, the blue and black solid lines represent the participant's and the lead vehicle's speed. The black and red dashed lines show the event onset and brake reaction time, respectively.

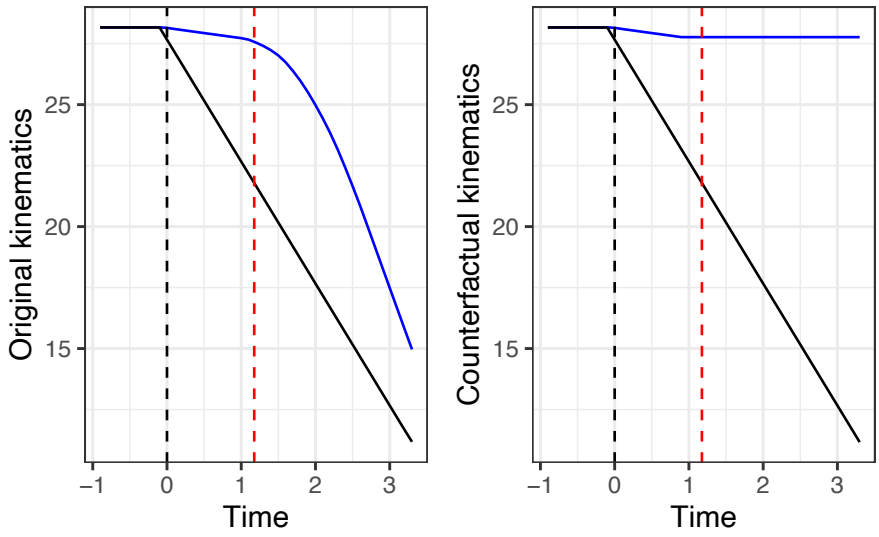

Figure 4.2 An example of the original and counterfactual speed following the event onset

4.1.1. Braking Reaction Model

The drivers brake reaction times were modeled by an evidence accumulation (Equation 4.1) model in which σ, k, and M were free model parameters.

$$\frac{dA}{dt} = k\varepsilon(t) - M + v(t) \qquad \textbf{Equation 4.1}$$

In this equation, $\varepsilon(t)$ is the looming prediction error and $v(t)$ is a zero-mean Gaussian white noise with standard deviation of σ. Brake adjustment will be executed if A exceeds a threshold. The accumulation threshold for braking, A, was set to 1 following the work in Svärd et al. (2020). The evidence accumulation braking model was compared with a reaction time distribution model. This model was created through sampling from

the lognormal model of observed braking reaction times presented by the experiment using the "fitdistrplus" package in R (Delignette-Muller & Dutang, 2015).

4.1.2. Braking Control Model

The brake control was modeled with a piecewise linear function assuming an initial constant deceleration of a_0, then a constant deceleration rate of j (the jerk), and a final constant deceleration of a_1. The transition between the first two phases was governed by t_b, which we defined based on the braking onset model prediction. Figure 4.3 shows the parameters of this model on an example deceleration.

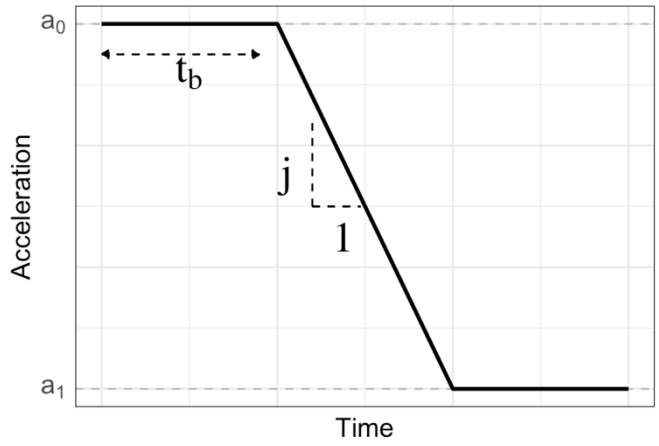

Figure 4.3 Piecewise linear model of braking

4.1.3. Model Fitting and Evaluation Process

The braking model parameters were optimized through a grid search across a set of fixed values for k, M, and σ for evidence accumulation in brake reaction time model

and for a_0 , j and a_1 in the braking control model—the range of the search is given in Table 4.1. The model was run for each combination of the parameters and for the two kinematic urgencies of the scenarios, resulted in a distribution of brake reaction times per scenario. The best combination of parameters for the brake reaction time model was selected based on the smallest difference—measured by a two sample Kolmogorov–Smirnov (KS)—between the observed braking reaction times and predicted reaction times from the model. The two models were compared with both the KS statistics and Kullback–Leibler (KL) divergence. The best combination of parameters for the brake control model was selected based on the root mean square error (RMSE).

Table 4.1 Parameters Search Range for Braking Models

Model	Parameter	Searched Range
Braking Onset	k	[1, 6]
	M	[-0.1, 0.1]
	σ	[0.1, 0.4]
Braking Control	a_0	[-2, 0]
	j	[-10, 0]
	a_1	[-8, 0]

4.2. Results

4.2.1. Simulated Braking Reaction

For the braking onset model, the results of the KS test across the search values of k, M, and σ suggested that $k = 7.7$, $M = -0.3$, and $\sigma = 0.5$ led to the best model fit. The KL divergence measure showed that the evidence accumulation model (0.06) had a smaller divergence from the experimental data compared to the lognormal distribution model (0.15). Figure 4.4 represents the cumulative density function with a histogram of

the models compared to the experimental data. The figure highlights that while both models qualitatively replicate the data, the evidence accumulation model is a closer approximation.

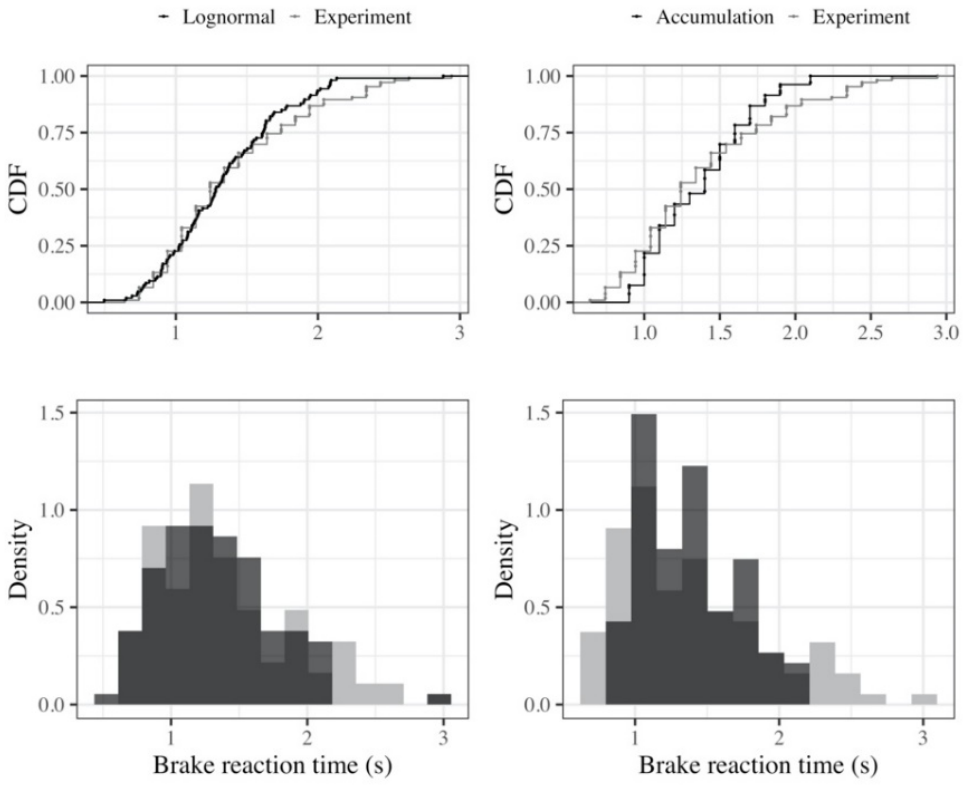

Figure 4.4 Cumulative density function (top plots) and histograms (bottom plots) of the accumulation model, lognormal, and experimental data distributions

4.2.2. Simulated Braking Control Behavior

For the braking control model, $a_0 = -0.4$, $j = -4.25$, $a_1 = -7.4$ resulted in the best model fit for critical and $a_0 = -0.4$, $j = -2.5$, $a_1 = -2.8$ resulted in the best model fit for the non-critical scenario. Figure 4.5 represents examples of the braking control model results, where the black and gray lines indicate the predicted braking profiles and

the observed data, respectively. The braking control models showed similar results to the brake onset models although the fit differed substantially between the critical (left two plots in Figure 4.5) and non-critical (right two plots in Figure 4.5) scenarios. In the critical scenario, the mean root mean square error (RMSE) was 1.23 (SD = 0.66) and the mean R^2 was 0.90 (0.11), whereas in the non-critical scenario the mean RMSE was 1.25 (0.65) and the mean R^2 was 0.50 (0.30).

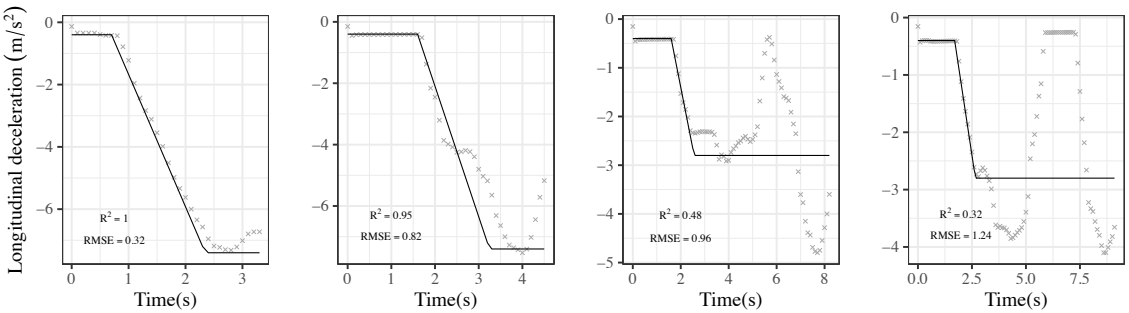

Figure 4.5 Examples of braking control maneuvers for the experiment and fitted model

4.3. Discussion

The results of the braking reaction analysis showed that the KL divergence measure for the evidence accumulation model (0.06) had a smaller divergence from the experimental data compared to the lognormal distribution model (0.15). This is consistent with the findings of prior work that showed looming-based evidence accumulation models can accurately predict the brake reaction times (Piccinini et al., 2019; Xue et al., 2018). The results of the braking control analysis showed a lower RMSE and a higher R^2 (1.23 and 90%, respectively) for the critical scenario compared to the non-critical (1.25 and

50%, respectively). One explanation for these results is that drivers in the non-critical scenario typically braked multiple times and therefore the piecewise linear braking pattern was a poor approximation of their behavior (note the right half of the rightmost plot in Figure 4.5). The results of the critical scenario are aligned with those in Markkula et al. (2016) during manual rear-end emergencies in which they showed for most cases the observed deceleration were closely estimated by the piecewise linear model (R^2>70%). In addition, a large difference was found for the deceleration rate (jerk) as well as the maximum deceleration level (a_1) in critical (-4.25 m/s^3 and -7.4 m/s^2, respectively) in comparison with non-critical scenario (-2.5 m/s^3 and -2.8 m/s^2, respectively). This is also aligned with prior work that showed the rate at which drivers increased their deceleration (towards a maximum) was highly dependent on urgency (Markkula et al., 2016; Svärd et al., 2017).

Overall, the results highlight that visual looming-based evidence accumulation models can effectively capture the brake onset time and the piecewise linear models can replicate the braking control behavior in critical events; however, it is limited in predicting the braking control in non-critical events, where several braking adjustments occur sequentially. Future research should capture these multiple braking adjustments by modifying the piecewise model to include a visual looming input.

5. MODELS OF POST-TAKEOVER STEERING BEHAVIOR*

The previous chapter focused on post-takeover braking behavior. While extensive work has been done with the braking models, steering models have received less attention. Steering maneuvers can be further partitioned into avoidance steering—initiation of an evasive maneuver—and stabilization steering—a series of corrective actions following the initial maneuver (Markkula et al., 2014). Evasive steering for manual emergencies has been modeled with open-loop, closed-loop, and hybrid models (Markkula et al., 2012; McDonald et al., 2019). Open-loop models represent the anticipatory behavior of the driver's response to an error in a series of preprogrammed control patterns (i.e., motor primitives) and closed-loop models represent the compensatory behavior of the driver in correcting a deviated situation. Prior studies showed that open-loop models best replicate manual emergency avoidance steering and that the closed-loop two-point visual control models best replicates stabilization steering. In this chapter, we extend the prior models to post-takeover steering control and fit a looming-based open-loop Gaussian model to the post-takeover avoidance steering. In addition, we fit a closed-loop two-point control model to drivers' subsequent post-takeover control maneuver (i.e., stabilization steering). To accomplish this goal, we have used the collected data from the obstacle reveal event explained in chapter 3.

---

* Parts of this chapter are reprinted with permission from "Alambeigi, H., & McDonald, A. (2020). Modeling Post-takeover Avoidance and Stabilization Steering Control in Automated Vehicles. Proceedings of the Human Factors and Ergonomics Society Annual Meeting, 64(1), 1999–2000."

5.1. Methods

From the total number of 128 obstacle reveal drives, 8 drives resulted in crashes. The data from these crashes was removed from the dataset because it did not include both avoidance and stabilization steering, resulting in a total of 120 complete datasets. Figure 5.1 illustrates these responses arranged by scenario criticality and the alert presence. The bottom and top dashed lines represent the center of the initial and the left adjacent lane.

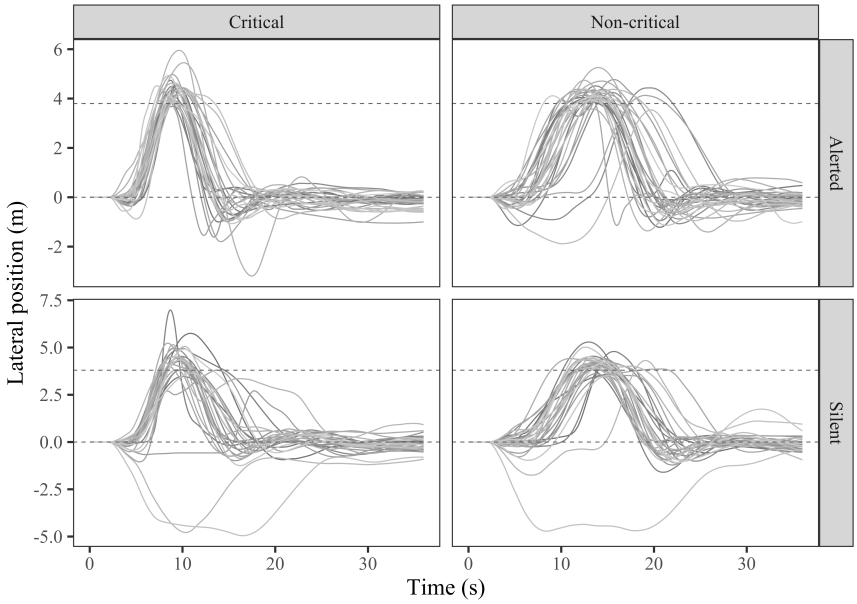

Figure 5.1 Lane changing vehicles' trajectories categorized by kinematic urgency of the event and presence or absence of the takeover request

The steering maneuvers were divided into three phases: takeover, avoidance steering, and stabilization steering. The takeover—defined by the time between the obstacle reveal (precipitating event onset) and the first evidence of avoidance steering was excluded from the modeling. The avoidance steering phase started after the steering

takeover time and ended at the last point of leftward steering wheel rotation. The stabilization steering phase was defined as the time between the end of avoidance phase and 35 seconds after the event onset. The threshold of 35 seconds for the corrective action was chosen from the literature where it has been shown that it takes 35-40 seconds for the drivers to stabilize their lateral control of the vehicle after the transition (Merat et al., 2014).

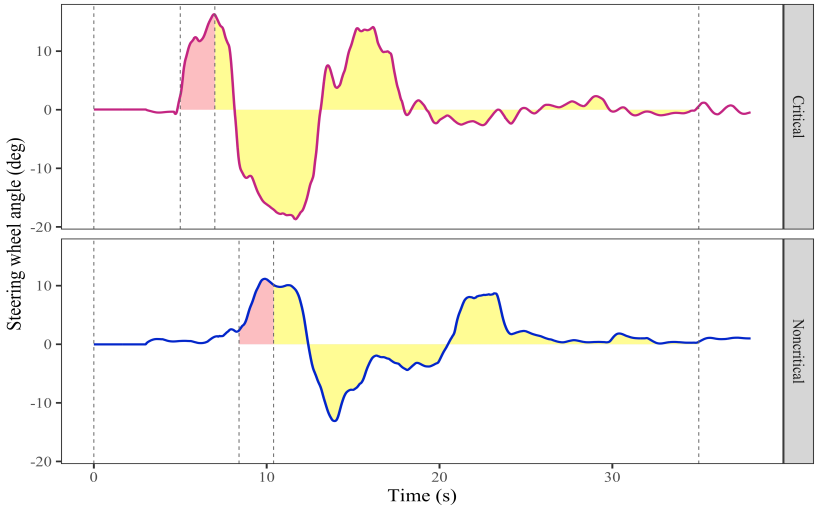

Figure 5.2 Illustration of avoidance and stabilization steering phases across the event criticality

Figure 5.2 illustrates a typical steering wheel angle rotation for the avoidance and stabilization phases across the criticality of the scenarios with the event onset set at time zero and the takeover time delineated by the second vertical dashed line. Top plot shows a critical scenario and bottom plot shows a non-critical scenario. The first and second shaded parts represent a typical range of the avoidance and stabilization maneuver in the collected data, respectively. The post-takeover steering maneuvers were modeled using a

baseline closed-loop steering model (Salvucci & Gray, 2004) and a two-part avoidance and stabilization model based on the findings in (Markkula et al., 2014). The two-part model contained an open-loop avoidance steering component and a closed-loop stabilization component—also based on Salvucci & Gray (2004).

5.1.1. Steering Avoidance Model

The avoidance steering maneuver comprises of a series of discrete open-loop corrections which suggests a predetermined amplitude at the maneuver onset (Markkula, 2014). Breuer (1998) showed that in an evasive maneuver the amplitude of steering wheel angle and maximum rate of the steering angle are linearly correlated which suggests a constant duration of steering corrections (Markkula, 2014). The steering wheel angle rates in open loop avoidance models have been shown to follow a Gaussian distribution function (Markkula et al., 2014) as shown in Figure 5.3 and is defined by Equation 5.1.

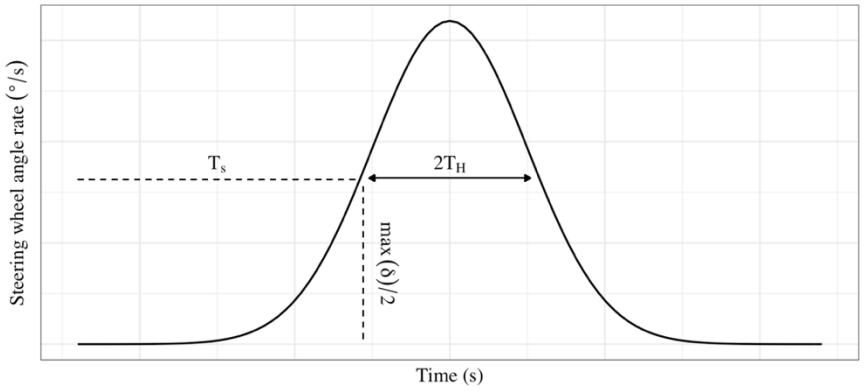

Figure 5.3 Steering wheel angle rate generated by an open-loop avoidance model

$$\dot{\delta}(t) = Ae^{-(\frac{(t-\mu)^2}{2\sigma^2})} \qquad \textbf{Equation 5.1}$$

In this Equation, $\dot{\delta}$ denotes the changes in the steering wheel angle, A is the amplitude of the pulse based on a constant variable k and maximum visual looming after the event onset and prior to the avoidance maneuver initiation, μ is the mean of the model input and was set to the time $T_S + T_A$ where T_S is the time when the steering input reaches half of its maximum value, and σ is the standard deviation of the model and was a function of time duration (T_H). Following the work in Markkula et al. (2014), k, T_A, and T_H are considered as free parameters. By fitting this model to the experimental data, the free parameters will be adjusted for the two scenarios. To determine the relationship between the maximum steering wheel angle and maximum steering rate a linear regression model was fit to the experimental data. Figure 5.4 shows the linear correlation for the two kinematic urgencies after initiation of the steering avoidance maneuver. The coefficient of determination in both events justifies the use of Gaussian models.

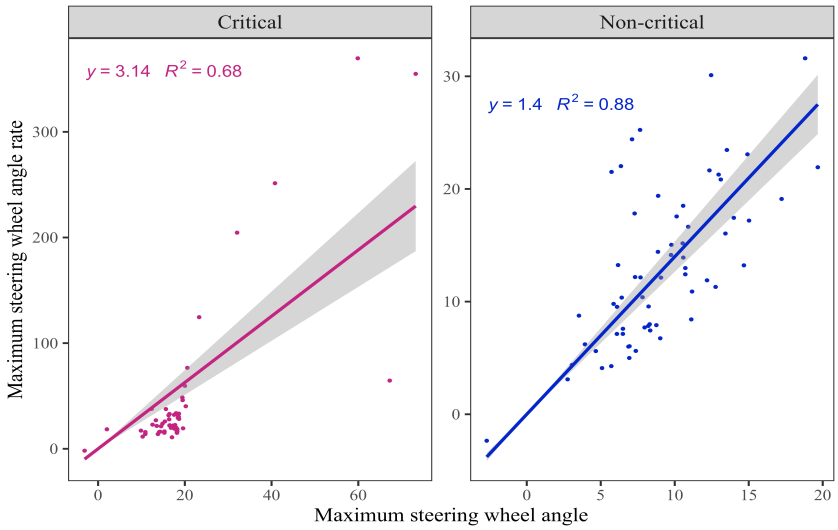

Figure 5.4 Correlation between max steering wheel angle and maximum steering wheel angle rate

5.1.2. Steering Stabilization Model

The stabilization steering component and baseline model used in this study is based on a two-point closed-loop stabilization model defined in Equation 5.2, initially proposed in Salvucci & Gray (2004). The model assumes that driver steering behavior is based on optimal control process to minimize the angles between the vehicle's heading and near and far anchor points.

$$\dot{\boldsymbol{\varphi}} = \boldsymbol{k_n}\dot{\boldsymbol{\theta}}_{\boldsymbol{n}} + \boldsymbol{k_f}\dot{\boldsymbol{\theta}}_{\boldsymbol{f}} + \boldsymbol{k_I}\boldsymbol{\theta_n} \qquad \textbf{Equation 5.2}$$

In this equation, φ is the steering wheel angle, θ_n is the near point sight angle, and $\dot{\theta}_n$ and $\dot{\theta}_f$ are the changes in the near and far point angles, respectively. k_n, k_f, and k_i are gain parameters. The distances between the vehicle and the near and far points are also typically free parameters. This equation imposes three constraints: a stable near point ($\dot{\theta}_n \approx 0$), a stable far point ($\dot{\theta}_f \approx 0$), and a near point at the center of the lane ($\theta_n \approx 0$). The gain parameters determine the weights of these constraints. Fitting the model to a new scenario consists of identifying the values of k_n, k_f, and k_I and the near and far point distances that minimize errors between observed behavior and model predictions. The near and far points were positioned on the center of the road way, although, any salient stable visual points could be used for the far point. To simplify the computational modeling efforts, a discrete form of equation 5.2 was used. To minimize the number of free parameters, the near point distance was fixed at 16 meters and the far point distance was fixed at 123 meters for this analysis. These values were selected based on the

comprehensive analysis in Markkula et al. (2014). Given the position and heading of the vehicle compared to the center lanes, the near and far points were either anchored at the current lane to account for the steering corrections within a lane or at the destination lane to capture the lane changing behavior. Figure 5.5 shows a schematic illustration of the two-point stabilization steering by Salvucci & Gray (2004) representing the end of the overtake maneuver in a straight road. The gray vehicle represents the stationary obstacle and D_f and D_n express the far and near point angles, respectively. The difference between the baseline and closed-loop stabilization models is that the baseline model was fit to the entire post-takeover steering whereas the closed-loop stabilization model was fit to only the stabilization phase of steering, starting after the avoidance steering and ending after the vehicle had stabilized in the original lane.

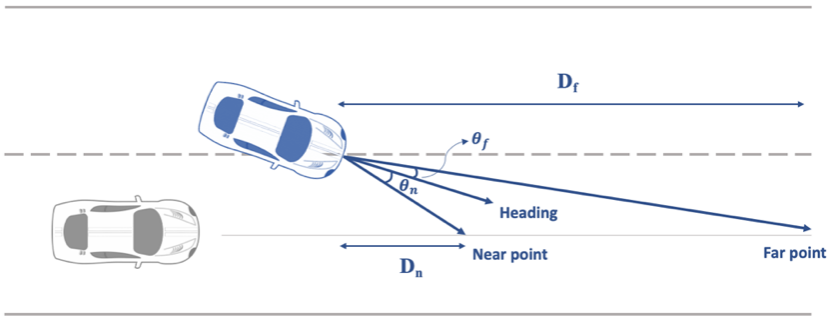

Figure 5.5 A schematic illustration of the two-point stabilization steering representing the end of the overtake maneuver in a straight road

5.1.3. Model Fitting and Evaluation Process

The parameters in each model were optimized by partitioning the experiment data into training and testing datasets conducting a grid search over a range of parameters (see

Table 5.1). The participants were randomly divided into two groups. For the first half, the model was trained on the critical drive and was tested on the non-critical drive. For the second group, the model was trained on the non-critical drive and tested on the critical drive. Each combination of parameters was evaluated based on the minimum RMSE between the model predictions and the observed training data and the best set of parameters was chosen for each participant. Following the model fitting, the results were validated against the test dataset. R^2 values were also calculated against the test data to allow for comparison with the results of other works.

Table 5.1 Parameter Search Range for Steering Models

Steering Model	Parameter	Searched Range
Avoidance	T_H	[0.1, 1]
	T_A	[-0.5, 0.5]
	k	[0, 100]
Stabilization	k_f	[0, 100]
	k_n	[0, 50]
	k_i	[0, 10]
Baseline	k_f	[0, 100]
	k_n	[0, 50]
	k_i	[0, 10]

5.2. Results

5.2.1. Simulated Steering Avoidance Behavior

The optimization results suggest that values of $k = [20, 70]$, $T_H = [0.2, 0.6]$, $T_A = [-0.5, 0.5]$ for the open-loop avoidance models correspond to more accurate models. Within the best regions, the model is not sensitive to the gain parameter settings. Table 5.2 presents the validation results against the test data. As this table shows, the open-loop

avoidance model generally replicates the trend in avoidance steering better than the closed-loop baseline model. Figure 5.6 provides examples of the avoidance steering profiles for the fitted model to the experimental data. In this figure, the black and grey lines represent the model and experiment, respectively. The first two examples represent good fits and the second two examples represent relatively poor fits.

Table 5.2 Model Fitting Results for the Post-takeover Avoidance Steering Models

	Avoidance: Open-loop	Avoidance: Baseline
RMSE	0.07 (0.065)	0.13 (0.33)
R^2	0.77 (0.29)	0.69 (0.27)

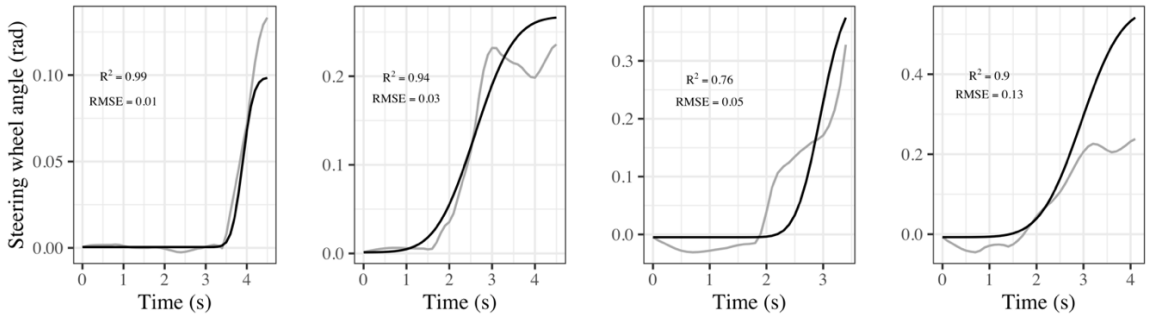

Figure 5.6 Examples of avoidance steering maneuvers for the experiment and fitted model

5.2.2. Simulated Steering Stabilization Behavior

The optimization results for the stabilization model suggest that values the lower values of k_f, k_n, and k_I, in particular, $k_f = [0, 25]$, $k_n = [0, 15]$, and $k_i = [0, 2]$, correspond to more accurate models. The stabilization modeling results, presented in Table 5.3, show similar R^2 values across the models, but a slightly better RMSE in the closed-loop model fit specifically to stabilization steering. Figure 5.7 provides examples

of the stabilization steering profiles for the fitted model to the experimental data. The black and grey lines represent the model and experiment, respectively. The first two examples represent good fits and the second two examples represent relatively poor fits.

Table 5.3 Model Fitting Results for the Post-takeover Stabilization Steering Models

	Stabilization: Closed-loop	Stabilization: Baseline
RMSE	0.12 (0.13)	0.12 (0.14)
R^2	0.32 (0.10)	0.31 (0.10)

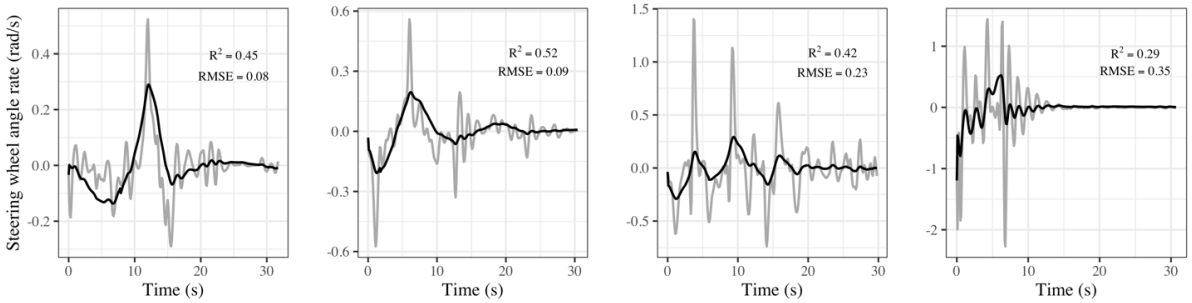

Figure 5.7 Examples of stabilization steering maneuvers for the experiment and fitted closed-loop stabilization model

5.3. Discussion

The validation results against the test data showed that the two-part model of visual looming-based open-loop avoidance and closed-loop stabilization are effective for predicting driver post-takeover performance. In particular, the results showed that the open-loop avoidance model generally replicated avoidance steering better than the closed-loop baseline model. The lower value of RMSE and higher value of R^2 for the open-loop model compared to the closed-loop baseline model (R^2: 77% vs. 69%) suggests that the drivers maximum looming prior to the takeover might determine the pattern of driver's

avoidance maneuver. The results are similar to that of Markkula et al. (2014), which showed an average R^2 of 71% for a manual driving emergency. The stabilization modeling results show similar RMSE values across the models, but a slightly better R^2 in the closed-loop model fit specifically to the stabilization steering (32% vs. 31%). In addition, the results showed that the stabilization part of the model is capable of capturing both lane changing behavior and steering corrections within a lane by switching the anchor points to the destination lane.

Overall, this model can effectively replicate the trends, although it has substantially less entropy than the observed data. While the analysis provides a promising replication of steering behavior, it is limited in determining the severe and quick corrections. In addition, regardless of the number of pulses in the avoidance steering rate profiles, only one Gaussian function was fit to the whole maneuver which can make the model less reliable for the data with more steering corrections. Despite these limitations, the findings suggest that open-loop looming-based Gaussian models accurately replicate post-takeover avoidance steering and that closed-loop models accurately replicate post-takeover stabilization steering. Future work should explore expansions to capture additional variability in avoidance steering and validate these models on real-world driving data or naturalistic steering dataset given the potential for differences in behavior between simulator and real-world scenarios.

6. HOLISTIC MODEL OF TAKEOVER BEHAVIOR

The analyses of the previous chapters highlight the need for a holistic model of driver behavior following an automation failure. So far, several models have been developed to predict separate components of a takeover process. In particular, the developed models have been focused on an avoidance strategy by either braking or steering alone, while in an on-road driving, drivers perform steering and braking with close temporal proximity, if not at the same time. The concept of parallel information processing follows the leaky competing accumulator models, in which the human brain can accumulate two sets of evidence simultaneously, rather than having a single accumulator with different thresholds, allowing them to have different choice alternatives (Usher & McClelland, 2001).

The current chapter addresses this gap by developing a holistic model of the drivers' perceptual decision-making and control response that integrates multiple responses and provides realistic predictions of human performance. The output of this model is the drivers' decision to steer or brake, takeover time, and control behavior. To evaluate the performance of the model, it was fit to the collected dataset—discussed in chapter 3. Developing such a comprehensive model can be used as a guideline to improve the design of advanced automated vehicle-related technologies. The rest of this chapter starts with a discussion on the model description, model formulation, and parameter fitting

and evaluation process, and ends with a presentation of the simulated decision-making, takeover time, and braking and steering control responses.

6.1. Model Description

Evidence accumulation models have been one of the most successful frameworks of perceptual decision-making within cognitive psychology over the last 50 years (Evans & Wagenmakers, 2020). The underlying assumption of these models is that the brain accumulates noisy evidence over time and a decision is made once enough evidence is extracted. Evidence accumulation models provide predictions for the decision being made and the time takes to make that decision, making them a good candidate for driver behavior modeling where rapid decision-making is required. In particular, these models decompose the response times into the underlying latent variables of decision-making process such as the drift rate and the decision threshold. The drift rate is the rate at which the evidence is integrated over time and the decision threshold is a boundary on the required evidence for triggering a response (Evans & Wagenmakers, 2020). Depending on the characteristics of these variables (e.g., constant or time-varying drift rate, stochastic or deterministic evidence), the evidence accumulation model has several variants such as the drift-diffusion or leaky competing accumulator model (Ratcliff, 1978; Usher & McClelland, 2001). The leaky accumulation model suggest that the evidence that has been collected over time may be subject to decay and has been shown to better explain the time-accuracy tradeoffs (Usher & McClelland, 2001). In addition, this model allows for lateral inhibition (i.e., simultaneous account for the choice response) of evidence through multiple

accumulators (one for each decision alternative). The inhibition among the accumulators reflects the relative-evidence decision criterion, in which the amount of information collected at each accumulator impacts every other accumulator. Upon stimulus presentation, the response is triggered by the accumulator with the strongest input.

The holistic framework follows the leaky competing evidence accumulation model and assumes that the driver is simultaneously accumulating evidence for steer and brake and that as the evidence builds up in favor of one decision choice it sends inhibition to the other. This model also assumes that the decision to steer or brake is guided by the predicted error in the drivers' visual looming of the lead vehicle and that the drivers are continuously accumulating this looming signal over time by looking at the forward roadway (zero gaze eccentricity). Following the decision-making process, the associated maneuver is activated and further adjusted if required.

6.2. Model Formulation

The evidence accumulator in this chapter modifies the basic accumulators, introduced in chapter 2, and adds parameters to better account for the human's perceptual decision-making and response time process. Figure 6.1 illustrates a schematic representation of the fundamentals of this model. In this figure, the dashed box indicates the driver's internal perceptual process and includes two parallel accumulators to account for the onset of each alternative response (i.e., steering and braking). The input to this perceptual process is environmental stimulus that the driver receives and the output is a

braking and/or steering control. Equation 6.1 shows the formulation of the evidence accumulation model.

$$\frac{d(A_i)}{dt} = k_i \varepsilon(t) + v(t) - CA_i \quad i = \{brake, steer\} \qquad \textbf{Equation 6.1}$$

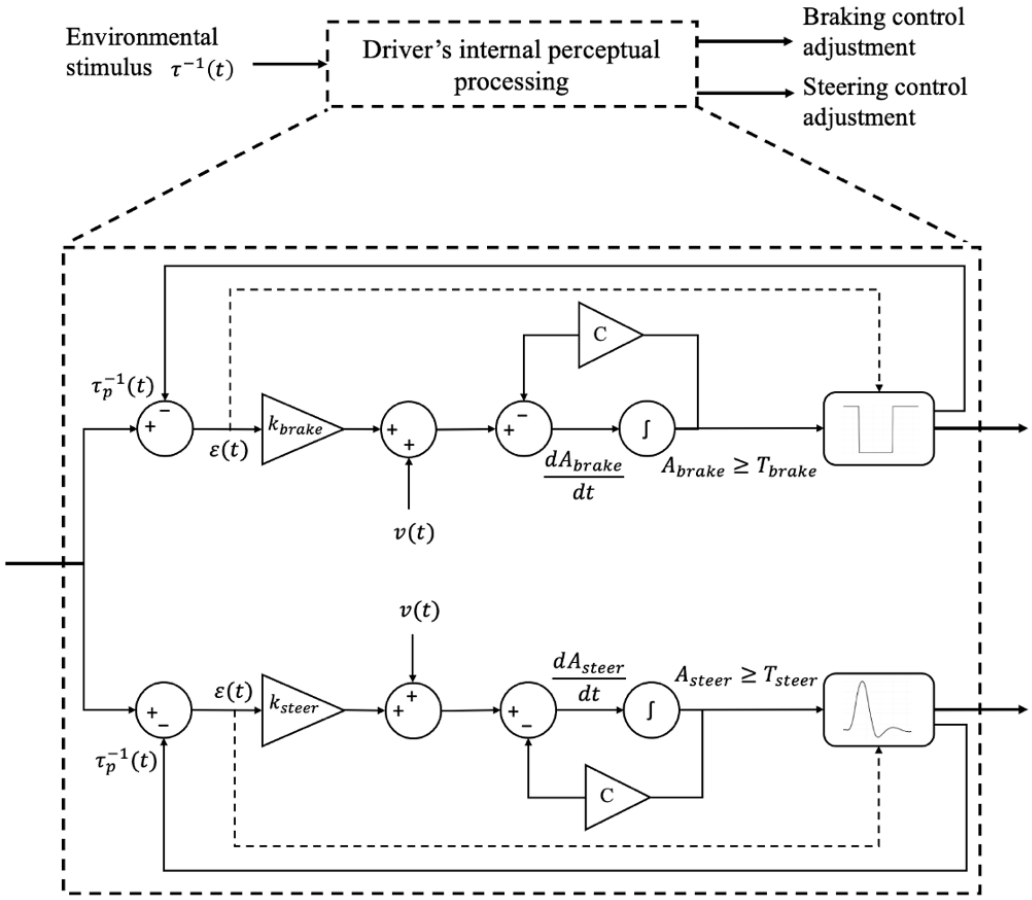

Figure 6.1 Schematic representation of the fundamentals of the holistic modelling framework including an accumulator for each alternative action and control action modules

In this Equation, A is the accumulator activity for braking or steering response, $\varepsilon(t)$ is the looming prediction error and is equivalent to $(\tau^{-1}(t) - \tau_p^{-1}(t))$, where $\tau^{-1}(t)$ is the perceptual quantity (i.e., looming signal in our model) that represents evidence for the need of an action and $\tau_p^{-1}(t)$ is the prediction of sensory consequences of control actions, $v(t)$ is the accumulator noise from a normal distribution with mean 0 and standard deviation σ. C is the leakage term corresponding to the decay in evidence accumulation over time (Usher & McClelland, 2001). The inclusion of the leakage term has the effect of a smoothing low-pass filter with a time constant equal to $1/C$ and can avoid an early detection of a response in slow looming conditions (Svärd et al., 2020).

k is the gain parameter or the proportion of the support for braking or steering determining the impact of looming prediction error and is defined as a function of sum of all looming and non-looming evidence (i.e., m) for or against the need for an evasive action. Traditionally, k was defined as a constant variable (McDonald et al., 2021; Piccinini et al., 2019; Svärd et al., 2020); however, following the work in a naturalistic setting that showed a substantially better fit for a visual looming with an exponential gain compared to a constant gain (although with a different goal), this model also uses an exponential gain for braking and steering (Sarkar, Alambeigi, et al., 2021). To reflect the inhibitory behavior of the leaky evidence accumulation model, the gain is set up in a way that as the support for braking increases the support for steering decreases, and vice versa, so that the overall looming gain will always add up to 1 (Equation 6.2). This allows the model to account for multiple responses at a single time unit.

$$k_{brake} = 1 - k_{steer} \qquad \textbf{Equation 6.2}$$

Figure 6.2 shows the effect of non-looming evidence (m) on the braking and steering gain parameters. As this figure shows, positive m values represent the non-looming evidence in favor of the steering decision, meaning that with very high visual looming and in the presence of a non-looming evidence, such as an empty adjacent lane, the driver accumulates more evidence in favor of changing lanes. The existence of other anticipatory perceptual cues such as the lead vehicle's brake lights can also provide evidence for the possible need to initiate the deceleration, if accompanied with other stimulus (Markkula et al., 2016). A negative value of m in this model can be an indicative of such an anticipatory cue, where it might increase the driver's tendency to brake if combined with sufficient visual looming evidence, as a brake light onset in itself is not enough to trigger a braking response (Markkula et al., 2016; Xue et al., 2018).

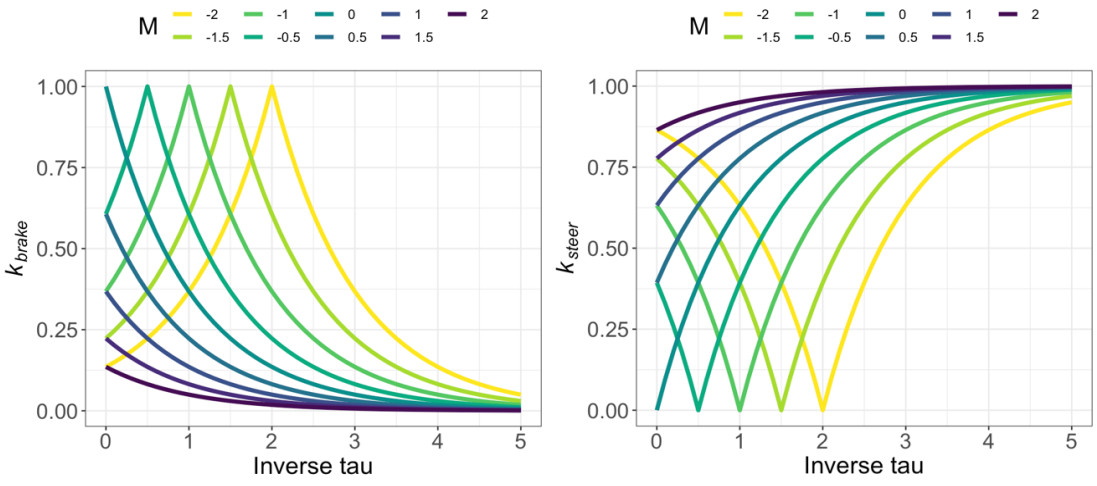

Figure 6.2 Visual representation of the braking and steering gain parameters

Another parameter that is missing in this model, is the effect of warning that the drivers received. It is expected that with the presence of a takeover request, it takes less time for the drivers to accumulate sufficient visual looming evidence to resume the vehicle control. Therefore, a constant variable, indicating the driver's initial readiness (r), is also added to the drift rate. Given the input of the model (τ^{-1}), drivers' choice of response is depended on the visual looming signal and how it evolves over time. If the visual evidence crosses the accumulator threshold (i.e., T in Figure 6.1), the driver initiates the response. The drivers' takeover time is then calculated as the minimum of braking and steering takeover times. In this model, σ, m, and r are considered as free parameters.

In the next step, the drivers' predicted decision and the takeover time is fed to the control part of the model. Based on the chosen response, drivers' control model was activated resulting in a braking control and/or steering avoidance behavior. After each control adjustment, the driver predicts how the looming will decay as a result, thus a new looming prediction (τ_p^{-1}) is fed back to the accumulator (the feedback in Figure 6.1).

For the brake control model, a modified version of the piecewise linear model discussed in chapter 4 (see Figure 4.3) was used. In contrast to the original piecewise model, in this model, the jerk was considered as a function of the visual looming signal. To this end, a linear regression model was fit to find the relationship between the deceleration rate and maximum visual looming prior to the maneuver. The analysis of the original piecewise model found a constant value of -0.4 for the initial deceleration (a_0) across all conditions. Therefore, this parameter was kept constant, while the final maximum deceleration (a_1) for each brake adjustment, and the jerk (j)—in the form of

j_0—were considered as free parameters. Equation 6.3 shows the relationship between jerk, visual looming, and the associated free parameter (j_0).

$$\boldsymbol{j = a\tau^{-1} + b + j_0} \qquad \textbf{Equation 6.3}$$

The avoidance steering model was fit using an extended version of the visual looming-based Gaussian model discussed in chapter 5 (see Figure 5.3). This model indicates that the drivers' steering wheel rate shows a normal bell-shaped pattern (also called a steering primitive) to adjust the steering wheel. The current avoidance model was modified to account for the number of steering primitives in the avoidance steering rate profiles. The input to this model is the maximum visual looming after the event onset and prior to the avoidance maneuver initiation, (τ_{max}^{-1}). The mean of the steering input and was set to the time T_S+T_A where T_S is the time when the steering input reaches half of its maximum value. The standard deviation of the model and was a function of time duration (T_H). In this model, the amplitude of the pulse, k, T_A, and T_H were considered as free parameters.

6.3. Methods

6.3.1. Takeover Response Analysis

To provide context for drivers' decision-making process, the observed responses from the experiment were analyzed based on their initial and aggregated avoidance strategies. The initial strategy refers to the drivers' first reaction following the automation

failure and the aggregated strategy includes any subsequent maneuver to their initial reaction. The drivers' avoidance strategies can be categorized into four different responses including braking, lane changing, both braking and lane changing, and no action. If the driver's initial response (e.g., braking) was followed by a second maneuver (e.g., lane changing), the aggregated response type included both braking and lane changing. Overall, out of 256 drives, 11 resulted in crashes (see section 3.2.2.1 for more details), out of which, in 2 cases the drivers did not initiate their maneuvers until after the crash occurred. Both of which were rear-end collisions with the lead vehicle. For the purpose of the response type analysis, these 2 drives were excluded. The count data from driver responses were analyzed with a two-sided Fisher's exact test as it works well with small sample sizes (Bower, 2003).

6.3.2. Model Fitting and Evaluation Process

The holistic model was fit to the automated vehicle takeover data collected from the simulator study, explained in chapter 3, using R (R Core Team, 2018). A good candidate for estimating the parameters of the evidence accumulation model is a Bayesian statistical inference approach as it naturally incorporates the perceptual uncertainty associated with the human behavior (Bitzer et al., 2014; Markkula et al., 2021). The Bayesian statistical approach has become significantly prominent in a variety of contexts across human decision-making and cognitive science as well as other behavioral research disciplines (M. D. Lee, 2008; van de Schoot et al., 2017). From the human cognition perspective, the perceptual representations of the environment are inferred from very

limited sensory inputs enforcing decisions to be made under uncertainty (Chater & Oaksford, 2008). This lack of certainty, highlights the importance of Bayesian statistical inference in simulating models of human cognition (Chater & Oaksford, 2008; M. D. Lee, 2011).

The Bayesian approach implements Bayes theorem and provides a comprehensive framework for making inferences by using prior beliefs (distributions) regarding the model parameters and making predictions using the probability of the parameters given the observed data and model. The prior distribution can be acquired from different sources including our prior understanding of likely values or experimental and theoretical studies (van de Schoot et al., 2017). In case of lack of knowledge or empirical evidence, an uninformative prior can be used. Whether the prior is informative or not, it gets updated after observing the data leading to an updated posterior distribution. This updated distribution then serves as the prior for future estimations (Turner & Van Zandt, 2012). A drawback of using a Bayesian approach is the computation of the model likelihood, which can be computationally expensive and intractable due to the large sample size, high number of parameters, or functional complexity (Karabatsos & Leisen, 2018). Alternatively, an approximate Bayesian Computation (ABC) can be employed when the data and parameter dimension is large.

ABC is a likelihood-free inference that follows the general steps of Bayesian inference by formulating a model with parameter values drawn from a prior distribution, estimating the model parameters by fitting the model to the observed data, comparing the simulation outputs to the data, and improving the model by checking its posterior

predictions (Csilléry et al., 2010; Jabot et al., 2013). Figure 6.3 represents a conceptual overview of the ABC.

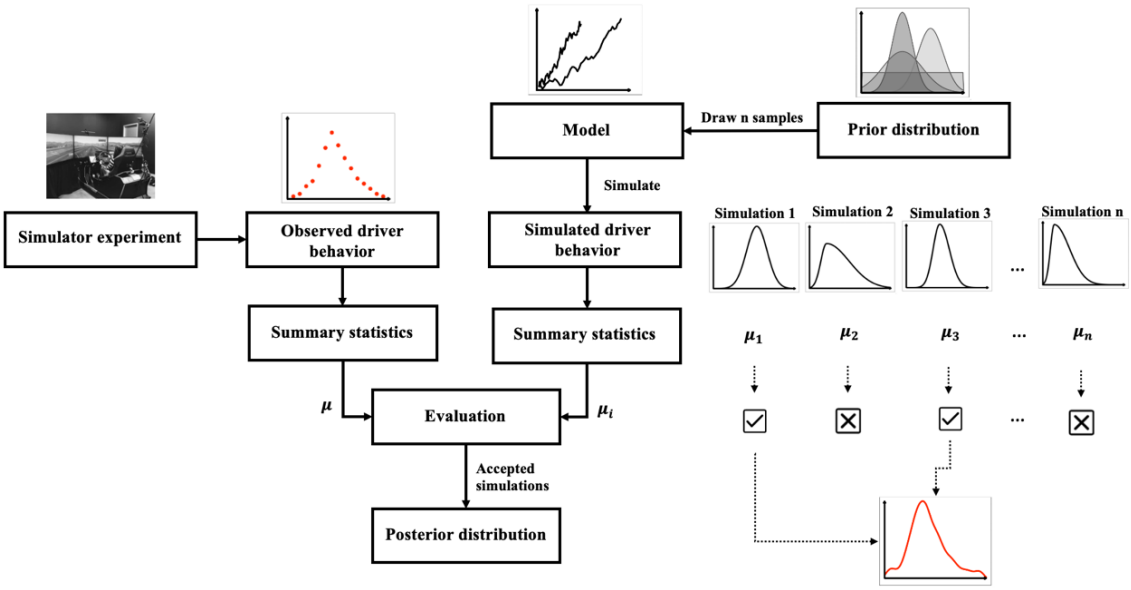

Figure 6.3 A conceptual overview of the Approximate Bayesian Computation (ABC) method

This approach explores the parameter space and replaces the likelihood ratio computation with simulations of the model and eventually provides the summary statistics of the parameters (Sunnåker et al., 2013). For the purpose of the analysis, the parameters for the reaction and control components of the model are estimated using a modified ABC-MCMC algorithm proposed in Marjoram et al. (2003). MCMC is a method that can simulate samples from the posterior distribution of the model parameters. ABC-MCMC uses the Metropolis–Hastings algorithm and explores the parameter space iteratively using the distance between the simulated and the observed summary statistics to update the

current parameter values (Csilléry et al., 2010; Marjoram et al., 2003). Marjoram et al.'s modified algorithm was selected as it proposed several improvements compared to their original algorithm including performing a calibration step so that the algorithm can automatically determines the tolerance threshold, the scaling of the summary statistics and the scaling of the jumps in the parameter space during the MCMC (Jabot et al., 2015).

ABC estimation process included 2,000 iterations of simulations for each 254 observations. Each iteration of the algorithm draws a random sample from a prior distribution for each parameter and predicts the mean effect from the simulated model using the sampled values (Vasishth, 2020). The number of simulations during the calibration step was set to 10,000. A uniform distribution was used for all free parameters of the model as shown in Table 6.1. For the jerk parameter in the brake control model only negative values were selected as the deceleration makes a linearly decreasing line over time. Similarly, for the final deceleration of this model only negative values were considered. Following the prior pioneering work, the accumulator threshold and the leakage term were set to 1 and 0.25, respectively (Svärd et al., 2020).

The simulations reported summary statistics of the parameters as the output of the model. A further step was needed to simulate the takeover response using the accepted range of the free parameters. To this end, random samples were drawn from the posterior distributions of the free parameters and were fed to the model to simulate the takeover times. The model evaluation phase included a comparison of the model to the observed takeover response, in terms of both the control choice and the posterior distribution of the takeover time.

In the braking and steering control models, the deceleration input and the steering wheel angle were estimated, and the accepted range of the parameter were provided. Drawing samples from the posterior distributions, the braking and steering inputs were simulated. Using RMSE, the performance of these models across all observations were compared with the performance of the basic braking and steering models, developed in previous chapters.

Table 6.1 Prior Distributions Used in the Holistic Model

Model	Parameter	Searched Range
Takeover response	m	Unif [-1,1]
	r	Unif [0,1]
	σ	Unif [0,1]
Braking control	j	Unif [-10,0]
	a_1	Unif [-8,0]
Steering control	k	Unif [0,100]
	T_A	Unif [-0.5,0.5]
	T_H	Unif [0,1]

6.3.2.1. Data Range

The end point of the experimental data, that was used for the model fitting, was the end of the avoidance maneuver—or the beginning of stabilization maneuver—for the steering control and the end of braking maneuver for the braking control. For each braking adjustment the minimum TTC + 0.5 s were considered, as the drivers generally maintain acceleration for that long (Markkula et al., 2016). If 95% of the minimum acceleration was not reached at minimum TTC + 0.5 s, the endpoint was set at the subsequent point in time when the acceleration reached 0.95% of the minimum acceleration, for the first time (Svärd et al., 2020).

6.4. Results

To investigate the underlying assumptions of the model on drivers' perceptual decision-making, this section starts with an overview of the observed takeover responses from the experiment. The rest of the sections present the simulated results for different phases of a takeover starting from decision-making and takeover times followed by braking and steering control behavior. The last section illustrates the relationship between these models from the holistic perspective.

6.4.1. Observed Takeover Behavior

Drivers' initial response is illustrated in Figure 6.4. In the unexpected braking scenario, the majority of drivers responded to the event by braking (116/126), while only a few performed lane-changing maneuver (10/126). The Fisher's Exact test showed significant differences in responses associated with scenario criticality ($p = 0.03$) in the unexpected braking scenario. Steering was significantly more common in critical scenarios compared to non-critical. In the obstacle reveal scenario, the most common response was steering to other lanes (112/128 events) followed by braking (16/128). All of the drivers included at least some steering response. Fisher's Exact test showed no significant effect of scenario criticality or alert type on driver responses in the obstacle reveal scenario.

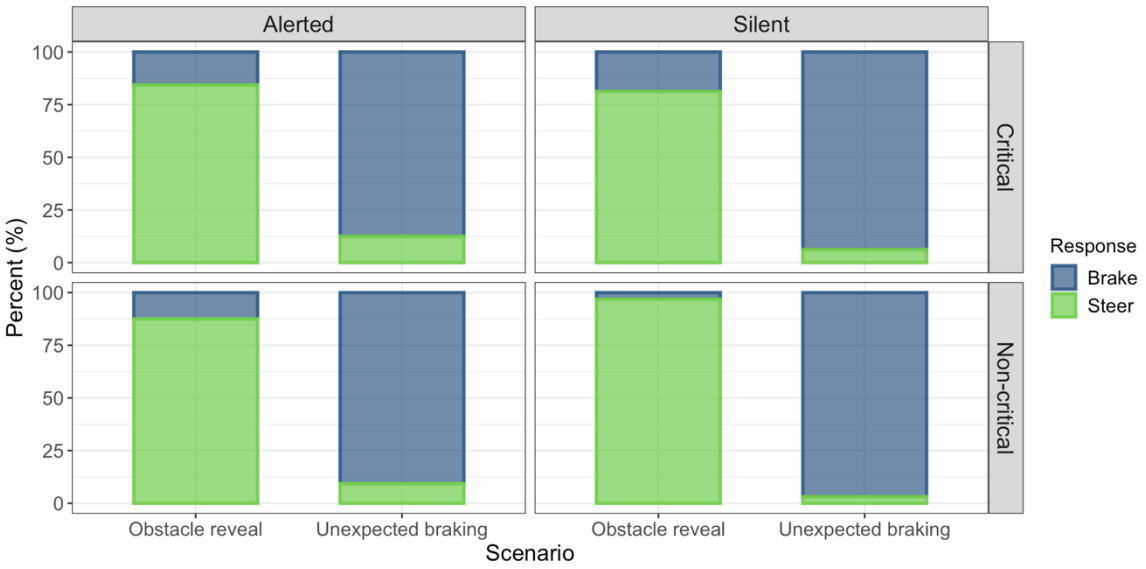

Figure 6.4 Drivers' takeover initial response (brake vs. steer) categorized by criticality, takeover request presence, and event type

Figure 6.5 shows the density plots of takeover times across all combinations of takeover request, criticality, and scenario types. Note that in this figure the groups with fewer than two data points have been dropped. The distributions were further categorized with respect to the drivers' initial response type after the failure. The blue and green distributions represent the brake and steer takeover times, respectively. The overall takeover times was defined as the minimum of brake and steer takeover times. Note that due to the lack of (or limited) observations in some cases only one of the braking or steering distributions are plotted (second and forth plots from top in the right panel of Figure 6.5). As this figure shows, in most cases the brake takeover times are shorter than steer takeover times. In addition, the width of distributions in critical scenarios represents a small range of observed values compared to the non-critical. With regards to the takeover

request type, there is a slight difference in the mean of alerted versus silent failure, where silent failures increased the takeover times compared to the alerted conditions.

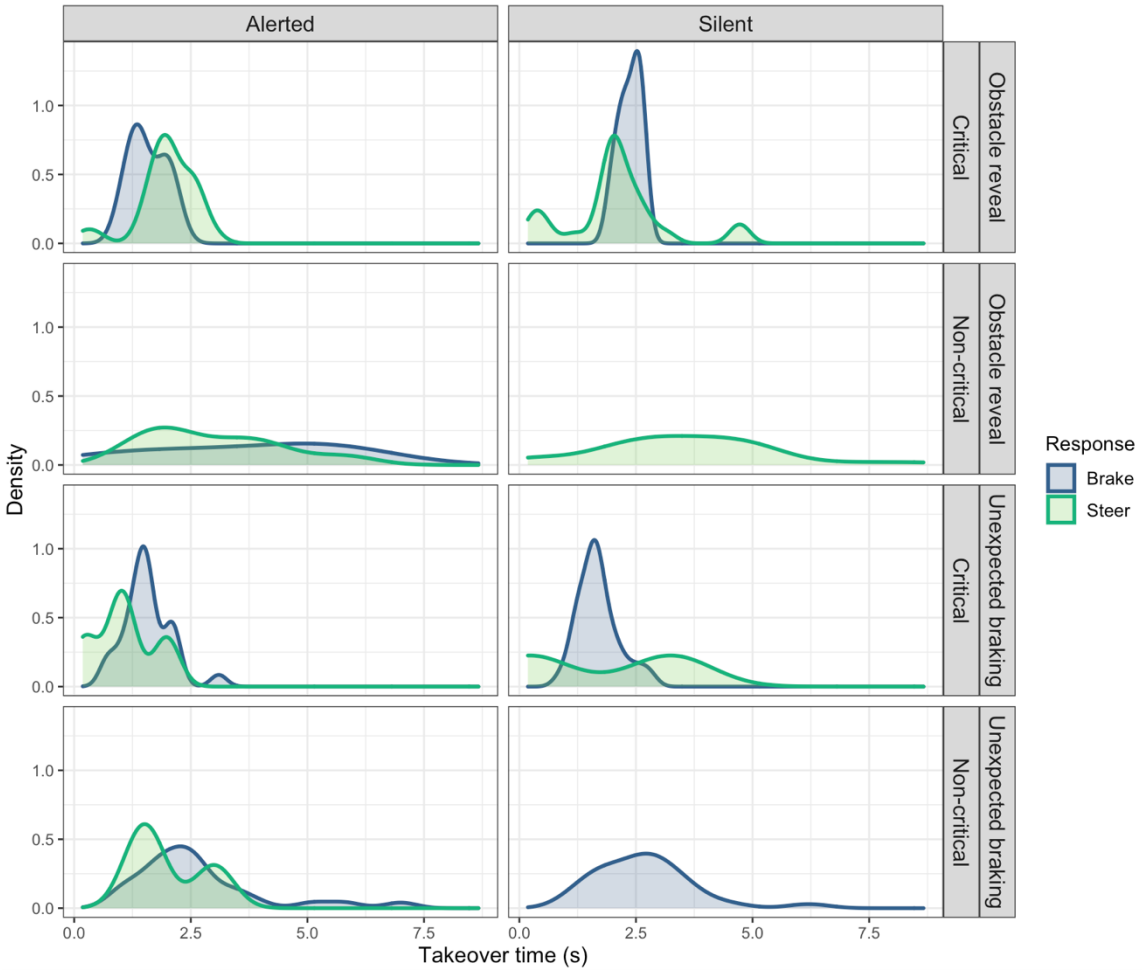

Figure 6.5 Density plots of takeover time categorized by the brake and steer response across criticality, takeover request presence, and event type

In addition to the initial maneuver, the drivers' aggregated response was analyzed. The aggregated response included subsequent maneuvers following the initial maneuver. This analysis is important from the modeling perspective as the driver's braking and

steering adjustments following the initial response can be an indicative of discrepancy between the real and predicted visual evidence (Markkula, Romano, et al., 2018). For example, the decision to steer to the adjacent lane following a braking might show that the attempted braking is not solving the conflict. This decision is mostly guided by the relative visual looming of vehicle in front.

Figure 6.6 shows the temporal illustration of braking and steering takeover times across criticality and scenario types, where the rows correspond to each individual's responses. Note that 4 outliers, that were beyond 10 s, were removed to improve readability. Due to the design of experiment, not all the participants experienced the alerted and silent failures; therefore, the takeover request type is not shown in this figure to allow for direct comparison of response types for each participant. In general, braking and steering takeovers happened with close proximity. Critical scenarios included more combination of braking and steering compared to non-critical scenarios with the occurrence of braking before steering. During emergency conflicts, braking only (i.e., without steering) has been found to be the most initial responses for most drivers (Markkula et al., 2012). Subsequently, steering was mostly observed in the situations where the driver may perceive that braking is insufficient to avoid the conflict (e.g., crash occurrence). This perception typically arises from high visual looming (low TTC), however, even in less critical situations with low visual looming, the drivers might still choose to respond with steering. This decision is normally motivated by an early detection of catching up with the lead vehicle and/or having sufficient time to plan a more confident maneuver. These findings were further supported by the cumulative distributions of the

takeovers. Figure 6.7 shows the cumulative density functions for the brake and steer takeover times aggregated with respect to the participants and scenarios. Overall, except a few early lane changing maneuvers, drivers' braking precedes the steering regardless of the criticality. Looking closely at the overlapping responses shows that in most cases as the evidence to execute a maneuver (e.g., steering) gets higher, the evidence for the other maneuver (e.g., braking) gets lower.

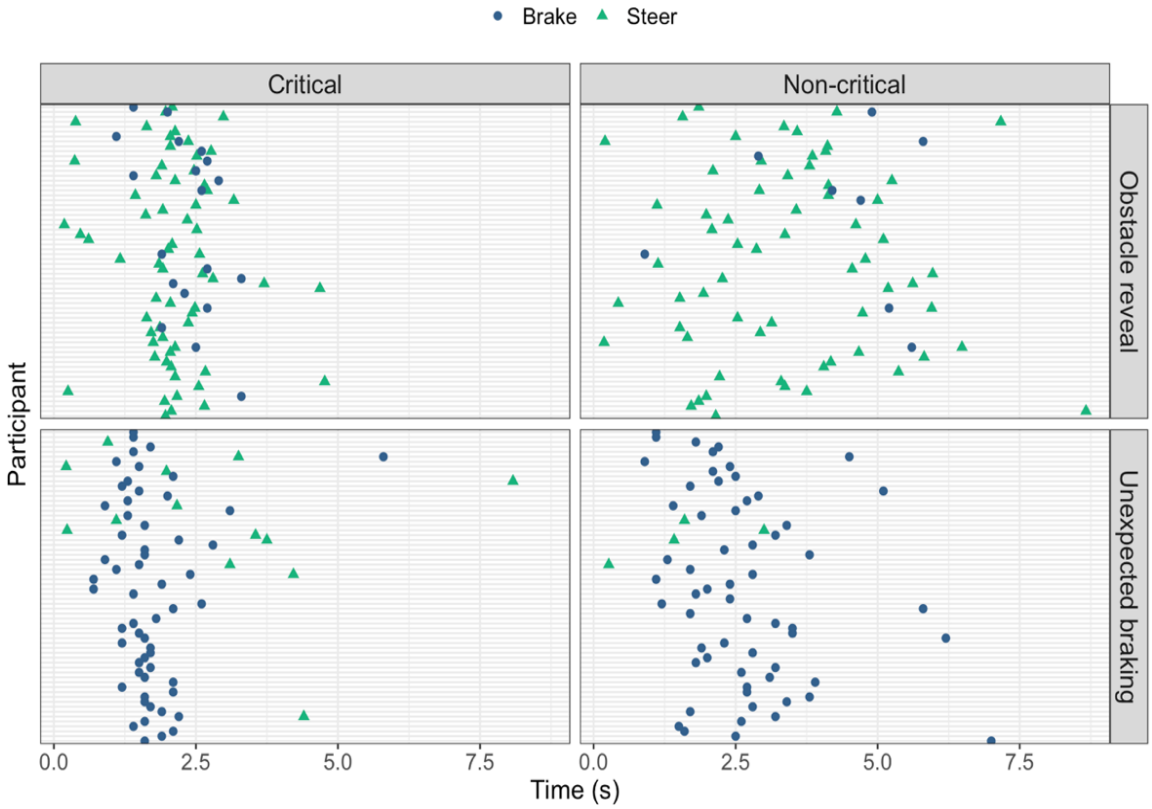

Figure 6.6 Temporal illustration of braking and steering takeover times across criticality and event types for each participant

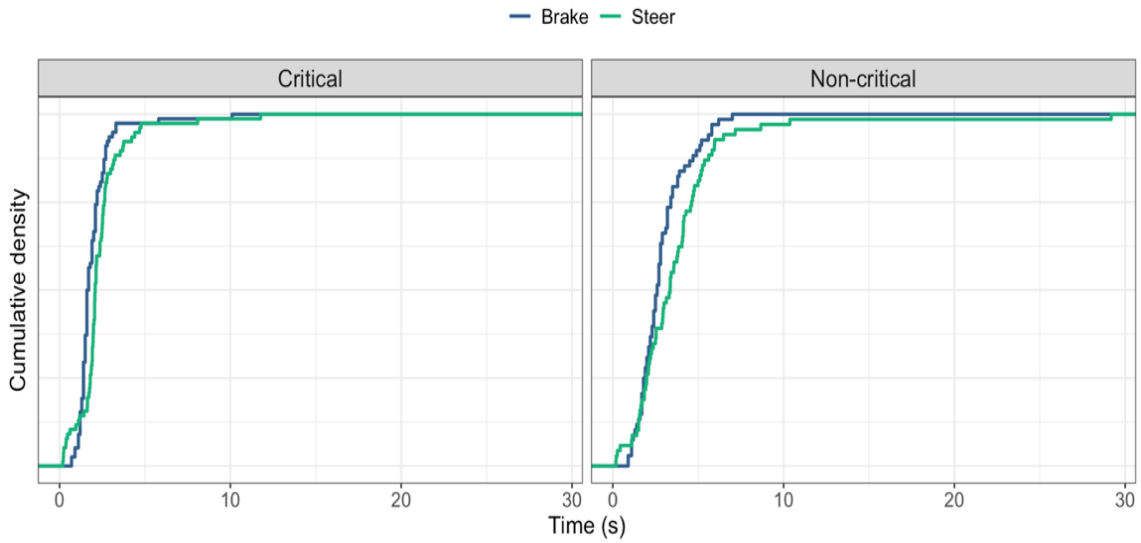

Figure 6.7 Cumulative density function associated with the braking and steering takeover times across the event criticality

Figure 6.8 represents two examples of the overlapping longitudinal deceleration and the steering wheel angle, representing the braking and steering behavior, respectively. In this figure, the black, blue, and green dashed lines show the failure onset, braking, and steering takeover times, respectively. Note that the steering input is scaled for the illustration purpose. The figure shows the close proximity of the control responses, in which the drivers initiated a braking maneuver followed by a lane change with a few seconds apart. The fact that drivers do not wait until the end of braking to initiate their steering responses is aligned with the idea of competing accumulator models, in which human brain can accumulate two sets of evidence in parallel (Usher & McClelland, 2001).

Collectively, the results of the response type analysis support the assumptions of the model regarding the braking and steering gain parameters, the association of visual

looming with the choice of response maneuver, as well as including two accumulators to account for each response.

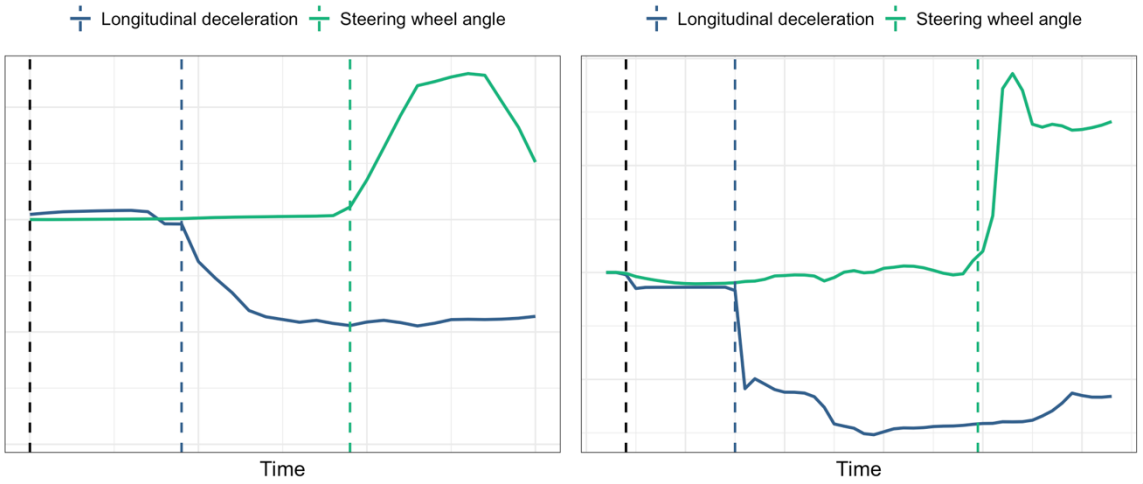

Figure 6.8 Examples of the steering and braking overlapping responses

6.4.2. Simulated Decision-making and Takeover Time

Figure 6.9 shows the posterior distributions of the non-looming evidence, m, driver's initial readiness, r, and standard deviation of the noise, σ. The drivers' takeover responses were estimated by drawing random samples from the posterior distributions of the parameters. Examining the parameter combinations across all conditions, the model predicted the choice of response (brake and steer) with 92% accuracy. Figure 6.10 shows the boxplots of the choice of response across the free parameters and the event type. Parameter σ and to a lesser extent r did not show substantial variability in terms of the response across different scenario types. Regardless of the scenario, parameter m resulted in more braking around the negative values and more steering around the positive values.

Similar to the observed experimental responses (see Figure 6.4), the model resulted in more braking in the unexpected braking and more steering in the obstacle reveal events. Although it is notable that the overall estimated braking decisions are higher.

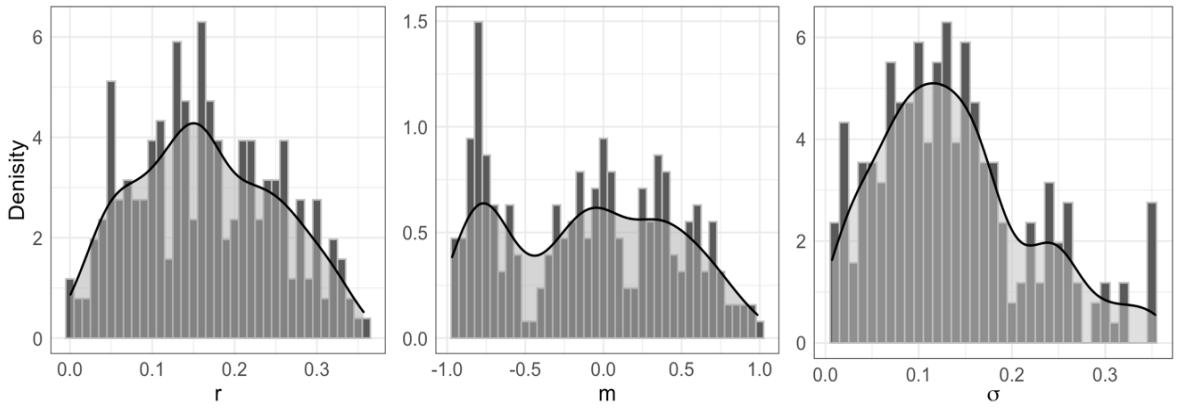

Figure 6.9 Posterior distributions of the takeover model parameters

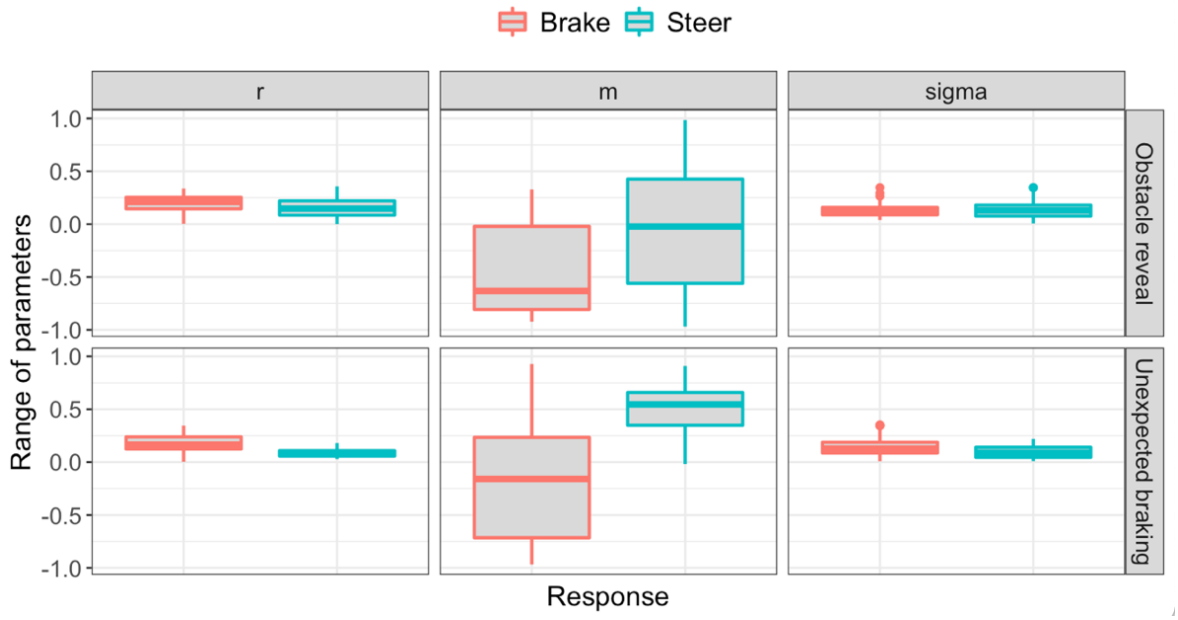

Figure 6.10 Boxplots of the parameters' posterior distributions across takeover response and event type

Figure 6.11 shows the distributions and cumulative densities of the simulated and observed takeover times across all the factors. As the figure shows, the model's estimation seems to capture the observed mean. Takeover time distributions were further explored across the experimental factors (i.e., takeover request presence, scenario criticality, and event type). Figure 6.12 illustrates these distributions. Overall, the critical scenarios showed a better fit than the non-critical scenarios, in which, the model estimates are mostly shorter than the observed data (note the left skewness in the right plots), in particular, in the unexpected braking event.

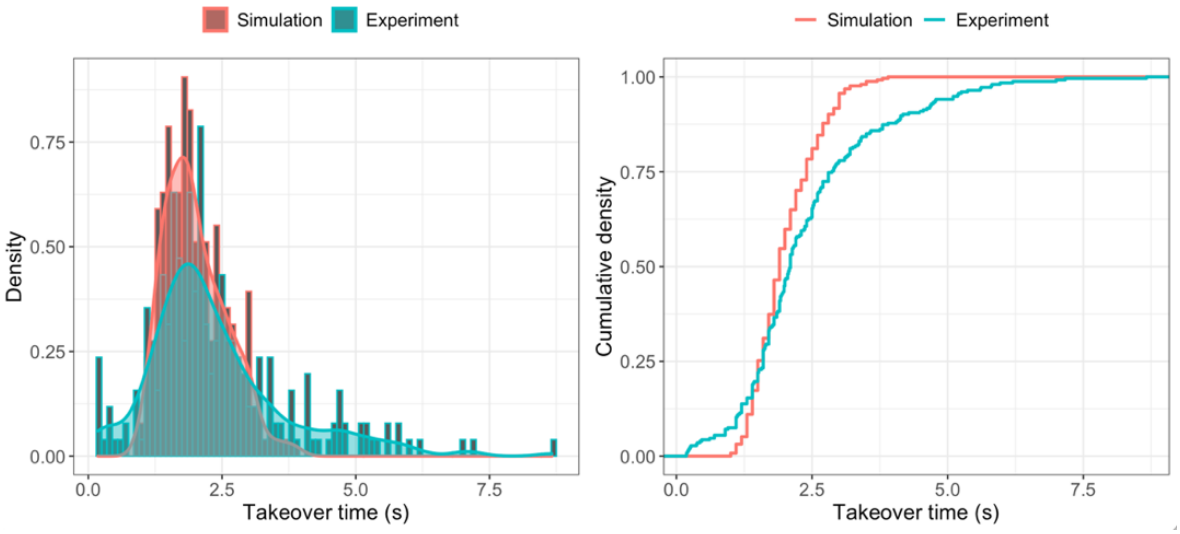

Figure 6.11 Simulated and experimental takeover time distributions

A correlation analysis has been performed to find the relationship between the posterior distributions of the free parameters. The correlation coefficient values were calculated based on the Pearson correlation method, a test statistic used to measure the statistical relationship or association between two continuous variables. The analysis

shows a slight positive correlation between the non-looming evidence and the drivers' takeover time and a slight negative correlation between the takeover time and the drivers' initial readiness and as well as the variability in the noise. However, we should be cautious in interpreting this figure as the correlations were not statistically significant.

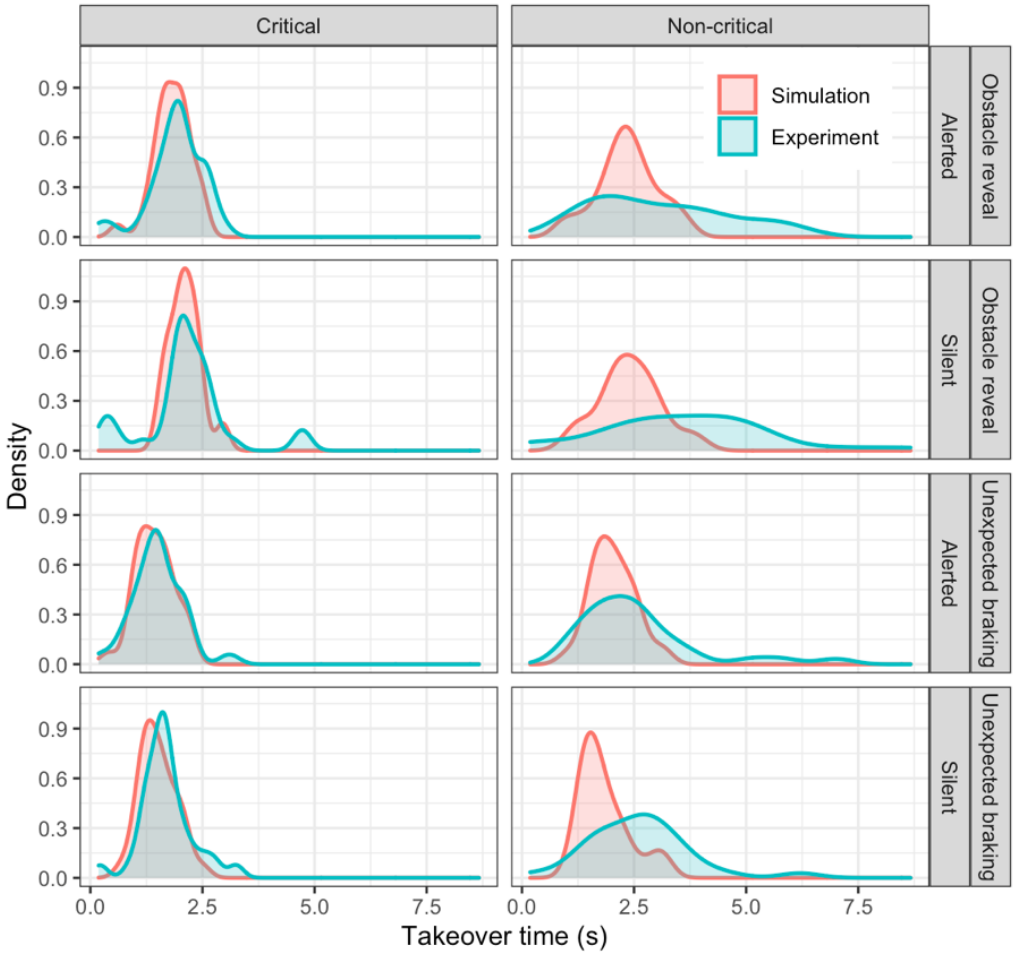

Figure 6.12 Simulated and experimental takeover time distributions across takeover request presence, event criticality, and event type

The correlations between the posterior distributions of the parameters revealed significant results among which the negative correlation between the driver's initial

readiness and non-looming evidence ($r = -0.6$) is interesting. It suggests that as the driver's readiness gets higher, for example by receiving an alert, drivers accumulate more evidence in favor of braking. This finding is consistent with the simulated response types that showed a slightly more braking with an increase in readiness. Figure 6.13 further supports these findings by showing the joint posterior distributions of the model parameters. Lighter and darker areas correspond to regions of higher and lower density.

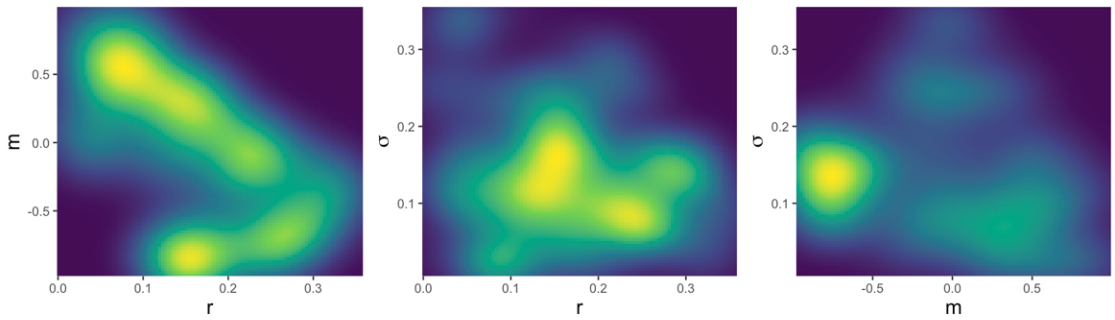

Figure 6.13 Joint posterior distributions of the model parameters

6.4.3. Simulated Control Behavior

Following the response choice and takeover time estimation, the predicted responses were fed to the control modules of the holistic framework. The rest of this section represents the simulated braking and steering responses.

6.4.3.1. Braking Control Behavior

The braking control model extends the basic piecewise linear model, developed in chapter 4 (see Figure 4.3), to directly include the perceptual cues into the model and capture the braking adjustments. Figure 6.14 shows an example of the multiple braking

applications, where each application is associated with a separate piecewise linear model. The first and second vertical dotted lines show the event onset and the onset of second brake adjustment. The dashed lines represent the release of the brake pedal. The first maneuver starts at the time of the brake takeover time and each subsequent adjustments uses the simulated data from the previous brake actuation plus a new reaction time for the starting point of each maneuver. Similar to the brake takeover time for the first braking maneuver, that was estimated in the previous section, this reaction time is estimated using an evidence accumulation model (see Equation 6.1). However, the parameters of the model are modified to only include braking. For example, the parameter m, the non-looming evidence in favor of steering, was held constant at -1, as the driver was already braking. So, setting the m value to -1 implies the accumulation of evidence in favor of braking. Similarly, the initial readiness was fixed at zero, as the drivers in the alerted condition received the warning only once. In addition, if we associate the initial readiness to the drivers' situation awareness as a result of receiving a warning, we don't expect to see any difference after the first takeover request. The variability in the noise was simulated iteratively with the range of [0:1] and eventually was set to 0.5. Following the initial reaction, the accumulator threshold was reset to 0.7, to reflect an increased brake readiness after the first brake application (Markkula, Romano, et al., 2018). In total, out of 254 observations, 108 drives didn't include any braking maneuvers. To pursue further evaluation of the model against the experimental data, these drives were excluded.

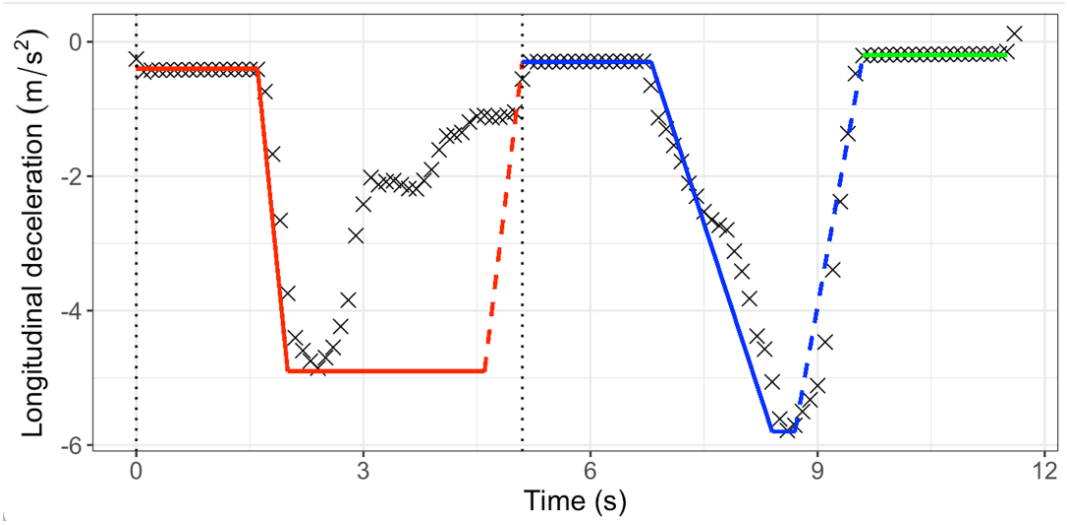

Figure 6.14 An example of multiple brake applications with the red and blue lines representing the expected fit to the experimental data

A strong relationship between the visual looming at the time of the brake and the jerk (rate of the deceleration) have been found (Bärgman et al., 2017; Markkula et al., 2016). To quantify this relationship, the jerk values were extracted from fitting a basic piecewise linear model to the experimental data for each brake adjustment. None of the drivers had more than two major brakes, made us to focus on the first two brakes following the takeover. Out of 146 observations that were initially braked, 39 continued braking. The evidence accumulation used to simulate the brake reaction times for these subsequent maneuvers successfully captured all 39 brakes. Interestingly, none of the ones who didn't feel the necessity to continue braking had accumulated evidence greater than the threshold. Figure 6.15 shows the jerk as a function of the visual looming signal for the initial (left plot) and the subsequent brake application (right plot). Next, a linear regression model was fit to the extracted values. Equation 6.3 and 6.4 show the fitted models.

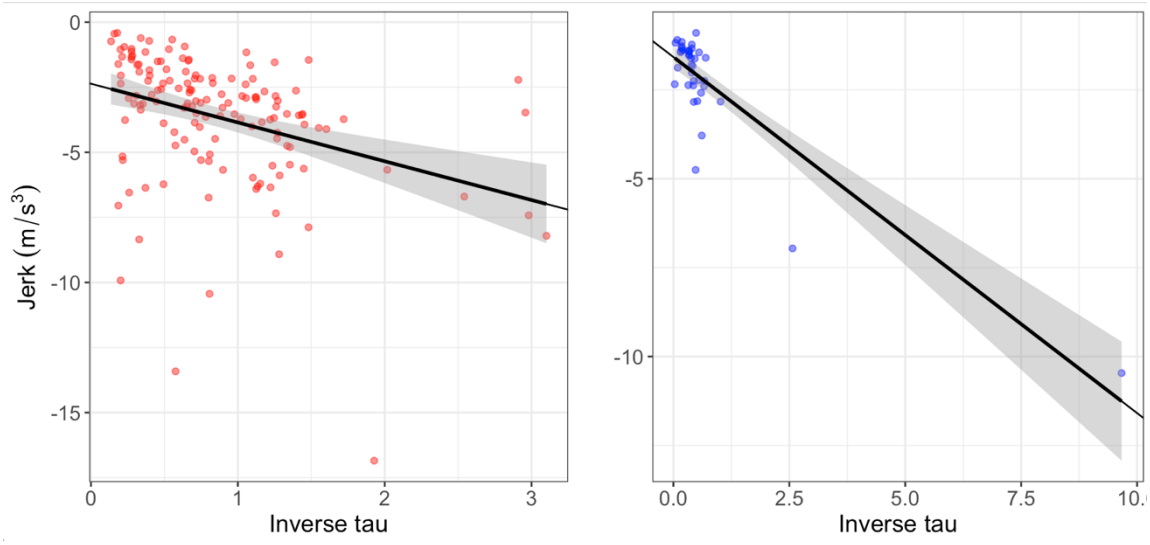

Figure 6.15 Model of jerk as a function of inverse tau at the start of the initial (left) and subsequent (right) braking maneuvers

$$j_i = -1.5\tau_{t_i}^{-1} - 2.36 \qquad \textbf{Equation 6.4}$$

$$j_s = -1\tau_{t_s}^{-1} - 1.60 \qquad \textbf{Equation 6.5}$$

Figure 6.16 shows the posterior distributions of the model parameters, in which a_{1i}, a_{1s}, and j_0 refer to the maximum deceleration of the initial braking maneuver, maximum deceleration of the subsequent braking maneuver, and the intercept of deceleration rate (jerk), respectively. The intercept of the jerk parameter (j_0) shows a relatively normal distribution, while both maximum decelerations (a_1) show a multimodal pattern, where the values are lower for the subsequent braking compared to the initial braking. One explanation for these lower values is the criticality of the events. Around 95% (37/39) of subsequent braking observations happened when the event was non-critical, while in the initial braking it was more evenly distributed (53% for critical vs.

47% for non-critical). This also justifies having two modes in the a_{1i} distribution, in which the cluster with the absolute larger values is associated with the critical events and the one with the absolute lower values is related to the non-critical events.

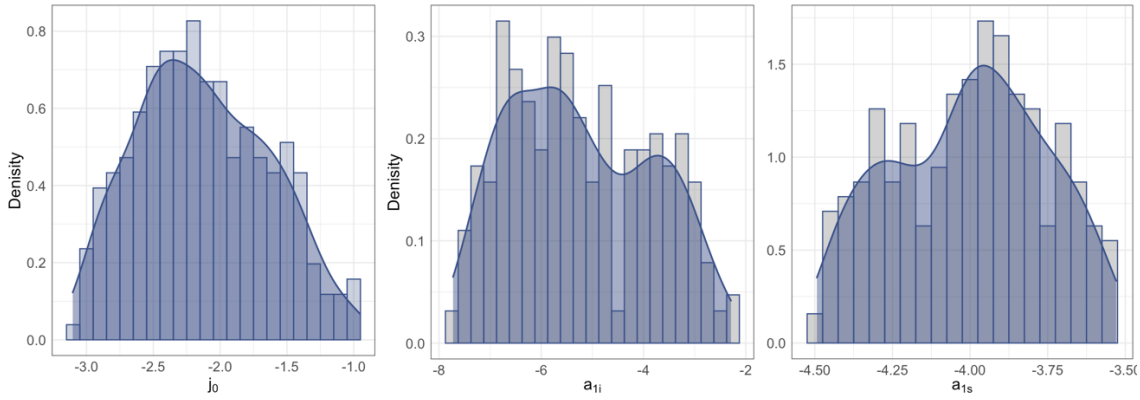

Figure 6.16 Posterior distributions of the brake control model parameters

Pearson correlation analysis showed significant positive correlations between intercept of jerk and both maximum decelerations ($r = 0.13$ for initial maximum deceleration and $r = 0.28$ for subsequent maximum deceleration). An increase in the intercept of jerk leads to an increase in the jerk (deceleration rate) itself and as the deceleration rate of the brake applications get higher, greater maximum decelerations are achieved showing some abrupt and full applications as well as some gradual and partial applications. Figure 6.17 shows the density of the joint posterior distributions, where lighter and darker areas correspond to regions of higher and lower density. Looking at the joint density plot of maximum decelerations (left plot) reveals three patterns of brake applications: A soft brake followed by a hard brake, two relatively even brakes, and a hard

brake followed by a soft with the focus being on the latter. The two right plots are mostly centered around higher jerk and maximum decelerations.

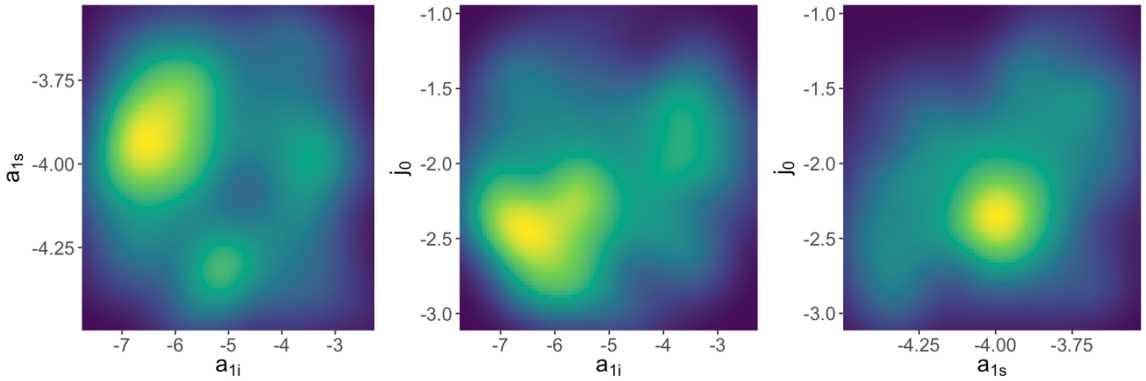

Figure 6.17 Joint posterior distributions of the braking model parameters

To simulate the brake maneuvers, for each observation random samples were drawn from the accepted range of posterior distributions. The outputs of model then were evaluated against the experimental data. Figure 6.18 shows the effect of j_0 on the simulated decelerations within the range of its posterior distribution, while the maximum deceleration was held constant. In this figure, the red line shows the observed braking maneuver from the experiment. As expected, with increasing the j_0 values, the deceleration rate gets higher, representing an acute deceleration. Figure 6.19 shows examples of the simulated (solid lines) and observed decelerations categorized by event criticality and presence or absence of the takeover request. Red dashed lines show the predicted brake takeover times. Overall, the model shows a good fit to the data. Simulating the decelerations for each observation resulted in a mean RMSE of 0.66 (0.19) between the model and observed braking inputs across the entire dataset.

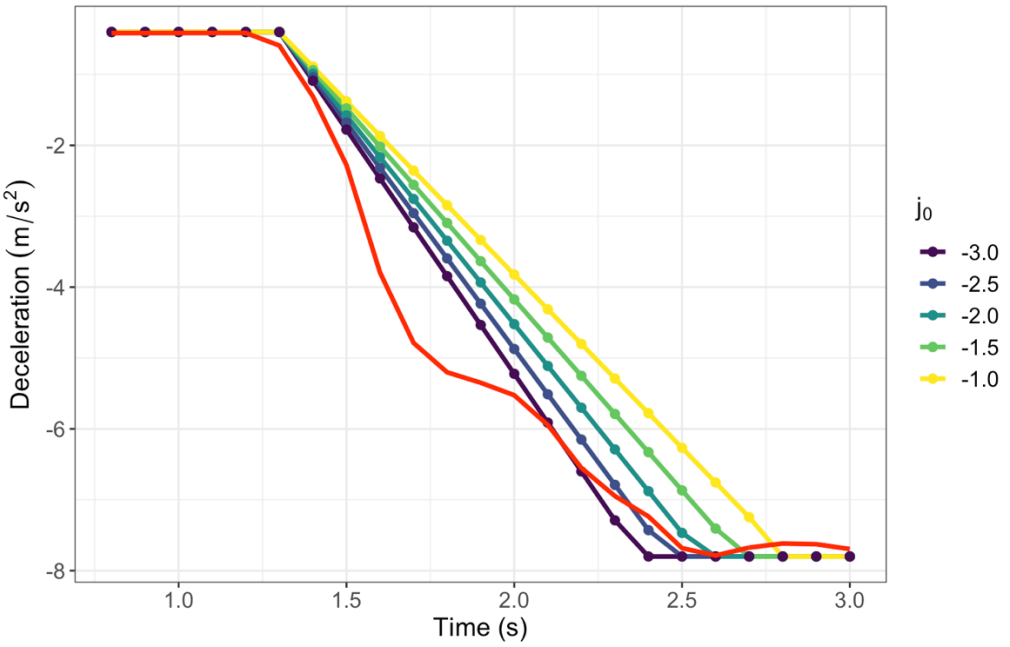

Figure 6.18 The effects of varying intercept of jerk on the simulated decelerations

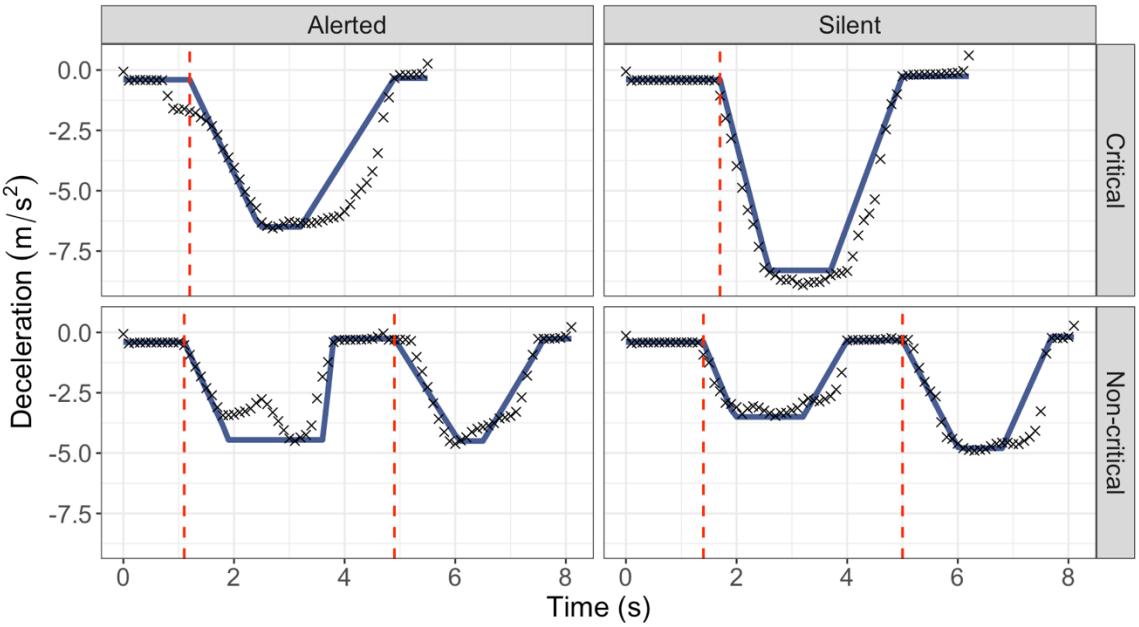

Figure 6.19 Examples of the simulated and observed brake maneuvers across criticality and takeover request types

6.4.3.2. Steering Control Behavior

The steering control model extends the open-loop avoidance model, developed in chapter 5 (see Figure 5.3 and Equation 5.1). Although most of the steering behaviors during the collision avoidance phase included a single steering primitive, a few avoidance maneuvers were composed of multiple peaks. To capture these multiple rotations, Gaussian function were applied to each peak. In total, out of 254 observations, 108 drives didn't include any steering maneuvers. For the purpose of the model evaluation against the experimental data, these drives were excluded. The avoidance steering phase, defined as the time between the steer takeover time and the last point of leftward steering wheel rotation (see Figure 5.2 for an illustration of the avoidance steering), were extracted from the entire steering profiles for further analysis. Figure 6.20 shows the relationship between the drivers' maximum steering wheel angle and maximum steering wheel angle rate in the avoidance phase. This figure indicates that the higher amplitudes of the steering rotations are associated with faster movements, in particular during the critical events. Also, there seems to be a very high inter-individual variations in the steering behavior. In most cases the maximum steering wheel rotation occurred while the driver was changing lanes. Pearson analysis shows a high correlation coefficient ($r^2 = 0.81$) across all conditions, making the Gaussian model a good candidate for the open-loop avoidance maneuver.

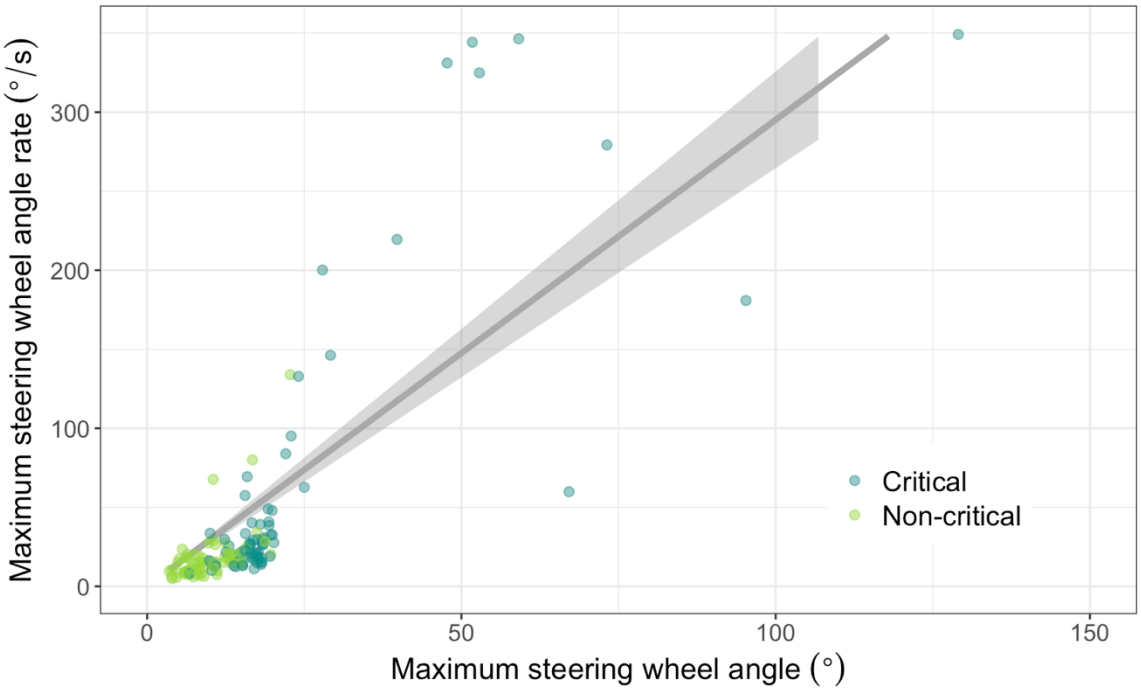

Figure 6.20 Maximum steering wheel as a function of maximum steering wheel angle rate

Figure 6.21 shows the posterior distributions of the model parameters, in which k, refers to the amplitude of the pulse, specifically the gain of the maximum visual looming after the event onset and prior to the avoidance maneuver initiation, T_A refers to the proportion of the time until driver's avoidance steering reaches its maximum value, and T_H is the pulse duration. All three posterior distributions are skewed mostly towards the lower values. The distribution of k and T_A are both aligned with the high intra variability in the maximum of the steering wheel rotation, that we observed in Figure 6.20. T_H shows a multimodal distribution, which perhaps is associated with the criticality of the event. When the event is non-critical, the steering rotations are smoother and more gradual, while in urgent events the steering wheel rotation happens in a short period of time. Figure 6.22

shows the joint posterior distributions of the model parameters, where lighter and darker areas correspond to regions of higher and lower density. The correlation analysis revealed significant correlations between all three parameters, where T_A showed negative correlations with the other two parameters while T_H and k are positively correlated.

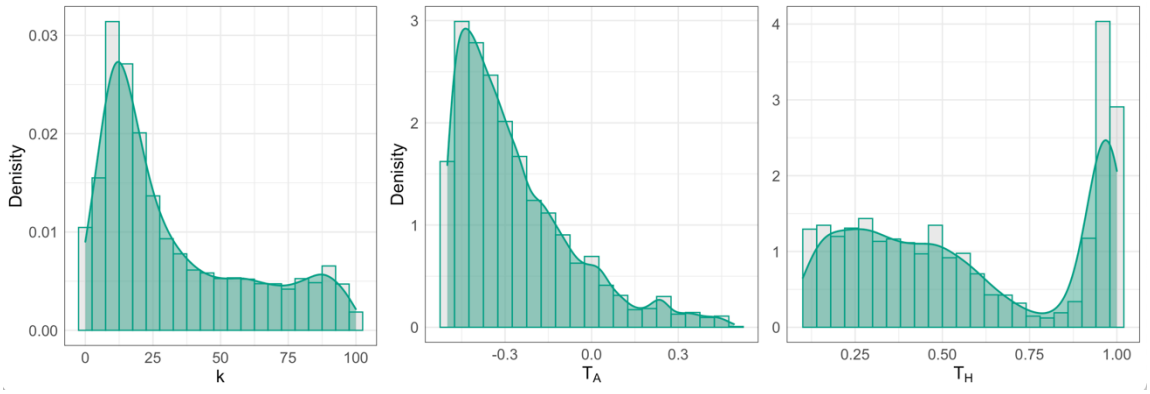

Figure 6.21 Posterior distributions of the steering control model parameters

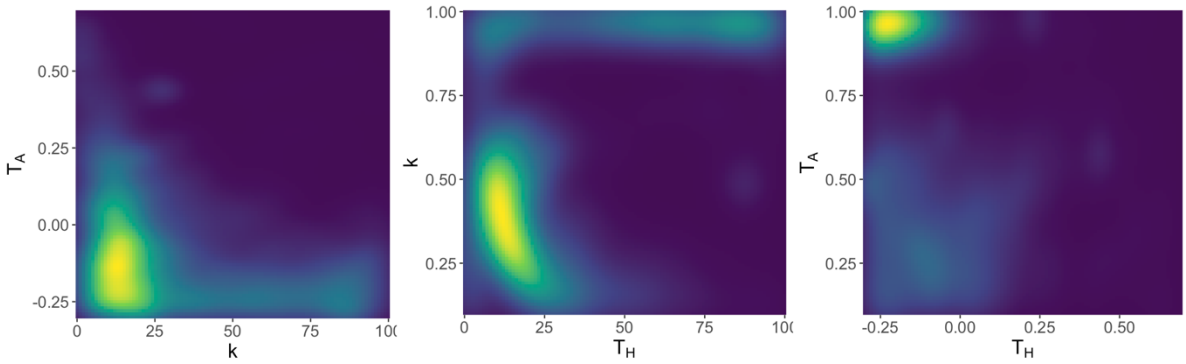

Figure 6.22 Joint posterior distributions of the steering model parameters

Drawing random samples from the posterior distributions, the steering wheel inputs were simulated. The outputs of model then were evaluated against the experimental data. Simulating the avoidance steering for each observation resulted in a mean RMSE of

2.91 (2.12) degrees between the model and the observed steering wheel angle across the entire dataset. Figure 6.23 shows examples of the simulated steering avoidance (solid lines) against the observed data across criticality and takeover request types. The red lines in this figure represent the steering takeover time. Figure 6.24 shows the effect of varying the free parameters on the simulated steering within the range of its posterior distribution. The red dots show the observed steering wheel angles from the experiment.

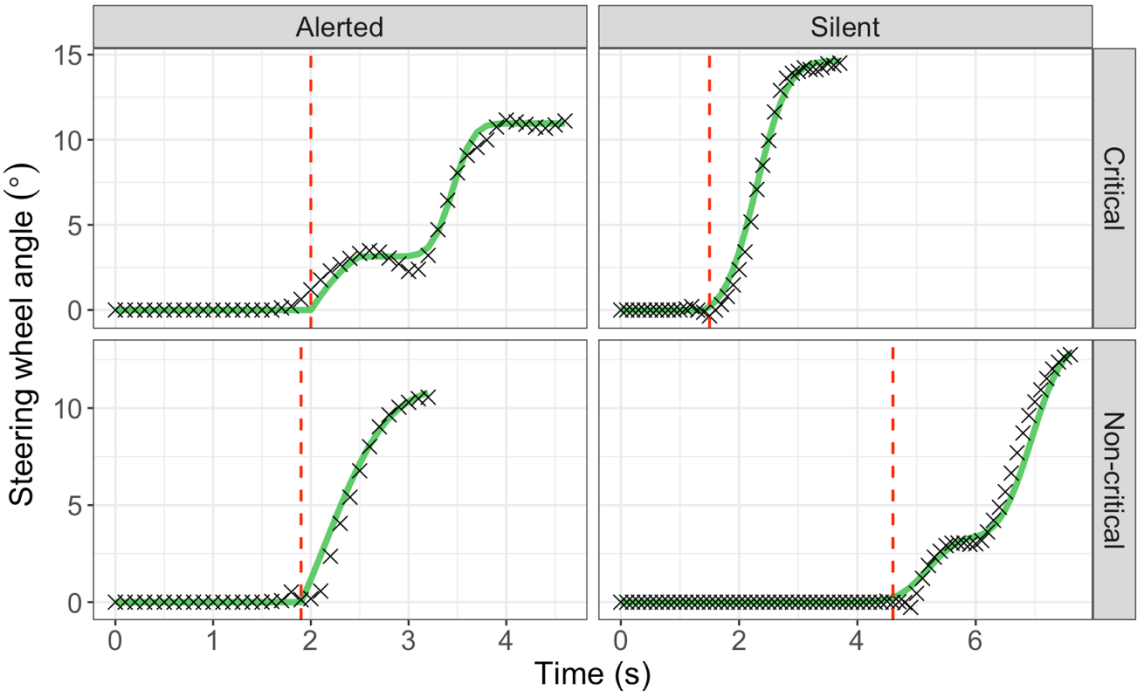

Figure 6.23 Examples of the simulated and observed steering maneuver across criticality and takeover request types during the avoidance phase

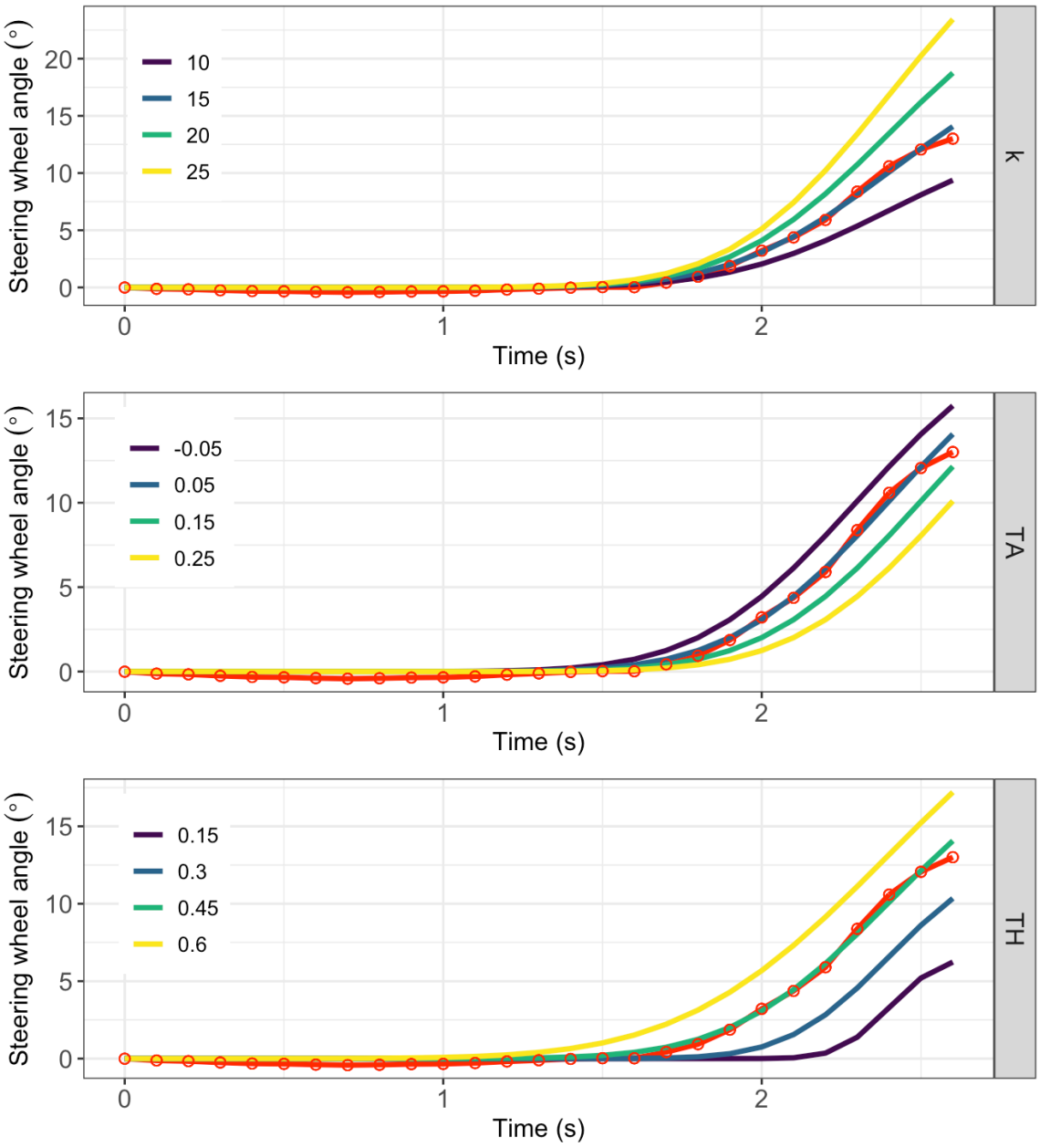

Figure 6.24 The effects of varying the model parameters on the simulated steering

6.4.3.3. Holistic View of The Takeover

After validating the individual models of decision-making, braking, and steering, the ability of the holistic model to predict the entire takeover behavior was assessed. Figure

6.25 shows an example of the simulated takeover response and control maneuvers from the holistic model.

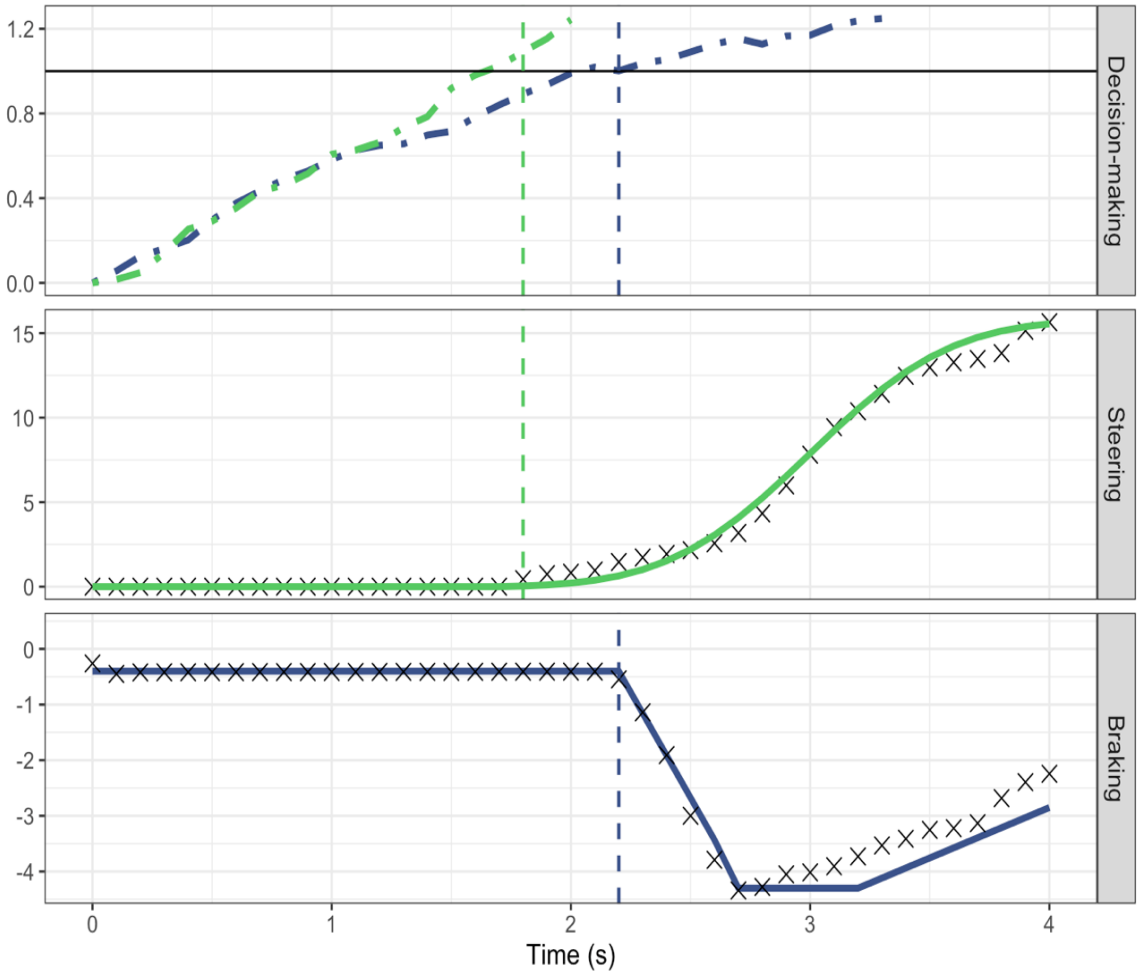

Figure 6.25 Takeover response and control behavior simulated from the holistic model

Following the automation failure, the evidence accumulation model started collecting evidence in favor of braking and/or steering. This model used visual looming of the drivers as an input and accumulated evidence up to a certain threshold (1 in our

case). Upon reaching to the desired threshold, a decision was triggered (the first accumulators reached to 1 in the top plot). In this example the steering accumulator dominated the braking, resulted in a faster reaction time for the steering rotation compared to the braking input; however, within a few seconds a braking deceleration was also applied. As the figure shows, the model can follow the observed driver behavior in both steering rotation and braking application.

6.5. Discussion

There have been several independent models that predict driver behavior in different phases of a takeover. However, a holistic modeling framework of drivers' perceptual decision-making and control response after a failure was missing. The perceptual decision-making process is typically described by evidence accumulation models, in which humans continuously collect perceptual cues for the decision alternatives and an action is triggered once this integration reaches a certain threshold. The holistic framework employed an evidence accumulation model with two accumulators associated with each decision alternative to collect the looming prediction error. The output of this model was the drivers' decision choice as well as the takeover times. The choice of response then activated the related control part of the framework and resulted in a braking and/or steering maneuver.

While, overall, the estimated takeover times showed a good fit to the observed data, in non-critical events the model predicted faster takeover times. One explanation for these shorter takeover times, is the drivers' glance location, in particular, towards the off-

road. Although the drivers can accumulate evidence using peripheral vision even when looking away from the roadway, the drift rate or the amount of evidence that the drivers accumulate during the off-road glances are less than those of looking directly at the forward roadway (Sarkar, Alambeigi, et al., 2021; Sarkar, Hickman, et al., 2021). Therefore, there is a time delay in the drivers' decision-making process compared to the simulations that the model did not capture. This is in line with our assumption that the model estimates the takeover times, given the drivers look directly at the forward roadway. Off-road glances reduce the visual looming subtending on the drivers' eyes leading to longer times to get to the required threshold. This speculation was confirmed by the videos of the drivers' glance location, that was collected using an eye-tracking device in the experimental data collection. However, the videos do not provide the drivers' specific gaze angles, that are typically used in modeling the drivers' glance direction (Sarkar, Alambeigi, et al., 2021), making it impractical to implement in the model. The next direction of this model can be extending the current evidence accumulation model to account for various gaze eccentricities. For example, yaw angle of the drivers' gaze from the forward roadway can be included as a gain to the visual looming signal.

The braking control model extended the basic piecewise linear function to capture multiple braking applications. In addition, the model was modified to associate the visual looming to the deceleration rate. The posterior distributions of the model showed that as the deceleration rate of the brake applications got higher, greater maximum decelerations were achieved, which shows that the braking inputs are either abrupt and full or more gradual and partial. This is consistent with prior work that showed the rate at which drivers

increased their deceleration (towards a maximum) was highly dependent on urgency (Markkula et al., 2016; Svärd et al., 2017). Simulating the brake input for each observation using the posterior distributions, showed an average RMSE of 0.66 (0.19) across the entire dataset, which highlights the improvement of the extended model compared to the basic piecewise linear model, developed in chapter 4 (Figure 4.5), with RMSE of 1.23 (0.66).

The steering control model modified the basic open-loop Gaussian model to account for multiple steering pulses during the takeover avoidance maneuver. Similar to the braking input, simulating the steering wheel angle rotation revealed the strength of the extended model compared to the basic open-loop model (Figure 5.6), developed in chapter 5. Posterior distribution of the parameters showed that in non-critical events, the steering rotations are smoother and more gradual, while in urgent events the steering wheel rotations are more oscillatory as they perhaps happen in a short period of time. The results of the RMSE for this model showed an average of 2.91 (2.12) degrees across the entire dataset, while this value was 4 (3.72) degree for the basic open-loop model (Alambeigi & McDonald, 2020).

The holistic model integrated different components and showed it can follow the observed driver behavior in predicting takeover time, steering rotation, and braking application. In comparison to the prior cognitive decision-making models, that predicted the drivers' braking and steering responses consecutive (Markkula, Romano, et al., 2018), this model is able to predict the steering and braking response, in parallel. In addition, it integrates the time and decision predictions with a control response. However, it should be noted that this model may suffer from error propagation after predicting the reaction

time. The evidence accumulation models for decision-making are driven by latent variables including the drift rate and the decision threshold. Using Bayesian approaches such as ABC do not provide direct access to the latent variables and rely on the input and output of the model to make inferences. Therefore, additional steps might be needed to constrain the accumulation process in order to achieve a more reliable prediction. In addition, using the common definition of takeover time (i.e., steering and braking input greater than a threshold) in the holistic model, might increase the rate of the mentioned error. The reaction time as a first demonstrable braking or steering input is a better substitute in the developed model. However, this metric should be constrained to avoid including unwanted reactions.

7. CONCLUSIONS

The advancement of automated vehicle technologies, in particular, automated vehicles, promises several socio-economic and safety advantages, (Casner et al., 2016; Fagnant & Kockelman, 2015). However, despite the benefits, many obstacles remain on the road to achieving the expected outcomes, in particular, for higher levels of automation. Driving technologies at higher levels of automation shift the allocation of function (e.g., monitoring the driving environment and executing an action) to automation. This shift can move the drivers out of the control loop and impede their ability to avoid a crash when the automation hits operational domain limits and an intervention from the driver is required (Louw & Merat, 2017). Therefore, the safety of automated vehicles is partially limited by the ability of the human driver to take over the control from automation (Brown, 2017; Lu & de Winter, 2015; McDonald et al., 2019), making it one of the most critical aspects in design considerations of automated driving systems.

During a takeover, the driver falls into completing a cognitive, physical, and visual perception-action loop to establish readiness, execute an action, evaluate, and modify it (McDonald et al., 2019). Understanding the driver's mental model of automation during this process is an essential first step in designing safer systems; however, additional steps are required to integrate these factors into the design process. Simulations represent integrative frameworks that capture bounds on human physical and cognitive performance for quantitative assessments of automated vehicle technologies (Page et al., 2015; Roesener et al., 2017). The basis for a simulation assessment can be derived from realistic

pre-crash scenarios integrated with mathematical models of driver behavior employing a particular system design. Driver model is a significant component of this process, as a poor model selection may undermine the accuracy of the safety benefit estimation (Bärgman et al., 2017; Roesener et al., 2017).

Reviewing the studies on automated vehicle takeovers as well as the models of driver behavior (chapter 2) revealed several gaps in the literature concerning the environmental, driver, or system-related factors and their impact on automated vehicle takeovers. In addition, the literature found a need for translating the existing model of driver behavior models during manual emergencies into models of automated vehicle takeovers. Chapter 3 to 6 of this dissertation addresses these gaps in an empirical study of takeovers and three studies of computational modeling using the data from a simulator experiment.

7.1. Theoretical Contributions

The first theoretical contribution of this dissertation is a comprehensive literature review on the automated vehicle takeovers as well as the driver behavior modeling (McDonald et al., 2019). The second contribution lies in investigating the effect of system design issues, including the criticality of the precipitating events (manipulated through takeover time budget) and silent failures (i.e., a failure to receive a takeover request) across various environmental conditions in a simulator experiment (Alambeigi & McDonald, 2021b). Finding silent failure as one of the prevalent causes of current on-road automated vehicle crashes highlights the theoretical contribution of exploring its effects on the

takeover performance (Alambeigi et al., 2019). A common approach to explore these effects is the frequentist null-hypothesis testing, which relies on the mean or median values for model fitting and might underestimate the safety consequences of extremes (DinparastDjadid et al., 2019; Eriksson & Stanton, 2017b). The experimental study, however, applied Bayesian multilevel regression models to this data to focus on the entire distribution of each safety metric and showed up to 84% probability of an increase in takeover time and 91% deterioration in post-takeover control associated with silent failures. This finding indicates that, even in the best case, silent failures present a risk of lower safety margins and more extreme post-takeover responses compared to alerted failures.

Further, by analyzing the posterior distributions, this study found that the minimal—yet negative—impact of the predicted takeover delays associated with silent failures, was carried over to the drivers' post-takeover behavior resulted in more aggressive responses. In line with the concept of the speed-accuracy tradeoff in decision-making processing, this finding implies that a short takeover time alone does not guarantee a safe evasive maneuver. In addition, the time given to a driver to respond to a transition of control (time budget) significantly impacts the quality of the post-takeover control and subsequent crash occurrence. These findings generate recommendations in automation system design explained later.

The next theoretical contribution of this dissertation is filling the gap in the automated vehicles' driver behavior modeling literature by developing computational models of a takeover process within the limits of system design and environmental

conditions. Different components of a takeover process were translated into models of driver behavior to assess the impacts of silent failures and event criticalities on drivers' performance across different precipitating events. Reviewing the literature on models of driver behavior showed in driver behavior during manual emergencies with that of automated vehicle transitions of control, making those validated models the first candidate for automated vehicle takeovers. One promising direction of these models was the use of visual looming-based models.

Taking the looming-based models into consideration, this dissertation extended the current braking models of manual emergencies to predict the driver's brake reaction time and control using an evidence accumulation model followed by a piecewise linear model (McDonald et al., 2021). The kinematic urgency of the scenario was captured by the driver's visual looming and the received alert was considered as an environmental cue for the need to initiate an action, therefore, captured by the non-looming evidence in the model. In addition to capturing the impacts of influential factors, the novelty of this model was feeding the brake reaction time to the control model to estimate the entire braking profile and evaluating the model on the collected experimental data.

The findings of the literature review highlighted that an effective steering model of a post-takeover control must represent both the initial avoidance maneuver and the subsequent stabilization steering. Therefore, we employed a visual-looming based open-loop Gaussian, to account for the anticipatory behavior, followed by a visual-based closed-loop model, to account for the compensatory behavior, and fitted those to the avoidance and stabilization steering profiles (Alambeigi & McDonald, 2020). One contribution of

this work is the comparison between the open-closed loop with a solely closed-loop model, where the open-closed loop model showed a better fit. The stabilization component of this model showed the capability of capturing both lane-changing behavior and steering corrections (i.e., lane-keeping) by switching the visual points. In addition, this study found that the maximum looming prior to the takeover determines the pattern of the drivers' avoidance maneuver.

The last theoretical contribution of this dissertation concerns the gap in the literature regarding the lack of a holistic model on an entire process of a takeover. We developed a comprehensive framework that can explain the underlying processes behind the drivers' decision-making and control behavior. In contrast to the prior works that modeled braking and steering responses separately, this model used two evidence accumulators and predicted the driver's action choice (i.e., braking and steering responses) and takeover times in parallel. The basic evidence accumulators, used in chapter 4, were modified to make the brake and steer gain parameters complementary. In addition, another novelty of this model was to include an additional parameter to the drift rate of the model. This parameter concerned the initial readiness of the driver in the decision-making process with the goal of capturing the impacts of the alert. Another novelty of this framework lies in the braking and steering control modules. The braking control model extended the basic piecewise linear function to account for multiple braking applications.

7.2. Practical Implications

Given the presented findings, one of the practical implications of this dissertation is in designing the human-machine interfaces (HMI). In automated driving systems, HMI should be designed to communicate the real-time system limitations and capabilities (i.e., automation state), proactively inform drivers about sensor degradation that could lead to system failures, and use cues or reminders to keep drivers engaged. To keep the drivers in the loop, tiered warnings, providing dynamic feedback, and technologies such as a switch device—that aims to engage the driver by continuously pressing a switch and warn the driver if there is no input—might be effective (May & Baldwin, 2009; B. Seppelt & Lee, 2019). Systems solutions that engage automated emergency braking or forward collision warnings following an automation disengagement rather than at safety-critical thresholds may help mitigate the effects of transitions during time-limited and critical conditions. Finally, strict operational domain limitations and geofencing should be explored.

Computational models, once validated, can be integrated into transportation safety simulation systems to encounter a variety of real traffic operational behaviors (Bärgman et al., 2017; Markkula, Romano, et al., 2018). This enables the evaluation of automated vehicle impacts on traffic safety and facilitates the subsequent potential design optimizations. The comprehensive framework developed here can serve as a baseline in these systems extending the existing driver models for virtual testing and leading to an enhancement in the design of automated vehicle technologies, an improvement in the human-automation interactions, and potentially a decrease in the consequences of automation failures.

7.3. Limitations and Future work

The studies discussed in this dissertation were conducted under a variety of constraints that might have limited their scope in multiple ways. First, the experiment represented a "best-case scenario", in which, the drivers' cognitive state (e.g., drowsiness, emotion, distraction) was not taken into account. For example, the drivers did not perform any non-driving tasks (e.g., text reading) while driving. Future work should investigate these findings with specific protocols to address the driver's cognitive state, such as distraction by having the driver to engage in a non-driving-related task.

In addition, the drivers received a generic auditory and visual warning, presented by a basic loud beep and a change in the color of the system icons at the time of the failure. Future work should investigate the impacts of ecological alerts that describe the features of the situation or provide some instruction to the driver. Some examples of these alerts include a verbal expression of "take over", a visual representation of resuming control such as hands on the steering wheel icon, or receiving a lane change suggestion presented on the forward roadway. A well-designed and timely ecological alert may decrease the takeover time (McDonald et al., 2019).

Given the controlled experimental setting of the experiment, we should be cautious in generalizing our findings to other, in particular, real-world driving conditions. Although providing a relative validity, driving in a simulator can bias the results in several ways. First, the impact of simulator realism, indicating how closely the simulator resembles an actual vehicle. While practice drivers were designed for participants to familiarize themselves with the simulator, a different feeling of the simulator's brake pedal (as an

example) from the one they used to can lead to a harsh deceleration. Next, the impact of expectancy, associating with the driver's mental model of the situation. In contrast to the real-world, the drivers' expectation of an event can impact the underlying processing times. Future studies should be conducted in on-road settings to validate the findings.

The models of driver behavior developed in this dissertation should also be the subject of future work. In order to capture the lane-changing and corrective steering, the stabilization steering model, used the crossing lane to switch the near and far visual points. This might result in a sudden drop in the model if the heading and the destination lane are not aligned. Including gaze locations in the model can guide the choice of visual points and smoothen the stabilization patterns. An explanation for the faster-predicted takeover times, found in the holistic model, particularly, in the non-critical events, is the driver's glance towards the off-road. Although the drivers can accumulate evidence using peripheral vision even when looking away from the roadway, the drift rate or the amount of information that the drivers collect during off-road glances are less than those of looking directly at the forward roadway (Sarkar, Alambeigi, et al., 2021; Sarkar, Hickman, et al., 2021). Therefore, the next step can be extending the current model to account for various gaze eccentricities.

While the models developed in this dissertation provide a promising direction in understanding the drivers' internal perceptual processing and control behavior, these models should incorporate the impacts of other system-, driver-, and environment-related factors and their interactions with the explored conditions to develop more generic models.

REFERENCES

Alambeigi, H., & McDonald, A. (2020). Modeling Post-takeover Avoidance and Stabilization Steering Control in Automated Vehicles. *Proceedings of the Human Factors and Ergonomics Society Annual Meeting*, *64*(1), 1999–2000. https://doi.org/10.1177/1071181320641483

Alambeigi, H., & McDonald, A. D. (2021a). *Investigating the effects of silent automation failure and scenario criticality on automated vehicle's takeover performance (03-036)*. https://doi.org/https://doi.org/10.15787/VTT1/C76VBC

Alambeigi, H., & McDonald, A. D. (2021b). A Bayesian Regression Analysis of the Effects of Alert Presence and Scenario Criticality on Automated Vehicle Takeover Performance. *Human Factors: The Journal of the Human Factors and Ergonomics Society*. https://doi.org/10.1177/00187208211010004

Alambeigi, H., McDonald, A. D., Manser, M., Shipp, E., & Lenneman, J. (2022). Predicting Driver Errors During Automated Vehicle Takeovers. *Transportation Research Record Journal of the Transportation Research Board*.

Alambeigi, H., McDonald, A. D., Shipp, E., & Manser, M. (2022). *Identifying Deviations from Normal Driving Behavior*. https://safed.vtti.vt.edu/sdm_downloads/identifying-deviations-from-normal-driving-behavior/

Alambeigi, H., McDonald, A. D., & Tankasala, S. R. (2019). Crash themes in automated vehicles: A topic modeling analysis of the California Department of Motor Vehicles automated vehicle crash database. *Transportation Research Board 99th Annual Meeting*. https://arxiv.org/abs/2001.11087

Alambeigi, H., Smith, A., Wei, R., McDonald, A., Arachie, C., & Huang, B. (2021). A Novel Approach to Social Media Guideline Design and Its Application to Automated Vehicle Events. *Proceedings of the Human Factors and Ergonomics Society Annual Meeting*, *65*(1), 1510–1514. https://doi.org/10.1177/1071181321651215

Anund, A., Fors, C., Hallvig, D., Åkerstedt, T., & Kecklund, G. (2013). Observer Rated Sleepiness and Real Road Driving: An Explorative Study. *PLoS ONE*, *8*(5), e64782. https://doi.org/10.1371/journal.pone.0064782

Bainbridge, L. (1983). Ironies of automation. In *Analysis, Design and Evaluation of Man–Machine Systems* (Vol. 19, Issue 6, pp. 129–135). Elsevier. https://doi.org/10.1016/B978-0-08-029348-6.50026-9

Banks, V. A., Eriksson, A., O'Donoghue, J., & Stanton, N. A. (2018). Is partially automated driving a bad idea? Observations from an on-road study. *Applied Ergonomics*, *68*(October 2017), 138–145. https://doi.org/10.1016/j.apergo.2017.11.010

Banks, V. A., Plant, K. L., & Stanton, N. A. (2017). Driver error or designer error: Using the Perceptual Cycle Model to explore the circumstances surrounding the fatal Tesla crash on 7th May 2016. *Safety Science*, *108*, 278–285. https://doi.org/10.1016/j.ssci.2017.12.023

Banks, V. A., & Stanton, N. A. (2015). Discovering Driver-vehicle Coordination Problems in Future Automated Control Systems: Evidence from Verbal Commentaries. *Procedia Manufacturing*, *3*(Ahfe), 2497–2504. https://doi.org/10.1016/j.promfg.2015.07.511

Banks, V. A., & Stanton, N. A. (2019). Analysis of driver roles: modelling the changing role of the driver in automated driving systems using EAST. *Theoretical Issues in Ergonomics Science*, *20*(3), 284–300. https://doi.org/10.1080/1463922X.2017.1305465

Bärgman, J., Boda, C.-N., & Dozza, M. (2017). Counterfactual simulations applied to SHRP2 crashes: The effect of driver behavior models on safety benefit estimations of intelligent safety systems. *Accident Analysis & Prevention*, *102*, 165–180. https://doi.org/10.1016/j.aap.2017.03.003

Bianchi Piccinini, G., Lehtonen, E., Forcolin, F., Engström, J., Albers, D., Markkula, G., Lodin, J., & Sandin, J. (2020). How Do Drivers Respond to Silent Automation Failures? Driving Simulator Study and Comparison of Computational Driver Braking Models. *Human Factors: The Journal of the Human Factors and Ergonomics Society*, *62*(7), 1212–1229. https://doi.org/10.1177/0018720819875347

Biever, W., Angell, L., & Seaman, S. (2020). Automated driving system collisions: Early lessons. *Human Factors*, *62*(2), 249–259. https://doi.org/10.1177/0018720819872034

Bitzer, S., Park, H., Blankenburg, F., & Kiebel, S. J. (2014). Perceptual decision making: drift-diffusion model is equivalent to a Bayesian model. *Frontiers in Human Neuroscience*, *8*(1 FEB), 1–17. https://doi.org/10.3389/fnhum.2014.00102

Blanco, M., Atwood, J., Russell, S., Trimble, T., McClafferty, J., & Perez, M. (2016). Automated vehicle crash rate comparison using naturalistic data. In *Virginia Tech Transportation Institute*. https://doi.org/10.13140/RG.2.1.2336.1048

Blincoe, L., Miller, T. R., Zaloshnja, E., & Lawrence, B. A. (2015). The Economic and Societal Impact of Motor Vehicle Crashes, 2010 (Revised). *Annals of Emergency*

Medicine, *66*(2), 194–196. https://doi.org/10.1016/j.annemergmed.2015.06.011

Blommer, M., Curry, R., Swaminathan, R., Tijerina, L., Talamonti, W., & Kochhar, D. (2017). Driver brake vs. steer response to sudden forward collision scenario in manual and automated driving modes. *Transportation Research Part F: Traffic Psychology and Behaviour*, *45*, 93–101. https://doi.org/10.1016/j.trf.2016.11.006

Boer, E. R. (1999). Car following from the driver's perspective. *Transportation Research Part F: Traffic Psychology and Behaviour*, *2*(4), 201–206. https://doi.org/10.1016/S1369-8478(00)00007-3

Bower, K. M. (2003). When to use Fisher's Exact Test. *American Society for Quality*, *2*(4), 35–37. http://www.keithbower.com/Miscellaneous/Fisher's Exact Test.htm

Brackstone, M., & McDonald, M. (1999). Car-following: a historical review. *Transportation Research Part F: Traffic Psychology and Behaviour*, *2*(4), 181–196. https://doi.org/10.1016/S1369-8478(00)00005-X

Brandenburg, S., & Skottke, E.-M. (2014). Switching from manual to automated driving and reverse: Are drivers behaving more risky after highly automated driving? *IEEE 17th International Conference on Intelligent Transportation Systems (ITSC) October 8-11, 2014. Qingdao, China*, 2978–2983. https://doi.org/10.1109/ITSC.2014.6958168

Breuer, J. J. (1998). Anlaysis of driver-vehicle-interactions in an evasive manoueuvre - results of "moose test" studies. *Distribution*, *1*, 620–627. http://www-nrd.nhtsa.dot.gov/pdf/Esv/esv16/98S2W35.PDF

Brown, B. (2017). The Social Life of Autonomous Cars. *Computer*, *50*(2), 92–96. https://doi.org/10.1109/MC.2017.59

Brown, B., & Laurier, E. (2017). The Trouble with Autopilots. *Proceedings of the 2017 CHI Conference on Human Factors in Computing Systems - CHI '17*, 416–429. https://doi.org/10.1145/3025453.3025462

Bueno, M., Dogan, E., Hadj Selem, F., Monacelli, E., Boverie, S., & Guillaume, A. (2016). How different mental workload levels affect the take-over control after automated driving. *IEEE 19th International Conference on Intelligent Transportation Systems (ITSC) International Conference on Intelligent Transportation Systems (ITSC)*, 2040–2045. https://doi.org/10.1109/ITSC.2016.7795886

Bürkner, P.-C. (2017). brms : An R Package for Bayesian Multilevel Models Using Stan. *Journal of Statistical Software*, *80*(1). https://doi.org/10.18637/jss.v080.i01

Bürkner, P.-C. (2018). Advanced Bayesian Multilevel Modeling with the R Package brms. *The R Journal*, *10*(1), 395. https://doi.org/10.32614/RJ-2018-017

Carsten, O., Lai, F. C. H., Barnard, Y., Jamson, A. H., & Merat, N. (2012). Control task substitution in semiautomated driving: Does it matter what aspects are automated? *Human Factors: The Journal of the Human Factors and Ergonomics Society*, *54*(5), 747–761. https://doi.org/10.1177/0018720812460246

Casner, S. M., Hutchins, E. L., & Norman, D. (2016). The challenges of partially automated driving. *Communications of the ACM*, *59*(5), 70–77. https://doi.org/10.1145/2830565

Chater, N., & Oaksford, M. (2008). *The Probabilistic Mind: Prospects for Bayesian Cognitive Science*. Oxford University Press. https://books.google.com/books?id=6Q-NS7CUTF0C

Cicchino, J. B. (2017a). Effectiveness of forward collision warning and autonomous emergency braking systems in reducing front-to-rear crash rates. *Accident Analysis and Prevention*, *99*, 142–152. https://doi.org/10.1016/j.aap.2016.11.009

Cicchino, J. B. (2017b). *Effects of blind spot monitoring systems on police-reported lane-change crashes* (Issue August).

Clark, H., & Feng, J. (2017). Age differences in the takeover of vehicle control and engagement in non-driving-related activities in simulated driving with conditional automation. *Accident Analysis and Prevention*, *106*, 468–479. https://doi.org/10.1016/j.aap.2016.08.027

Csilléry, K., Blum, M. G. B., Gaggiotti, O. E., & François, O. (2010). Approximate Bayesian Computation (ABC) in practice. *Trends in Ecology and Evolution*, *25*(7), 410–418. https://doi.org/10.1016/j.tree.2010.04.001

de Winter, J. C. F., Happee, R., Martens, M. H., & Stanton, N. A. (2014). Effects of adaptive cruise control and highly automated driving on workload and situation awareness: A review of the empirical evidence. *Transportation Research Part F: Traffic Psychology and Behaviour*, *27*(PB), 196–217. https://doi.org/10.1016/j.trf.2014.06.016

Dekker, S. W. A., & Woods, D. D. (2002). MABA-MABA or Abracadabra? Progress on Human-Automation Co-ordination. *Cognition, Technology & Work*, *4*(4), 240–244. https://doi.org/10.1007/s101110200022

Delignette-Muller, M. L., & Dutang, C. (2015). fitdistrplus: An R package for fitting distributions. *Journal of Statistical Software*, *64*(4), 1–34. https://doi.org/10.18637/jss.v064.i04

DinparastDjadid, A., Lee, J., Domeyer, J., Schwarz, C., Brown, T. L., & Gunaratne, P. (2019). Designing for the Extremes: Modeling Drivers' Response Time to Take Back Control From Automation Using Bayesian Quantile Regression. *Human Factors*. https://doi.org/10.1177/0018720819893429

Dixit, V. V., Chand, S., & Nair, D. J. (2016). Autonomous vehicles: Disengagements, accidents and reaction times. *PLOS ONE*, *11*(12), e0168054. https://doi.org/10.1371/journal.pone.0168054

Dogan, E., Rahal, M. C., Deborne, R., Delhomme, P., Kemeny, A., & Perrin, J. (2017). Transition of control in a partially automated vehicle: Effects of anticipation and non-driving-related task involvement. *Transportation Research Part F: Traffic Psychology and Behaviour*, *46*, 205–215. https://doi.org/10.1016/j.trf.2017.01.012

Driver Metrics Performance Behaviors and States Committee. (2015). *Operational definitions of driving performance measures and statistics J2944_201506*. https://doi.org/https://doi.org/10.4271/J2944_201506

Elster, C., & Wübbeler, G. (2015). Bayesian regression versus application of least squares - An example. *Metrologia*, *53*(1), S10–S16. https://doi.org/10.1088/0026-1394/53/1/S10

Endsley, M. R., & Kaber, D. B. (1999). Level of automation effects on performance, situation awareness and workload in a dynamic control task. In *Ergonomics* (Vol. 42, Issue 3). https://doi.org/10.1080/001401399185595

Endsley, M. R., & Kiris, E. O. (1995). The Out-of-the-Loop Performance Problem and Level of Control in Automation. *Human Factors: The Journal of the Human Factors and Ergonomics Society*, *37*(2), 381–394. https://doi.org/10.1518/001872095779064555

Engström, J. (2010). Scenario criticality determines the effects of working memory load on brake response time. In J. F. Krems, T. Petzoldt, & M. Henning (Eds.), *Proceedings of the European conference on human centred design for intelligent transport systems (HUMANIST)* (pp. 25–36). http://conference2010.humanist-vce.eu/document/Proceedings/1a_Engstrom.pdf

Engström, J., Bärgman, J., Nilsson, D., Seppelt, B., Markkula, G., Piccinini, G. B., & Victor, T. W. (2018). Great expectations: a predictive processing account of automobile driving. *Theoretical Issues in Ergonomics Science*, *19*(2), 156–194. https://doi.org/10.1080/1463922X.2017.1306148

Engström, J., Markkula, G., & Merat, N. (2017). Modelling the effect of cognitive load on driver reactions to a braking lead vehicle : A computational account of the cognitive control hypothesis. *Fifth International Conference on Driver Distraction*

and Inattention, 1–13.

Eriksson, A., Banks, V. A., & Stanton, N. A. (2017). Transition to manual: Comparing simulator with on-road control transitions. *Accident Analysis & Prevention*, *102*, 227–234. https://doi.org/10.1016/j.aap.2017.03.011

Eriksson, A., Petermeijer, S. M., Zimmermann, M., De Winter, J. C. F., Bengler, K. J., & Stanton, N. A. (2019). Rolling out the red (and Green) Carpet: Supporting driver decision making in automation-to-manual transitions. *IEEE Transactions on Human-Machine Systems*, *49*(1), 20–31. http://dx.doi.org/10.1109/THMS.2018.2883862

Eriksson, A., & Stanton, N. A. (2017a). Driving Performance After Self-Regulated Control Transitions in Highly Automated Vehicles. *Human Factors*, *59*(8), 1233–1248. https://doi.org/10.1177/0018720817728774

Eriksson, A., & Stanton, N. A. (2017b). Takeover time in highly automated vehicles: Noncritical transitions to and from manual control. *Human Factors*, *59*(4), 689–705. https://doi.org/10.1177/0018720816685832

Evans, N. J., & Wagenmakers, E.-J. (2020). Evidence Accumulation Models: Current Limitations and Future Directions. *The Quantitative Methods for Psychology*, *16*(2), 73–90. https://doi.org/10.20982/tqmp.16.2.p073

Fagnant, D. J., & Kockelman, K. (2015). Preparing a nation for autonomous vehicles: Opportunities, barriers and policy recommendations. *Transportation Research Part A: Policy and Practice*, *77*, 167–181. https://doi.org/10.1016/j.tra.2015.04.003

Favarò, F. M., Eurich, S. O., & Rizvi, S. S. (2019). "Human" Problems in Semi-Autonomous Vehicles: Understanding Drivers' Reactions to Off-Nominal Scenarios. *International Journal of Human–Computer Interaction*, *00*(00), 1–16. https://doi.org/10.1080/10447318.2018.1561784

Favarò, F. M., Nader, N., Eurich, S. O., Tripp, M., & Varadaraju, N. (2017). Examining accident reports involving autonomous vehicles in California. *PLOS ONE*, *12*(9), e0184952. https://doi.org/10.1371/journal.pone.0184952

Feldhütter, A., Gold, C., Schneider, S., & Bengler, K. (2017). How the Duration of Automated Driving Influences Take-Over Performance and Gaze Behavior. In B. Deml, P. Stock, R. Bruder, & C. M. Schlick (Eds.), *Advances in Ergonomic Design of Systems, Products and Processes* (pp. 309–318). Springer Berlin Heidelberg. https://doi.org/10.1007/978-3-662-53305-5_22

Fildes, B., Keall, M., Bos, N., Lie, A., Page, Y., Pastor, C., Pennisi, L., Rizzi, M., Thomas, P., & Tingvall, C. (2015). Effectiveness of low speed autonomous

emergency braking in real-world rear-end crashes. *Accident Analysis and Prevention*, *81*, 24–29. https://doi.org/10.1016/j.aap.2015.03.029

Forster, Y., Naujoks, F., Neukum, A., & Huestegge, L. (2017). Driver compliance to take-over requests with different auditory outputs in conditional automation. *Accident Analysis and Prevention*, *109*(October), 18–28. https://doi.org/10.1016/j.aap.2017.09.019

Gazis, D. C., Herman, R., & Rothery, R. W. (1961). Nonlinear Follow-the-Leader Models of Traffic Flow. *Operations Research*, *9*(4), 545–567. https://doi.org/10.1287/opre.9.4.545

General Motors. (2018). *GM Cruise LLC*. https://getcruise.com

Ghazizadeh, M., Lee, J., & Boyle, L. N. (2012). Extending the Technology Acceptance Model to assess automation. *Cognition, Technology and Work*, *14*(1), 39–49. https://doi.org/10.1007/s10111-011-0194-3

Gipps, P. G. (1981). A behavioural car-following model for computer simulation. *Transportation Research Part B: Methodological*, *15*(2), 105–111. https://doi.org/10.1016/0191-2615(81)90037-0

Gold, C., Berisha, I., & Bengler, K. J. (2015). Utilization of drivetime - Performing non-driving related tasks while driving highly automated. *Proceedings of the Human Factors and Ergonomics Society*, *2015-Janua*(2013), 1666–1670. https://doi.org/10.1177/1541931215591360

Gold, C., Damböck, D., Bengler, K. J., & Lorenz, L. (2013). Partially Automated Driving as a Fallback Level of High Automation. In *6. Tagung Fahrerassistenzsysteme. Der Weg zum automatischen Fahren.*

Gold, C., Damböck, D., Lorenz, L., & Bengler, K. J. (2013). Take over! How long does it take to get the driver back into the loop? *Proceedings of the Human Factors and Ergonomics Society*, 1938–1942. https://doi.org/10.1177/1541931213571433

Gold, C., Happee, R., & Bengler, K. J. (2017). Modeling take-over performance in level 3 conditionally automated vehicles. *Accident Analysis & Prevention*, *116*, 3–13. https://doi.org/10.1016/j.aap.2017.11.009

Gold, C., Körber, M., Lechner, D., & Bengler, K. (2016). Taking Over Control From Highly Automated Vehicles in Complex Traffic Situations. *Human Factors: The Journal of the Human Factors and Ergonomics Society*, *58*(4), 642–652. https://doi.org/10.1177/0018720816634226

Gonçalves, J., Happee, R., & Bengler, K. J. (2016). Drowsiness in conditional

automation: Proneness, diagnosis and driving performance effects. *IEEE Conference on Intelligent Transportation Systems, Proceedings, ITSC*, *31*(15), 873–878. https://doi.org/10.1109/ITSC.2016.7795658

Goncalves, R. C., Louw, T., Markkula, G., & Merat, N. (2019). Applicability of risky decision-making theory to understand drivers ' behaviour during transitions of control in vehicle automation. *Ergodesign & USIHC*.

Gray, R., & Regan, D. (1998). Accuracy of estimating time to collision using binocular and monocular information. *Vision Research*, *38*(4), 499–512. https://doi.org/10.1016/S0042-6989(97)00230-7

Greenlee, E. T., DeLucia, P. R., & Newton, D. C. (2018). Driver Vigilance in Automated Vehicles: Hazard Detection Failures Are a Matter of Time. *Human Factors: The Journal of the Human Factors and Ergonomics Society*, 1–12. https://doi.org/10.1177/0018720818761711

Hamdar, S. H., Treiber, M., Mahmassani, H. S., & Kesting, A. (2008). Modeling Driver Behavior as Sequential Risk-Taking Task. *Transportation Research Record: Journal of the Transportation Research Board*, *2088*(2088), 208–217. https://doi.org/10.3141/2088-22

Hancock, P. A. (2007). On the process of automation transition in multitask human-machine systems. *IEEE Transactions on Systems, Man, and Cybernetics Part A:Systems and Humans*, *37*(4), 586–598. https://doi.org/10.1109/TSMCA.2007.897610

Hancock, P. A., Jagacinski, R. J., Parasuraman, R., Wickens, C. D., Wilson, G. F., & Kaber, D. B. (2013). Human-automation interaction research: Past, present, and future. *Ergonomics in Design*, *21*(2), 9–14. https://doi.org/10.1177/1064804613477099

Happee, R., Gold, C., Radlmayr, J., Hergeth, S., & Bengler, K. J. (2017). Take-over performance in evasive manoeuvres. *Accident Analysis and Prevention*, *106*, 211–222. https://doi.org/10.1016/j.aap.2017.04.017

Hergeth, S., Lorenz, L., & Krems, J. F. (2017). Prior Familiarization with Takeover Requests Affects Drivers' Takeover Performance and Automation Trust. *Human Factors*, *59*(3), 457–470. https://doi.org/10.1177/0018720816678714

Hu, M., Liao, Y., Wang, W., Li, G., Cheng, B., & Chen, F. (2017). Decision Tree-Based Maneuver Prediction for Driver Rear-End Risk-Avoidance Behaviors in Cut-In Scenarios. *Journal of Advanced Transportation*, 1–12. https://doi.org/10.1155/2017/7170358

Inagaki, T., & Sheridan, T. B. (2018). A critique of the SAE conditional driving automation definition, and analyses of options for improvement. *Cognition, Technology and Work*, *Sae 2016*, 1–10. https://doi.org/10.1007/s10111-018-0471-5

Isaksson-Hellman, I., & Lindman, M. (2016). Evaluation of the crash mitigation effect of low-speed automated emergency braking systems based on insurance claims data. *Traffic Injury Prevention*, *17*(sup1), 42–47. https://doi.org/10.1080/15389588.2016.1186802

Jabot, F., Faure, T., & Dumoulin, N. (2013). EasyABC: Performing efficient approximate Bayesian computation sampling schemes using R. *Methods in Ecology and Evolution*, *4*(7), 684–687. https://doi.org/10.1111/2041-210X.12050

Jabot, F., Faure, T., & Dumoulin, N. (2015). *EasyABC : a R package to perform efficient approximate Bayesian computation sampling schemes Overview of the package EasyABC*. 1–18.

Jamson, A. H., Merat, N., Carsten, O. M. J., & Lai, F. C. H. (2013). Behavioural changes in drivers experiencing highly-automated vehicle control in varying traffic conditions. *Transportation Research Part C: Emerging Technologies*, *30*, 116–125. https://doi.org/10.1016/J.TRC.2013.02.008

Jin, S., Wang, D.-H., & Yang, X.-R. (2011). Non-Lane-Based Car-Following Model with Visual Angle Information. *Transportation Research Record: Journal of the Transportation Research Board*, *2249*, 7–14. https://doi.org/10.3141/2249-02

Jurgensohn, T. (2007). Control theory models of the driver. In P. C. Cacciabue (Ed.), *Modelling Driver Behaviour in Automotive Environments: Critical Issues in Driver Interactions with Intelligent Transport Systems* (pp. 277–292). Springer. https://doi.org/10.1007/978-1-84628-618-6

Kaber, D. B., & Endsley, M. R. (2004). The effects of level of automation and adaptive automation on human performance, situation awareness and workload in a dynamic control task. In *Theoretical Issues in Ergonomics Science* (Vol. 5, Issue 2). Taylor & Francis. https://doi.org/10.1080/1463922021000054335

Kaplan, S., & Prato, C. G. (2012). Associating Crash Avoidance Maneuvers With Driver Attributes and Accident Characteristics: A Mixed Logit Model Approach. *Traffic Injury Prevention*, *13*(3), 315–326. https://doi.org/10.1080/15389588.2011.654015

Karabatsos, G., & Leisen, F. (2018). An approximate likelihood perspective on ABC methods. *Statistics Surveys*, *12*(630677), 66–104. https://doi.org/10.1214/18-SS120

Kerschbaum, P., Lorenz, L., & Bengler, K. J. (2015). A transforming steering wheel for highly automated cars. *IEEE Intelligent Vehicles Symposium (IV) . COEX, Seoul,*

Korea. COEX, Seoul, Korea, 1287–1292.

Kiefer, R. J., Flannagan, C. A., & Jerome, C. J. (2006). Time-to-Collision Judgments Under Realistic Driving Conditions. *Human Factors: The Journal of the Human Factors and Ergonomics Society*, *48*(2), 334–345. https://doi.org/10.1518/001872006777724499

Kiefer, R. J., Leblanc, D. J., & Flannagan, C. A. (2005). Developing an inverse time-to-collision crash alert timing approach based on drivers' last-second braking and steering judgments. *Accident Analysis and Prevention*, *37*(2), 295–303. https://doi.org/10.1016/j.aap.2004.09.003

Körber, M., Baseler, E., & Bengler, K. J. (2018). Introduction matters: Manipulating trust in automation and reliance in automated driving. *Applied Ergonomics*, *66*, 18–31. https://doi.org/10.1016/j.apergo.2017.07.006

Körber, M., Cingel, A., Zimmermann, M., & Bengler, K. (2015). Vigilance Decrement and Passive Fatigue Caused by Monotony in Automated Driving. *6th International Conference on Applied Human Factors and Ergonomics (AHFE 2015) and the Affiliated Conferences, AHFE 2015*, *3*(Ahfe), 2403–2409. https://doi.org/10.1016/j.promfg.2015.07.499

Körber, M., Gold, C., Lechner, D., Bengler, K. J., & Koerber, M. (2016). The influence of age on the take-over of vehicle control in highly automated driving. *Transportation Research Part F: Traffic Psychology and Behaviour*, *39*, 19–32. https://doi.org/10.1016/j.trf.2016.03.002

Kreuzmair, C., & Meyer, M. L. (2017). The Influence of Driver Fatigue on Take-over Performance in Highly Automated Vehicles. *25th International Technical Conference on the Enhanced Safety of Vehicles (ESV) National Highway Traffic Safety Administration*, 1–7. http://indexsmart.mirasmart.com/25esv/PDFfiles/25ESV-000199.pdf

Kruschke, J. K., & Liddell, T. M. (2018). Bayesian data analysis for newcomers. *Psychonomic Bulletin and Review*, *25*(1), 155–177. https://doi.org/10.3758/s13423-017-1272-1

Lee, D. (1976). A Theory of Visual Control of Braking Based on Information about Time-to-Collision. *Perception*, *5*(4), 437–459. https://doi.org/10.1068/p050437

Lee, J. D. (2018). Perspectives on Automotive Automation and Autonomy. *Journal of Cognitive Engineering and Decision Making*, *12*(1), 53–57. https://doi.org/10.1177/1555343417726476

Lee, J., & Kolodge, K. (2018). Understanding Attitudes Towards Self-Driving Vehicles:

Quantitative Analysis of Qualitative Data. *Proceedings of the Human Factors and Ergonomics Society Annual Meeting*, *62*(1), 1399–1403. https://doi.org/10.1177/1541931218621319

Lee, J., & See, K. A. (2004). Trust in Automation: Designing for Appropriate Reliance. *Human Factors: The Journal of the Human Factors and Ergonomics Society*, *46*(1), 50–80. https://doi.org/10.1518/hfes.46.1.50_30392

Lee, M. D. (2008). Three case studies in the Bayesian analysis of cognitive models. *Psychonomic Bulletin and Review*, *15*(1), 1–15. https://doi.org/10.3758/PBR.15.1.1

Lee, M. D. (2011). How cognitive modeling can benefit from hierarchical Bayesian models. *Journal of Mathematical Psychology*, *55*(1), 1–7. https://doi.org/10.1016/j.jmp.2010.08.013

Li, S., Blythe, P., Guo, W., & Namdeo, A. (2018). Investigation of older driver's take-over control performance in highly automated vehicles in adverse weather conditions. *IET Intelligent Transport Systems*.

Li, Y., Zhang, L., Zhang, B., Zheng, T., Feng, H., & Li, Y. (2016). Non-lane-discipline-based car-following model considering the effect of visual angle. *Nonlinear Dynamics*, *85*(3), 1901–1912. https://doi.org/10.1007/s11071-016-2803-4

Lorenz, L., Kerschbaum, P., & Schumann, J. (2014). Designing take over scenarios for automated driving: How does augmented reality support the driver to get back into the loop? *Proceedings of the Human Factors and Ergonomics Society*, *51*, 1681–1685. https://doi.org/10.1177/1541931214581351

Louw, T., Kountouriotis, G., Carsten, O., & Merat, N. (2015). Driver Inattention During Vehicle Automation: How Does Driver Engagement Affect Resumption Of Control? *4th International Driver Distraction and Inattention Conference*, 9–11.

Louw, T., Madigan, R., Carsten, O., & Merat, N. (2017). Were they in the loop during automated driving? Links between visual attention and crash potential. *Injury Prevention*, *23*(4), 281–286. https://doi.org/10.1136/injuryprev-2016-042155

Louw, T., Markkula, G., Boer, E., Madigan, R., Carsten, O., & Merat, N. (2017). Coming back into the loop: Drivers' perceptual-motor performance in critical events after automated driving. *Accident Analysis & Prevention*, *108*, 9–18. https://doi.org/10.1016/j.aap.2017.08.011

Louw, T., & Merat, N. (2017). Are you in the loop? Using gaze dispersion to understand driver visual attention during vehicle automation. *Transportation Research Part C: Emerging Technologies*, *76*, 35–50. https://doi.org/10.1016/j.trc.2017.01.001

Louw, T., Merat, N., & Jamson, A. H. (2015). Engaging with highly automated driving. To be or not to be in the loop. *8th International Driving Symposium on Human Factors in Driver Assessment, Training and Vehicle Design, Salt Lake City, Utah, USA*, *1996*, 190–196. https://doi.org/10.13140/RG.2.1.2788.9760

Lu, Z., & de Winter, J. C. F. (2015). A Review and Framework of Control Authority Transitions in Automated Driving. *Procedia Manufacturing*, *3*(Ahfe), 2510–2517. https://doi.org/10.1016/j.promfg.2015.07.513

Lu, Z., Happee, R., Cabrall, C. D. D., Kyriakidis, M., & de Winter, J. C. F. (2016). Human factors of transitions in automated driving: A general framework and literature survey. *Transportation Research Part F: Traffic Psychology and Behaviour*, *43*, 183–198. https://doi.org/10.1016/j.trf.2016.10.007

Macadam, C. C. (2003). Understanding and Modeling the Human Driver. *Vehicle System Dynamics*, *40*(1–3), 101–134. https://doi.org/10.1076/vesd.40.1.101.15875

Madigan, R., Louw, T., & Merat, N. (2018). The effect of varying levels of vehicle automation on drivers' lane changing behaviour. *PLoS ONE*, *13*(2), 1–17. https://doi.org/10.1371/journal.pone.0192190

Margiotta, R., & Washburn, S. (2017). *Simplified Highway Capacity Calculation Method for the Highway Performance Monitoring System* (Issue October). https://trid.trb.org/view/1528420

Marjoram, P., Molitor, J., Plagnol, V., & Tavaré, S. (2003). Markov chain Monte Carlo without likelihoods. *Proceedings of the National Academy of Sciences of the United States of America*, *100*(26), 15324–15328. https://doi.org/10.1073/pnas.0306899100

Markkula, G. (2014). Modeling driver control behavior in both routine and near-accident driving. *Proceedings of the Human Factors and Ergonomics Society*, *2014-Janua*, 879–883. https://doi.org/10.1177/1541931214581185

Markkula, G., Benderius, O., & Wahde, M. (2014). Comparing and validating models of driver steering behaviour in collision avoidance and vehicle stabilisation. *Vehicle System Dynamics*, *52*(12), 1658–1680. https://doi.org/10.1080/00423114.2014.954589

Markkula, G., Benderius, O., Wolff, K., & Wahde, M. (2012). A Review of Near-Collision Driver Behavior Models. *Human Factors: The Journal of the Human Factors and Ergonomics Society*, *54*(6), 1117–1143. https://doi.org/10.1177/0018720812448474

Markkula, G., Boer, E., Romano, R., & Merat, N. (2018). Sustained sensorimotor

control as intermittent decisions about prediction errors: computational framework and application to ground vehicle steering. *Biological Cybernetics*, *112*(3), 181–207. https://doi.org/10.1007/s00422-017-0743-9

Markkula, G., Engström, J., Lodin, J., Bärgman, J., & Victor, T. W. (2016). A farewell to brake reaction times? Kinematics-dependent brake response in naturalistic rear-end emergencies. *Accident Analysis & Prevention*, *95*, 209–226. https://doi.org/10.1016/j.aap.2016.07.007

Markkula, G., Romano, R., Madigan, R., Fox, C. W., Giles, O. T., & Merat, N. (2018). Models of Human Decision-Making as Tools for Estimating and Optimizing Impacts of Vehicle Automation. *Transportation Research Record: Journal of the Transportation Research Board*, *2672*(37), 153–163. https://doi.org/10.1177/0361198118792131

Markkula, G., Uludağ, Z., Wilkie, R. M., & Billington, J. (2021). Accumulation of continuously time-varying sensory evidence constrains neural and behavioral responses in human collision threat detection. *PLOS Computational Biology*, *17*(7), e1009096. https://doi.org/10.1371/journal.pcbi.1009096

May, J. F., & Baldwin, C. L. (2009). Driver fatigue: The importance of identifying causal factors of fatigue when considering detection and countermeasure technologies. *Transportation Research Part F: Traffic Psychology and Behaviour*, *12*(3), 218–224. https://doi.org/10.1016/j.trf.2008.11.005

McDonald, A. D., Alambeigi, H., Engström, J., Markkula, G., Vogelpohl, T., Dunne, J., & Yuma, N. (2019). Toward Computational Simulations of Behavior During Automated Driving Takeovers: A Review of the Empirical and Modeling Literatures. *Human Factors: The Journal of the Human Factors and Ergonomics Society*, *61*(4), 642–688. https://doi.org/10.1177/0018720819829572

McDonald, A. D., Sarkar, A., Hickman, J. S., Alambeigi, H., Markkula, G., & Vogelpohl, T. (2021). *Modeling driver behavior during automated vehicle platooning failures*. https://safed.vtti.vt.edu/wp-content/uploads/2021/01/Safe-D-Final-Research-Report-03-036_Submitted.pdf

Melcher, V., Rauh, S., Diederichs, F., Widlroither, H., Bauer, W., HaraldWidlroither, & Bauer, W. (2015). Take-Over Requests for Automated Driving. *Procedia Manufacturing*, *3*, 2867–2873. https://doi.org/10.1016/j.promfg.2015.07.788

Merat, N., Jamson, A. H., Lai, F. C. H., & Carsten, O. (2012). Highly automated driving, secondary task performance, and driver state. *Human Factors*, *54*(5), 762–771. https://doi.org/10.1177/0018720812442087

Merat, N., Jamson, A. H., Lai, F. C. H., Daly, M., & Carsten, O. M. J. (2014). Transition

to manual: Driver behaviour when resuming control from a highly automated vehicle. *Transportation Research Part F: Traffic Psychology and Behaviour*, *27*(PB), 274–282. https://doi.org/10.1016/j.trf.2014.09.005

Michon, J. A. (1985). A Critical View of Driver Behavior Models: What Do We Know, What Should We Do? In *Human Behavior and Traffic Safety* (pp. 485–520). Springer US. https://doi.org/10.1007/978-1-4613-2173-6_19

Miller, D., Sun, A., Johns, M., Ive, H. P., Sirkin, D., Aich, S., & Ju, W. (2015). Distraction becomes engagement in automated driving. *Proceedings of the Human Factors and Ergonomics Society*, *59*(1), 1676–1680. https://doi.org/10.1177/1541931215591362

Mok, B. K.-J., Johns, M., Lee, K. J., Miller, D., Sirkin, D., Ive, P., & Ju, W. (2015). Emergency, Automation Off: Unstructured Transition Timing for Distracted Drivers of Automated Vehicles. *IEEE Conference on Intelligent Transportation Systems, Proceedings, ITSC*, *2015-Octob*, 2458–2464. https://doi.org/10.1109/ITSC.2015.396

Mok, B. K.-J., Sirkin, D., Sibi, S., Miller, D., & Ju, W. (2015). Understanding Driver - Automated Vehicle Interactions Through Wizard of Oz Design Improvisation. *Proceedings of the Eighth International Driving Symposium on Human Factors in Driver Assessment, Training and Vehicle Design*, *Dahlbäck 1993*, 386–392. https://doi.org/10.17077/drivingassessment.1598

Mole, C., Pekkanen, J., Sheppard, W., Louw, T., Romano, R., Merat, N., Markkula, G., & Wilkie, R. (2020). Predicting takeover response to silent automated vehicle failures. *PLOS ONE*, *15*(11), e0242825. https://doi.org/10.1371/journal.pone.0242825

Nalborczyk, L., Batailler, C., Lœvenbruck, H., Vilain, A., & Bürkner, P.-C. (2019). An introduction to Bayesian Multilevel Models using brms: A case study of gender effects on vowel variability in standard Indonesian. *Journal of Speech, Language, and Hearing Research*, *62*(5), 1225–1242. https://doi.org/10.1044/2018_JSLHR-S-18-0006

Naujoks, F., Mai, C., & Neukum, A. (2014). The Effect of Urgency of Take-Over Requests During Highly Automated Driving Under Distraction Conditions. In T. Ahram, W. Karwowski, & T. Marek (Eds.), *Proceedings of the 5th International Conference on Applied Human Factors and Ergonomics AHFE* (Issue July, pp. 2099–2106).

Naujoks, F., Purucker, C., Wiedemann, K., Neukum, A., Wolter, S., & Steiger, R. (2017). Driving performance at lateral system limits during partially automated driving. *Accident Analysis and Prevention*, *108*, 147–162.

https://doi.org/10.1016/j.aap.2017.08.027

Neubauer, C., Matthews, G., & Saxby, D. (2014). Fatigue in the automated vehicle: Do games and conversation distract or energize the driver? *Proceedings of the Human Factors and Ergonomics Society 58th Annual Meeting*, 2053–2057. https://doi.org/10.1177/1541931214581432

Page, Y., Fahrenkrog, F., Fiorentino, A., Gwehenberger, J., Helmer, T., Lindman, M., Op den Camp, O., van Rooij, L., Puch, S., Fränzle, M., Sander, U., & Wimmer, P. (2015). A comprehensive and harmonized method for assessing the effectiveness of advanced driver assistance systems by virtual simulation: The P.E.A.R.S. initiative. *The 24th International Technical Conference on the Enhanced Safety of Vehicles (ESV)*, 1–12. http://www-esv.nhtsa.dot.gov/Proceedings/24/isv7/main.htm

Parasuraman, R., & Riley, V. (1997). Humans and automation: Use, misuse, disuse, abuse. *Human Factors: The Journal of the Human Factors and Ergonomics Society*, *39*(2), 230–253.

Payre, W., Cestac, J., & Delhomme, P. (2016). Fully Automated Driving: Impact of Trust and Practice on Manual Control Recovery. *Human Factors*, *58*(2), 229–241. https://doi.org/10.1177/0018720815612319

Pekkanen, J., Lappi, O., Rinkkala, P., Tuhkanen, S., Frantsi, R., & Summala, H. (2018). A computational model for driver's cognitive state, visual perception and intermittent attention in a distracted car following task. *Royal Society Open Science*, *5*(9), 2014–2018. https://doi.org/10.1098/rsos.180194

Petermeijer, S. M., Bazilinskyy, P., Bengler, K. J., & de Winter, J. C. F. (2017). Take-over again: Investigating multimodal and directional TORs to get the driver back into the loop. *Applied Ergonomics*, *62*, 204–215. https://doi.org/10.1016/j.apergo.2017.02.023

Petermeijer, S. M., Cieler, S., & de Winter, J. C. F. (2017). Comparing spatially static and dynamic vibrotactile take-over requests in the driver seat. *Accident Analysis & Prevention*, *99*(A), 218–227. https://doi.org/10.1016/j.aap.2016.12.001

Petermeijer, S. M., Doubek, F., & de Winter, J. C. F. (2017). Driver response times to auditory, visual, and tactile take-over requests: A simulator study with 101 participants. *2017 IEEE International Conference on Systems, Man, and Cybernetics (SMC)*, *April*, 1505–1510. https://doi.org/10.1109/SMC.2017.8122827

Piccinini, G. B., Lehtonen, E., Engstrom, J., Deike, A., Markkula, G., Lodin, J., Sandin, J., Bianchi Piccinini, G., Lehtonen, E., Forcolin, F., Engström, J., Albers, D., Markkula, G., Lodin, J., & Sandin, J. (2019). How do drivers respond to silent automation failures ? Driving simulator study and comparison of computational

driver braking models. *Human Factors: The Journal of the Human Factors and Ergonomics Society (Under Review)*, 001872081987534. https://doi.org/10.1177/0018720819875347

Pipes, L. A. (1953). An operational analysis of traffic dynamics. *Journal of Applied Physics*, *24*(3), 274–281. https://doi.org/10.1063/1.1721265

Pipkorn, L., Victor, T. W., Dozza, M., & Tivesten, E. (2021). Driver conflict response during supervised automation: Do hands on wheel matter? *Transportation Research Part F: Traffic Psychology and Behaviour*, *76*, 14–25. https://doi.org/10.1016/j.trf.2020.10.001

R Core Team. (2018). R: A language and environment for statistical computing. In *R Foundation for Statistical Computing* (4.0.3). R Foundation for Statistical Computing. https://www.r-project.org/

Radlmayr, J., Gold, C., Lorenz, L., Farid, M., & Bengler, K. J. (2014). How traffic situations and non-driving related tasks affect the take-over quality in highly automated driving. *Proceedings of the Human Factors and Ergonomics Society*, *58*(1), 2063–2067. https://doi.org/10.1177/1541931214581434

Radlmayr, J., Weinbeer, V., Löber, C., Farid, M., & Bengler, K. (2018). How Automation Level and System Reliability Influence Driver Performance in a Cut-In Situation. In N. A. Stanton (Ed.), *Advances in Human Aspects of Transportation* (Vol. 597, pp. 684–694). Springer International Publishing. https://doi.org/10.1007/978-3-319-60441-1_66

Ratcliff, R. (1978). A theory of memory retrieval. *Psychological Review*, *85*(2), 59–108. https://doi.org/10.1037/0033-295X.85.2.59

Ratcliff, R., Smith, P. L., Brown, S. D., & McKoon, G. (2016). Diffusion Decision Model: Current Issues and History. *Trends in Cognitive Sciences*, *20*(4), 260–281. https://doi.org/10.1016/j.tics.2016.01.007

Risto, M., & Martens, M. H. (2014). Driver headway choice: A comparison between driving simulator and real-road driving. *Transportation Research Part F: Traffic Psychology and Behaviour*, *25*(PART A), 1–9. https://doi.org/10.1016/j.trf.2014.05.001

Road safety facts. (2019). *Road safety facts*. https://www.asirt.org/safe-travel/road-safety-facts/

Roesener, C., Hiller, J., Weber, H., & Eckstein, L. (2017). How safe is automated driving? Human driver models for safety performance assessment. *2017 IEEE 20th International Conference on Intelligent Transportation Systems (ITSC)*, *October*,

1–7. https://doi.org/10.1109/ITSC.2017.8317706

Russell, H. E. B., Harbott, L. K., Nisky, I., Pan, S., Okamura, A. M., & Gerdes, J. C. (2016). Motor learning affects car-to-driver handover in automated vehicles. *Science Robotics*, *1*(1), eaah5682. https://doi.org/10.1126/scirobotics.aah5682

SAE International. (2016). *Surface Vehicle Information Report: Human factors definitions for automated driving and related research topics (Technical Report No. J3114)*. https://saemobilus.sae.org/content/j3114_201612

SAE International. (2021). *Taxonomy and Definitions for Terms Related to Driving Automation Systems for On-Road Motor Vehicles*.

Saifuzzaman, M., & Zheng, Z. (2014). Incorporating human-factors in car-following models: A review of recent developments and research needs. *Transportation Research Part C*, *48*, 379–403. https://doi.org/10.1016/j.trc.2014.09.008

Salvucci, D. D., & Gray, R. (2004). A two-point visual control model of steering. *Perception*, *33*(10), 1233–1248. https://doi.org/10.1068/p5343

Sarkar, A., Alambeigi, H., Mcdonald, A., Markkula, G., & Hickman, J. (2021). Role of Peripheral Vision in Brake Reaction Time During Safety Critical Events. *Proceedings of the Human Factors and Ergonomics Society*.

Sarkar, A., Hickman, J. S., McDonald, A. D., Huang, W., Vogelpohl, T., & Markkula, G. (2021). Steering or braking avoidance response in SHRP2 rear-end crashes and near-crashes: A decision tree approach. *Accident Analysis & Prevention*, *154*, 106055. https://doi.org/10.1016/j.aap.2021.106055

Sarter, N. B., & Woods, D. D. (2000). Team Play with a Powerful and Independent Agent: A Full-Mission Simulation Study. *Human Factors: The Journal of the Human Factors and Ergonomics Society*, *42*(3), 390–402. https://doi.org/10.1518/001872000779698178

Schmidt, J., Dreißig, M., Stolzmann, W., & Rötting, M. (2017). The Influence of Prolonged Conditionally Automated Driving on the Take-Over Ability of the Driver. *Proceedings of the Human Factors and Ergonomics Society Annual Meeting*, *61*(1), 1974–1978. https://doi.org/10.1177/1541931213601972

Schoettle, B., & Sivak, M. (2015). *A Preliminary Analysis of Real-World Crashes Involving Self-Driving Vehicles* (Issue October). https://doi.org/UMTRI-2015-34

Seppelt, B. D. (2009). Supporting operator reliance on automation through continuous feedback [University of Iowa]. In *ProQuest Dissertations and Theses* (Vol. 3390204).

http://ezproxy.net.ucf.edu/login?url=http://search.proquest.com/docview/304902478?accountid=10003%5Cnhttp://sfx.fcla.edu/ucf?url_ver=Z39.88-2004&rft_val_fmt=info:ofi/fmt:kev:mtx:dissertation&genre=dissertations+&+theses&sid=ProQ:ProQuest+Dissertations+&+T

Seppelt, B., & Lee, J. (2015). Modeling Driver Response to Imperfect Vehicle Control Automation. *Procedia Manufacturing*, *3*(Ahfe), 2621–2628. https://doi.org/10.1016/j.promfg.2015.07.605

Seppelt, B., & Lee, J. (2019). Keeping the driver in the loop: Dynamic feedback to support appropriate use of imperfect vehicle control automation. *International Journal of Human Computer Studies*, *125*(March 2018), 66–80. https://doi.org/10.1016/j.ijhcs.2018.12.009

Seppelt, B., & Victor, T. W. (2016). Potential solutions to human factors challenges in road vehicle automation. In G. Meyer & S. Beiker (Eds.), *Road Vehicle Automation 3* (Issue August, pp. 131–148). Springer International Publishing. https://doi.org/10.1007/978-3-319-40503-2

Sharp, R. S., Casanova, D., & Symonds, P. (2000). Mathematical model for driver steering control, with design, tuning and performance results. *Vehicle System Dynamics*, *33*(5), 289–326.

Shen, S., & Neyens, D. M. (2014). Assessing drivers' performance when automated driver support systems fail with different levels of automation. *Proceedings of the Human Factors and Ergonomics Society*, *58*(1), 2068–2072. https://doi.org/10.1177/1541931214581435

Society of Automation Engineers (SAE). (2018). J3016B Taxonomy and Definitions for Terms Related to Driving Automation Systems for On-Road Motor Vehicles. In *SAE International*. https://www.sae.org/standards/content/j3016_201806/

State of California Department of Motor Vehicles. (2014). *Testing of Autonomous Vehicles with a Driver*. https://www.dmv.ca.gov/portal/dmv/detail/vr/autonomous/testing

Strand, N., Nilsson, J., Karlsson, I. C. M. A., & Nilsson, L. (2014). Semi-automated versus highly automated driving in critical situations caused by automation failures. *Transportation Research Part F: Traffic Psychology and Behaviour*, *27*, 218–228. https://doi.org/10.1016/j.trf.2014.04.005

Sultan, B., Brackstone, M., & McDonald, M. (2004). Drivers use of deceleration and acceleration information in car-following process. *Transportation Research Record*, *1*(1883), 31–39. https://doi.org/10.3141/1883-04

Sunnåker, M., Busetto, A. G., Numminen, E., Corander, J., Foll, M., & Dessimoz, C. (2013). Approximate Bayesian Computation. *PLoS Computational Biology*, *9*(1). https://doi.org/10.1371/journal.pcbi.1002803

Svärd, M., Markkula, G., Bärgman, J., & Victor, T. (2020). *Computational modeling of driver pre-crash brake response, with and without off-road glances: Parameterization using real-world crashes and near-crashes*. https://doi.org/10.31234/osf.io/6nkgv

Svärd, M., Markkula, G., Engström, J., Granum, F., & Bärgman, J. (2017). A quantitative driver model of pre-crash brake onset and control. *Proceedings of the Human Factors and Ergonomics Society Annual Meeting*, *61*(1), 339–343. https://doi.org/10.1177/1541931213601565

Teoh, E. R., & Kidd, D. G. (2017). Rage against the machine? Google's self-driving cars versus human drivers. *Journal of Safety Research*, *63*, 57–60. https://doi.org/10.1016/j.jsr.2017.08.008

Tesla Motors. (2018). *Model S software* (7.0). Tesla, Inc. https://www.teslamotors.com/presskit/autopilot

Turner, B. M., & Van Zandt, T. (2012). A tutorial on approximate Bayesian computation. *Journal of Mathematical Psychology*, *56*(2), 69–85. https://doi.org/10.1016/j.jmp.2012.02.005

Usher, M., & McClelland, J. L. (2001). The time course of perceptual choice: The leaky, competing accumulator model. In *Psychological Review* (Vol. 108, Issue 3, pp. 550–592). https://doi.org/10.1037/0033-295X.108.3.550

van de Schoot, R., Winter, S. D., Ryan, O., Zondervan-Zwijnenburg, M., & Depaoli, S. (2017). A systematic review of Bayesian articles in psychology: The last 25 years. *Psychological Methods*, *22*(2), 217–239. https://doi.org/10.1037/met0000100

van den Beukel, A. P., & van der Voort, M. C. (2013). The Influence of Time-criticality on Situation Awareness when Retrieving Human Control after Automated Driving. *The Influence of Time-Criticality on Situation Awareness When Retrieving Human Control after Automated Driving*, *Itsc*, 2000–2005. https://doi.org/10.1007/978-3-319-00476-1_5

van Winsum, W. (1999). The human element in car following models. *Transportation Research Part F: Traffic Psychology and Behaviour*, *2*(4), 207–211. https://doi.org/10.1016/S1369-8478(00)00008-5

Vasishth, S. (2020). Using approximate Bayesian computation for estimating parameters in the cue-based retrieval model of sentence processing. *MethodsX*, *7*(October

2019). https://doi.org/10.1016/j.mex.2020.100850

Venkatraman, V., Lee, J., & Schwarz, C. W. (2016). Steer or Brake? Modeling Drivers' Collision Avoidance Behavior Using Perceptual Cues. *Transportation Research Record: Journal of the Transportation Research Board*, *2602*, 97–103. https://doi.org/10.3141/2602-12

Victor, T. W., Tivesten, E., Gustavsson, P., Johansson, J., Sangberg, F., & Ljung Aust, M. (2018). Automation Expectation Mismatch: Incorrect Prediction Despite Eyes on Threat and Hands on Wheel. *Human Factors: The Journal of the Human Factors and Ergonomics Society*, *60*(8), 1095–1116. https://doi.org/10.1177/0018720818788164

Vogelpohl, T., Kühn, M., Hummel, T., Gehlert, T., & Vollrath, M. (2018). Transitioning to manual driving requires additional time after automation deactivation. *Transportation Research Part F: Traffic Psychology and Behaviour*, *55*, 464–482. https://doi.org/10.1016/j.trf.2018.03.019

Vogelpohl, T., Kühn, M., Hummel, T., & Vollrath, M. (2018). Asleep at the automated wheel—Sleepiness and fatigue during highly automated driving. *Accident Analysis and Prevention*. https://doi.org/10.1016/j.aap.2018.03.013

Volvo Cars. (2018). *IntelliSafe Autopilot*. https://www.volvocars.com/us/about/our-innovations/intellisafe

Walch, M., Lange, K., Baumann, M., & Weber, M. (2015). Autonomous Driving: Investigating the Feasibility of Car-driver Handover Assistance. *Proceedings of the 7th International Conference on Automotive User Interfaces and Interactive Vehicular Applications*, 11–18. https://doi.org/10.1145/2799250.2799268

Wan, J., & Wu, C. (2018). The Effects of Lead Time of Take-Over Request and Nondriving Tasks on Taking-Over Control of Automated Vehicles. *IEEE Transactions on Human-Machine Systems*, *48*(6), 582–591. https://doi.org/10.1109/THMS.2018.2844251

Wandtner, B., Schömig, N., & Schmidt, G. (2018a). Secondary task engagement and disengagement in the context of highly automated driving. *Transportation Research Part F: Traffic Psychology and Behaviour*, *58*, 253–263. https://doi.org/10.1016/j.trf.2018.06.001

Wandtner, B., Schömig, N., & Schmidt, G. (2018b). Effects of Non-Driving Related Task Modalities on Takeover Performance in Highly Automated Driving. *Human Factors: The Journal of the Human Factors and Ergonomics Society*, *XX*(X), 1–12. https://doi.org/10.1177/0018720818768199

Waymo. (2018). *Waymo self-driving car*. https://waymo.com

Wickens, C. (1984). *Processing resources and attention, varieties of attention* (R. Parasuraman & D. D. (eds.)). Academic Press.

Wiedemann, K., Naujoks, F., Wörle, J., Kenntner-Mabiala, R., Kaussner, Y., & Neukum, A. (2018). Effect of different alcohol levels on take-over performance in conditionally automated driving. *Accident Analysis & Prevention*, *115*, 89–97. https://doi.org/10.1016/j.aap.2018.03.001

Wintersberger, P., Green, P., & Riener, A. (2017). Am I Driving or Are You or Are We Both? A Taxonomy for Handover and Handback in Automated Driving. *Proceedings of the 9th International Driving Symposium on Human Factors in Driver Assessment, Training, and Vehicle Design: Driving Assessment 2017*, 333–339. https://doi.org/10.17077/drivingassessment.1655

World Health Organization. (2015). *Global status report on road safety*.

Xue, Q., Markkula, G., Yan, X., & Merat, N. (2018). Using perceptual cues for brake response to a lead vehicle: Comparing threshold and accumulator models of visual looming. *Accident Analysis & Prevention*, *118*(June), 114–124. https://doi.org/10.1016/j.aap.2018.06.006

Yang, H. H., & Peng, H. (2010). Development of an errorable car-following driver model. *Vehicle System Dynamics*, *48*(6), 751–773. https://doi.org/10.1080/00423110903128524

Young, M. S., & Stanton, N. A. (2002). Malleable attentional resources theory: A new explanation for the effects of mental underload on performance. *Human Factors*, *44*(3), 365–375. https://doi.org/10.1518/0018720024497709

Zeeb, K., Buchner, A., & Schrauf, M. (2015). What determines the take-over time? An integrated model approach of driver take-over after automated driving. *Accident Analysis and Prevention*, *78*, 212–221. https://doi.org/10.1016/j.aap.2015.02.023

Zeeb, K., Buchner, A., & Schrauf, M. (2016). Is take-over time all that matters? the impact of visual-cognitive load on driver take-over quality after conditionally automated driving. *Accident Analysis and Prevention*, *92*, 230–239. https://doi.org/10.1016/j.aap.2016.04.002

Zeeb, K., Härtel, M., Buchner, A., & Schrauf, M. (2017). Why is steering not the same as braking? The impact of non-driving related tasks on lateral and longitudinal driver interventions during conditionally automated driving. *Transportation Research Part F: Traffic Psychology and Behaviour*, *50*, 65–79. https://doi.org/10.1016/j.trf.2017.07.008

Zhang, B., de Winter, J., Varotto, S., Happee, R., & Martens, M. (2019). Determinants of take-over time from automated driving: A meta-analysis of 129 studies. *Transportation Research Part F: Traffic Psychology and Behaviour*, *64*, 285–307. https://doi.org/10.1016/j.trf.2019.04.020

Zhang, B., Wilschut, E., Willemsen, D., & Martens, M. H. (2017). Driver Response Times when Resuming Manual Control from Highly Automated Driving in Truck Platooning Scenarios. *RSS2017*, *October*, 7522. https://doi.org/10.13140/RG.2.2.28249.01127